ผลกระทบจากผนังอิฐก่อเยื้องออกนอกแนวเสาต่อพฤติกรรมของอาคารคอนกรีตเสริมเหล็กในประเทศภูฏานภายใต้แผ่นดินไหว

นายเทค นาท คาราเรีย

วิทยานิพนธ์นี้เป็นส่วนหนึ่งของการศึกษาตามหลักสูตรปริญญาวิศวกรรมศาสตรมหาบัณฑิต
สาขาวิชาวิศวกรรมโยธา ภาควิชาวิศวกรรมโยธา
คณะวิศวกรรมศาสตร์ จุฬาลงกรณ์มหาวิทยาลัย
ปีการศึกษา 2560

SEISMIC EFFECTS OF CORNICE PROJECTION IN MASONRY-INFILL REINFORCED CONCRETE BUILDINGS IN BHUTAN

Mr. Tek Nath Kararia

A Thesis Submitted in Partial Fulfillment of the Requirements
for the Degree of Master of Engineering Program in Civil Engineering
Department of Civil Engineering
Faculty of Engineering
Chulalongkorn University
Academic Year 2017

Thesis Title	SEISMIC EFFECTS OF CORNICE PROJECTION IN MASONRY-INFILL REINFORCED CONCRETE BUILDINGS IN BHUTAN
By	Mr. Tek Nath Kararia
Field of Study	Civil Engineering
Thesis Advisor	Assistant Professor Chatpan Chintanapakdee, Ph.D.

Accepted by the Faculty of Engineering, Chulalongkorn University in Partial Fulfillment of the Requirements for the Master's Degree

.....Dean of the Faculty of Engineering
(Associate Professor Supot Teachavorasinskun, D.Eng.)

THESIS COMMITTEE

.....Chairman
(Associate Professor Anat Ruangrassamee, Ph.D.)

.....Thesis Advisor
(Assistant Professor Chatpan Chintanapakdee, Ph.D.)

.....External Examiner
(Nuttawut Thanasisathit, Ph.D.)

เทค นาท คาราเรีย : ผลกระทบจากผนังอิฐก่อเยื้องออกนอกแนวเสาต่อพฤติกรรมของอาคารคอนกรีตเสริมเหล็กในประเทศภูฏานภายใต้แผ่นดินไหว (SEISMIC EFFECTS OF CORNICE PROJECTION IN MASONRY-INFILL REINFORCED CONCRETE BUILDINGS IN BHUTAN) อ.ที่ปรึกษาวิทยานิพนธ์หลัก: ผศ. ดร. ฉัตรพันธ์ จินตนาภักดี, 103 หน้า.

ประเทศภูฏานตั้งอยู่ในพื้นที่ที่เกิดแผ่นดินไหวเป็นประจำและรุนแรงในแถบเทือกเขาหิมาลัย แต่ทว่ามีข้อกฎหมายกำหนดให้การออกแบบอาคารเชิงสถาปัตยกรรมต้องมีการยื่นพื้นและคิ้วบัวออกจากแนวเสาโดยมีระยะยื่นห่างจากตัวอาคารเพิ่มขึ้นที่ระดับชั้นที่สูงขึ้นไปเพื่อเพิ่มพื้นที่ใช้สอยและคงเอกลักษณ์ทางสถาปัตยกรรมของอาคารในประเทศภูฏาน การยื่นพื้นและคิ้วบัวรวมถึงการใช้กำแพงอิฐที่มีความหนาส่งผลต่อการตอบสนองของอาคารต่อแผ่นดินไหวขนาดใหญ่ ปัจจุบันยังไม่ได้มีการศึกษาอย่างเพียงพอเกี่ยวกับผลของการยื่นพื้นและคิ้วบัวดังกล่าวต่อสมรรถนะในการต้านทานแผ่นดินไหวของอาคาร การศึกษานี้จึงใช้วิธีวิเคราะห์การตอบสนองของโครงสร้างไม่เชิงเส้นแบบประวัติเวลาตรวจสอบประสิทธิภาพของโครงสร้างอาคารเรียนสามชั้นจำลองแบบสามมิติซึ่งเป็นตัวแทนอาคารโครงข้อแข็งมีผนังอิฐก่อซึ่งพบได้ทั่วไปในประเทศภูฏานภายใต้ความเร่งแผ่นดินไหวทั้งในแนวราบและแนวดิ่ง การศึกษานี้ได้เปรียบเทียบการตอบสนองของอาคารที่ไม่มีและมีผนังอิฐและกรณีที่มีระยะยื่นของพื้นและคิ้วบัวอีกหกแบบต่างๆ กันเพื่อศึกษาถึงผลของการยื่นพื้นและคิ้วบัวต่อการตอบสนองต่อแผ่นดินไหวของอาคาร ค่าการตอบสนองที่พิจารณาได้แก่ การเคลื่อนตัวของชั้น การเคลื่อนที่สัมพันธ์ระหว่างชั้น แรงในองค์อาคาร การโก่งตัวในแนวดิ่ง ซึ่งผลการศึกษาพบว่าการยื่นพื้นและคิ้วบัวทำให้ โมเมนต์ในคานยื่นเพิ่มขึ้น ๑.๖๕ เท่าและการโก่งตัวของคานยื่นเพิ่มขึ้น ๑.๘๐ เท่าเทียบกับผลจากน้ำหนักบรรทุกแนวดิ่งในสภาวะที่ไม่มีแผ่นดินไหว และจากกำลังต้านทานของโครงสร้างที่ออกแบบตามปกติไม่ควรยื่นพื้นและคิ้วบัวเกิน ๑.๔๐ เมตร

ภาควิชา วิศวกรรมโยธา ลายมือชื่อนิสิต .....

สาขาวิชา วิศวกรรมโยธา ลายมือชื่อ อ.ที่ปรึกษาหลัก .....

ปีการศึกษา 2560

5970421221 : MAJOR CIVIL ENGINEERING
KEYWORDS: REINFORCED CONCRETE / CORNICE PROJECTION / NONLINEAR RESPONSE HISTORY ANALYSIS / VERTICAL ACCELERATION

TEK NATH KARARIA: SEISMIC EFFECTS OF CORNICE PROJECTION IN MASONRY-INFILL REINFORCED CONCRETE BUILDINGS IN BHUTAN. ADVISOR: ASST. PROF. CHATPAN CHINTANAPAKDEE, Ph.D., 103 pp.

Bhutan is located in utmost active seismic zone in the belt of the Himalayan region. However, there is a prevailing architectural requirement of cornice projections away from the perimeter columns at each floor proportional to the floor level to increase floor area and retain Bhutanese architectural style. This irregular projection with thick solid brick walls resting at the edge of cantilever projection affects the structural response during a strong earthquake. To date, there is not adequate investigation on the effects of such cornice projection on seismic performance of buildings. In this study, Nonlinear Response History Analysis (NLRHA) using vertical ground acceleration of relevant earthquakes was performed to assess performance of a three-dimensional three-story typical school building, which represents stock of structures in Bhutan. This study compares response parameters of the bare frame, in-filled frame, and six models with different projection lengths to comprehend the collective effects. Relevant global and local response parameters such as lateral story displacements, inter-story drifts, internal force demands, vertical deflections and its amplifications were assessed. The results indicate that bending moment and vertical deflection of the cantilevered beams are significantly affected due to the presence of cornice projection under vertical acceleration. The bending moment is amplified by a factor of 1.65, whereas the vertical deflection is amplified by a factor of 1.80, compared to the effect of gravity load alone. Based on typical design and acceptance criteria of ACI codes, the cornice projection length should not exceed 1.4m.

Department:	Civil Engineering	Student's Signature	.....
Field of Study:	Civil Engineering	Advisor's Signature	.....
Academic Year:	2017		

ACKNOWLEDGEMENTS

I wish to express my sincere gratitude to my supervisor Asst. Professor Dr. Chatpan Chintanapakdee for his continuous guidance, motivation, for his patience, and for constructive technical and moral support to complete this study smoothly. It was truly a blessing to have you as my supervisor who had immense knowledge in this field. Further, I wish to extend my sincere gratitude to the committee members Assoc. Professor Dr. Anat Ruangrassamee and Dr. Nuttawut Thanasisathit for your insights, constructive comments, and ideas after carefully reviewing this thesis work at the initial and final stages.

Secondly, Thailand International Cooperation Agency (TICA) Award is gratefully acknowledged for the full scholarship provided for me to undertake the Master of Engineering study. This scholarship and research fund provided a great opportunity for me to study in the Master program at Chulalongkorn University and completion of this research work.

Thirdly, my colleagues in the university as well as in the Structural Engineering Research Laboratory of Chulalongkorn University for the positive atmosphere, especially, Mr. Nattanai Kuangmia, Mr. Bach Kim Do , Mr. Kimleng Khy, Mr. Khonesavanh Pormeuangpieng and Miss Kanchana Thapthim among others for the helpful technical discussions, sharing ideas and generous supports for making the duration of research work more conducive, productive and interesting. Altogether, it made my stay and research work lively throughout the year.

Last but not least, my friends and my family especially my parents for their encouragement and support throughout my study period.

I express thanks to all of those who helped me directly or indirectly in the successful completion of this thesis work. Anyone missed in this acknowledgment is also thanked.

This work is dedicated to my parents.

CONTENTS

Page

Page

LIST OF FIGURES

LIST OF TABLES

CHAPTER 1
INTRODUCTION

1.1 Background

Cultural heritage is highly regarded and it is the subject of the Constitution of Bhutan. In addition, it is one of the nine guiding principles for modern development goals of the country. Accordingly, advanced work is done to develop codes which are consistent to support the modern development at the same time preserve the Bhutan iconic unique traditions.

There are building rules in place to facilitate safe building construction with the professional approach to building design (DuDH, 2002) and also to promote the traditional architecture. It aims to achieve design requirements. The architectural features and outer façade of all buildings shall conform to the Bhutanese Architecture guidelines 2014 (MoWHS, 2014).

One of the highly focused topic in the recent time is the study of the response of buildings during the strong ground motion of an earthquake. Bhutan's geographical position falls along tectonic boundary of the two plates of Indo-Eurasian. The earthquake itself is very complex phenomena, previous studies had not found the ways to predict of magnitude and probabilities of occurrence. We need to prepare and build our environment and facility resilience to seismic forces. Some countries with the active seismic fault suffered numerous devastating loss of properties and lives around the world in recent times. Typical buildings are mainly consist of reinforced concrete (RC) frame structure with brick masonry in-fill walls and cantilever projections (cornice or rabsel) from the main superstructure.

Typical buildings in Bhutan range from single story to seven stories and until the late 1990s there was no regulation regarding design and construction of buildings

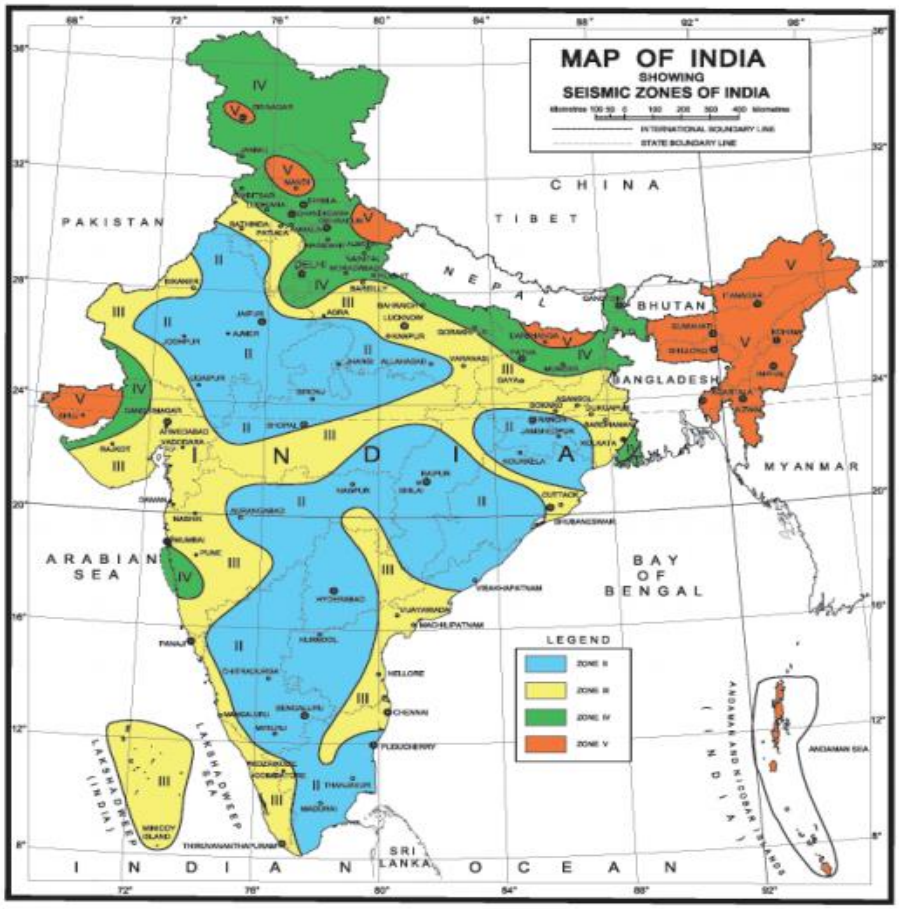

Figure 1-1 Seismic Zones of India (IS1893, 2002)

to resisting strong earthquakes. Currently, most were designed for gravity loads only. However, over time the importance of having strong buildings against the strong ground motions in the region had been seriously considered. Since 1997, Bhutan had been strictly following Indian seismic codes for all new RC frame structure buildings. The seismic zone for Bhutan is considered as seismic zone V based on seismic zonation map of India. To date Bhutan does not have its own seismic map and has to refer to Indian seismic map.

The traditional architecture (MoWHS, 2014) is a most beautiful expression of ancient culture that reflect and mirror the integration of the simple daily lives of the Bhutanese people. Bhutanese architecture preservation for future rests mainly on the understanding of values attached to it and consequent concrete actions taken to promote and develop these values. The mandatory requirement to integrate components of

Bhutanese architecture beside structural component is to preserve traditional architecture with its values along with modern development. With rapid modernization in constructions with new materials and latest technologies, our cultural heritage and traditional buildings, old low-rise structures are replaced by more complex and high rise modern structures. Thus, there is a high risk of losing the traditional architecture such as the scale, details, proportion, materials, and others.

Currently, there is Bhutanese Architecture Guidelines 2014 with the objective to support the construction of traditional structures and construction of modern buildings that are harmonious with traditional architectural design and proportion. The main concern is that in the current practice that structural designers do not consider these additional components in the analysis even though it is detailed in architectural requirement. Thus, there is a gap between the architectural requirement and structural analysis procedure. The main reason, they do not consider in modeling structural element as well as non-structural element together is due to difficulties in understanding the complex structural behavior, when the structure is exposed to gravity and random earthquake loads.

There had been limited study done on cornice projection (cantilever projection). Since 2014, compulsory requirements of cornice projections to all buildings are necessary and it is important to make sure building design considers this architectural/ non-structural component in structural analysis. Recently, this cornice projection is away from main structure perimeter column grid around building with varying projection length however, there is no clear attempt or breakthrough to understanding the issue related to such unique projection.

Witnessing the frequent large magnitude earthquake in the country as well as neighboring countries which had triggered policymakers and builders a bigger concern to be more responsible and prepare for such a devastating event. The damages caused by earthquakes in 2009 and 2011 to specially to shelter (buildings) are approximately USD 52 million and USD 24.46 million respectively (Bhutan Joint Assessment Report to World Bank and United Nations for earthquakes of 2011 and 2009). So, recommendations after proper understanding of the more accurate behavior of typical in-filled wall frame structure with cornice projections will be useful for decision making to build more resilient buildings.

Many literatures are available for only in-filled masonry in-filled frame structure, however, literature on typical Bhutanese building with unique cornice projection is not available. Thus, the focus of this paper is to comprehend the effect of projections on structural behavior such as a change in response and stability when exposed to strong ground motions.

A. Research problems

The architecture guideline 2014 requires that all newly designed and build houses strictly follow the guideline where the proportional projection of walls have to be made at each story above ground. Thus, dead load of the wall above will be placed on the eccentric beam offset from the column gridline. These offset walls induce bending moment to the cantilever beam. This paper aims to find the more accurate behavior of load transfer mechanism and the maximum safe projection length that can be constructed to fulfill the architectural requirements without excessively affecting the responses of structure during vertical acceleration of earthquakes. The typical contemporary building has projections as shown in Figure 1-1 and the component outer elevation view in Figure 1-2.

Figure 1-2 Typical Bhutanese building (Dorji et al., 2009)

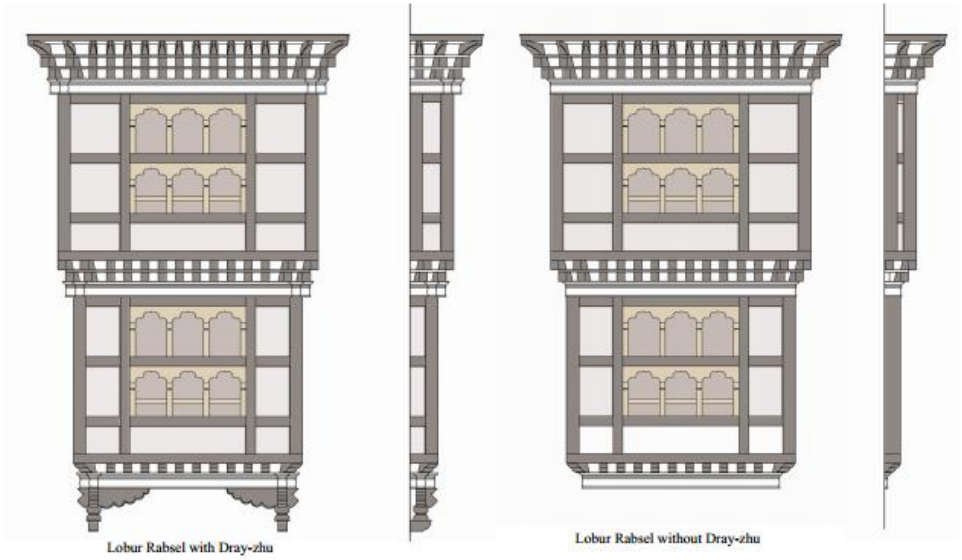

Figure 1-3 Proportionate cornice projection (MoWHS, 2014)

B. Research questions

1. What is the responses of the structure with cornice projections to the seismic loading?
2. What is the maximum safe limit length of cornice projection for structures subjected to earthquake ground motions?
3. How much is the dynamic amplification of internal forces and deflections due to the influence of cornice projections?

1.2 Objectives of research

This study has the following objectives:

1. To determine response of a typical structure which is a school building with cornice projection representing stocks of masonry in-filled frame structure in Bhutan.
2. To determine the safe limit for the cornice projection length.
3. To evaluate dynamic amplification factor of internal forces and deflections of structures with cornice projection.

1.3 Scope and assumptions

1. Typically, masonry in-filled frame structures representing the stock of buildings in Bhutan are considered in this study, details of model were obtained from structural drawing of School Planning and Building Division (SPBD), Ministry of Education.
2. The building is investigated using 7 sets of relevant strong ground motions of the similar earthquake in the region. Two horizontal and one vertical components of earthquake ground motions are applied simultaneously to the structures.
3. Non-linear Response History Analysis (NLRHA) procedure is used for evaluating the performance of the structures. Tools used is ETABS 2015 for the NLRHA.
4. Seismic design codes IS1893, FEMA356, ASCE41 and few others as necessary are referred.
5. It is assumed that full height of masonry wall rest on the cantilever beam at the end of projection in terms of lumped mass.
6. Projection is assumed to be uniform throughout length of front façade of building.

Limitations

1. Cornice at different sides of building is not included in this study. Cornice projection at the front side only is considered.
2. Complex shapes of cornice projection are simplified as cantilever beam in mathematical model.
3. Later stiffness of in-filled wall with opening more than 50% is not considered in the model based on previous study.
4. Different types of wall materials such as interlocking cement earth block, Bhutan concrete bricks are Bamboo mat-based walls (ekra walls) not included. Only RCC cornice are used for this study.
5. Irregular projection away from gridline of column are not considered

1.4 Significance

1. Current practice of structural analysis practice does not capture all architectural/non-structural component that is cornice projection. However, since 2014, it has become compulsory requirement with Bhutanese Architectural Guidelines in place (MoWHS, 2014).
2. Cornice projection has become important aspect and concern as there is no detail study has been conducted before. The integration of cornice component as a part of main structure became the requirement and applicable to almost all types of building in Bhutan. So, it is recommended area of study in recent time.
3. Replacing existing traditional one or two stories building to increased number of stories by changing the construction material and technology. These changes may lead to drastic change in strength and behavior of the structure which need to be studies.
4. Bhutan fall on the active faults and past studies (Drukpa et al., 2006) predicted there is huge accumulated strain over long period of time and it may lead to large magnitude earthquake in future, similar to Nepal Gorkha Earthquake M7.8 ,2015 with many aftershocks.
5. The damage caused by Earthquakes in Bhutan due to earthquake in 2009 and 2011 which especially affected shelters (MoHCA, 2009, MoHCA, 2011) as follows:

1. USD 52 million loss 2009
2. USD 24.46 million Loss 2011 (Total USD 77.46 Million)

If the total damages caused by all natural disasters are considered , 50% of the causalities is attributed to earthquakes especially due to collapse of structures (Walling et al., 2009) .

1.5 Outline of thesis

This thesis work consists of six Chapters as briefly described below:

Chapter 1 gives the overview of seismic code used in Bhutan, backgrounds of Bhutanese architectural requirements. It also includes statement of research problem, objectives, scope and assumptions.

Chapter 2 elaborates quite detail about the seismicity, types of building such are traditional and modern buildings in Bhutan and importance of unique cornice projection and its structural details. This chapter also includes literature review on important component "cornice projection element" used in this research work especially RC in-filled wall represented by diagonal compression struts, earthquake ground motions which includes both horizontal and vertical components.

Chapter 3 gives thermotical backgrounds on different analysis procedures such as static, dynamic and modal analysis. It also includes reasons for using Nonlinear Response History Analysis (NLRHA) with amplitude scaling of ground motions to the target spectrum.

Chapter 4 focuses on the development of simplified mathematic models from physical model which includes the cornice projections and approach for the analysis to achieve the objectives. It also covers details of preparation of input earthquake accelerations, gravity loading, properties of all structural elements.

Chapter 5 mainly emphasis on NLRHA and important parameters considered for seismic performance assessments. The result of response parameters and discussions are also covered in this chapter.

Chapter 6 includes conclusions and recommendations of the research findings and also identify the scope for future work.

CHAPTER 2
LITERATURE REVIEW

2.1 Seismicity of Bhutan

One of the most devastating natural disasters of all time is an earthquake. It is considered to be a most destructive natural disaster causing more than 50% of the causalities from a natural disaster is attributed to earthquakes besides damaging huge amount of properties (Walling et al., 2009). There is no exception from the fatalities and damage of properties due to earthquakes for a tiny Himalayan country, Bhutan. The most recent earthquake (MoHCA, 2011) that rocked Bhutan causing widespread damages.

Two consecutive earthquake of 2009 and 2011 reminded that Bhutan is vulnerable to such earthquake events. The 2011 earthquake caused huge damages and killed at least 99 people in Bhutan, Nepal and India and over 200 are injured.

In last several decades, there were 32 significant earthquakes occurred in Bhutan, the most important one being 1941 with the magnitude of 6.75 (Thinley et al., 2015). There are many earthquakes that occurred around Bhutan which specifically falls in India such as in M8.7 Shillong Plateau (1897); M8.3, Bihar and Nepal Border (1934), M8.6 Arunachal Pradesh (1950) earthquakes among many others (Walling et al., 2009).

Bhutan being the already faced many earthquakes, still not fully prepared for similar or high magnitude future events. Currently, Bhutanese building are designed using Indian Seismic Code IS1893(2002). This may lead to the inaccurate prediction of peak ground acceleration (PGA) and the response spectrum are quite different for Bhutan as a whole which could lead to different structural responses.

However, all building built prior to 1997 both in urban and rural areas either built following thumb rules or design is done considering gravity load only without any seismic check. Due to that many rural houses as well as old government office structures were heavily damaged all over districts in recent two earthquakes. Thus, there are hundreds of buildings which are potentially vulnerable to earthquakes (Thinley et al., 2015)

The investigation (Drukpa et al., 2006) most of the past earthquakes in the Bhutan Himalaya covering between period 1937-2003 was done. It is found that focal mechanisms are consisting of typically strike slip with mid to deep crustal depths. In the recent earthquake events shows that Indian plate significantly undergoing mid to deep crustal depths with oblique convergence of Indo-Asian plates collision. The seismicity of the Himalayan region has shallow and deeper earthquakes.

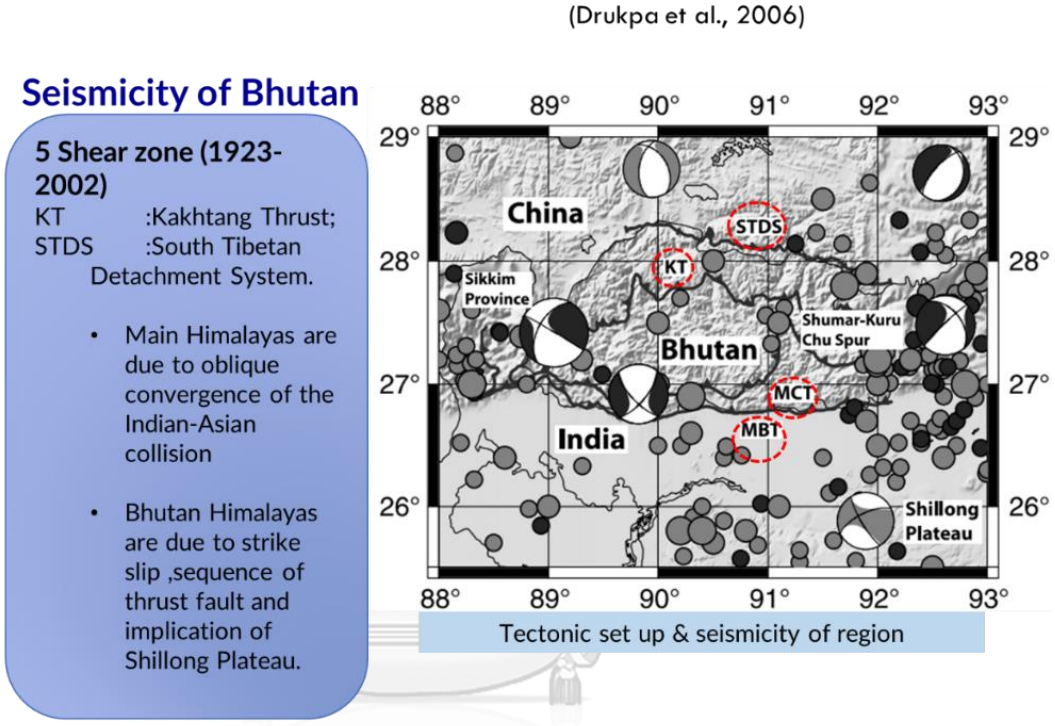

Figure 2-1 Tectonic setup & seismicity of Bhutan

(Drukpa et al., 2006)

Main Central Thrust (MCT), Main Boundary Thrust (MBT)

Currently, Bhutan do not have its own seismic zonation map however, Bhutan is surrounded at three sides by Indian states where Bhutan is considered as a part of adjoining areas while developing the seismic zonation of India.

Figure 2-2 shows the seismic zonation map of the India from which currently Bhutan also derived the seismic zone for earthquake design. Bhutan consider itself in seismic zone. Most of Bhutan region border with India falls in zone V and other region in western part of country falls in zone IV. Thus, it is further required proper microzonation and subdivision of areas of similar exposure to earthquake events. This

will definitely help Bhutan understand the seismic hazard within Bhutan and take more necessary measure to build safer structures. The gap between the approximate PGA derive from Indian seismic map and the real PGA value observed at site will be reduced if we have proper microzonation map of Bhutan. This can lead to appropriate design of structures with valuable analysis information, helpful for hazard assessment of important areas (urban) and understand local site conditions. The informed decision can be taken based on seismic hazard for future plan and construction at different areas.

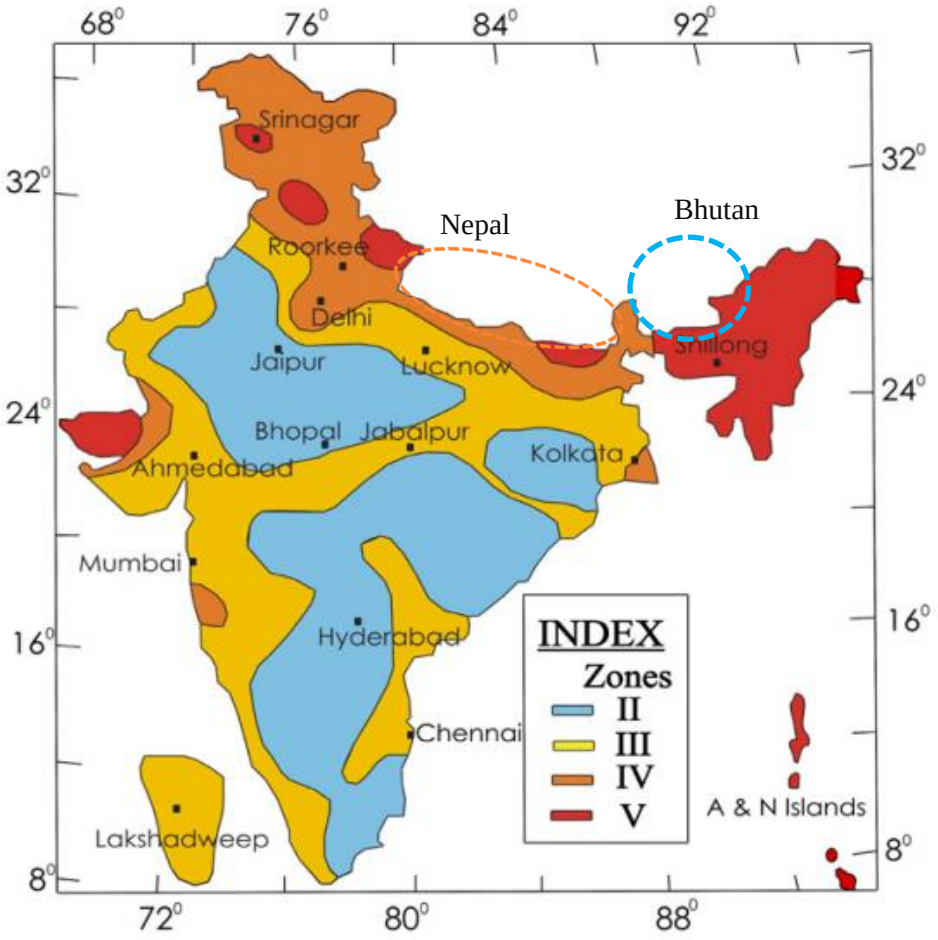

Figure 2-2 Zonation map of India (BIS, 2002)

The continuous subduction (Walling et al., 2009) of Indian plate causing seismic activity which makes whole region vulnerable to devastating hazards of large earthquake in the region including Bhutan. The Himalayan region starting from north to south has 5 different main shear zones.

In April 2015 (Takai et al., 2016) large Gorkha earthquake of M7.8 occurred that originates from Main Himalayan Thrust fault located central part of Nepal. This

also shook Bhutan quite strongly and causes minor damages. These strong ground motions represent typical kind of earthquake in the Himalayan region so that using this ground motion in the study would be more appropriate representing the countries in the region besides other.

Therefore, this paper aims to presents the seismic response behavior considering the typical masonry in-filled frame masonry structure with Bhutanese architectural components (cornice projections) using the vertical acceleration of eathquakes. Non-linear Response History Analysis (NLRHA) is performed using software ETABS. The seismic performance of building with various projection length of cornice is evaluated in terms of relevant response parameters.

2.2 Typical building structures in Bhutan

2.2.1 Traditional building

Architectural (MoWHS, 2014) elements in traditional Bhutanese architecture enhance or upgrade the hierarchy and values of a design. The architectural elements in traditional Bhutanese architecture may be divided into two categories. The Main Architectural Elements are those that are mainly structural elements and are commonly found in traditional Bhutanese architecture. Secondary Architectural Elements are those that are usually installed to enhance aesthetics and create higher standards of hierarchy and value in traditional Bhutanese architecture.

The projection of cornice as part of Cornice is secondary. Currently, when the material for secondary architectural elements are changed in terms of material and design of elements it definitely has some change in the building response during the earthquake. This research focuses on to investigate the safe limits of cantilever projections and change in structural behavior when exposed to the strong ground motion.

Figure 2-3 Traditional house with wooden cornice

(MoWHS, 2014)

2.2.2 Modern buildings

The modern building also includes the projection of cornice similar to that of traditional building, however with the new construction materials and techniques. Figure 2-4 and 2-5 shows the typical contemporary building during construction stage

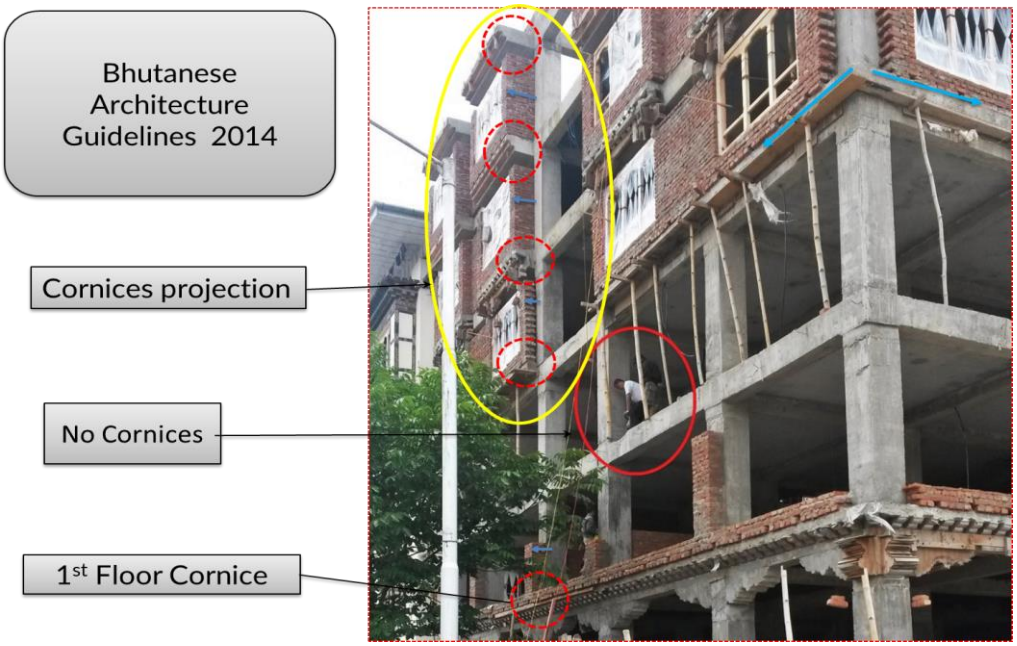

Figure 2-4 Modern building during construction

(https://jeninbhutan.wordpress.com)

with cornice projection of different length at a different floor level of integrating traditional architectural components. Cornice projection length at level 1 in Figure 2-5 is first projection and next projection is at level 2 with increased length of projections. Similarly, projection length for different level like level 3 and level 4 increases proportionally starting from level 1. In my study, level 1 to level 3 projection were studied. There has been drastic modifications of construction technique and material however at the same time maintaining the same architectural outlook following the Bhutanese Architectural Guideline.

Figure 2-5 Modern building during constrution

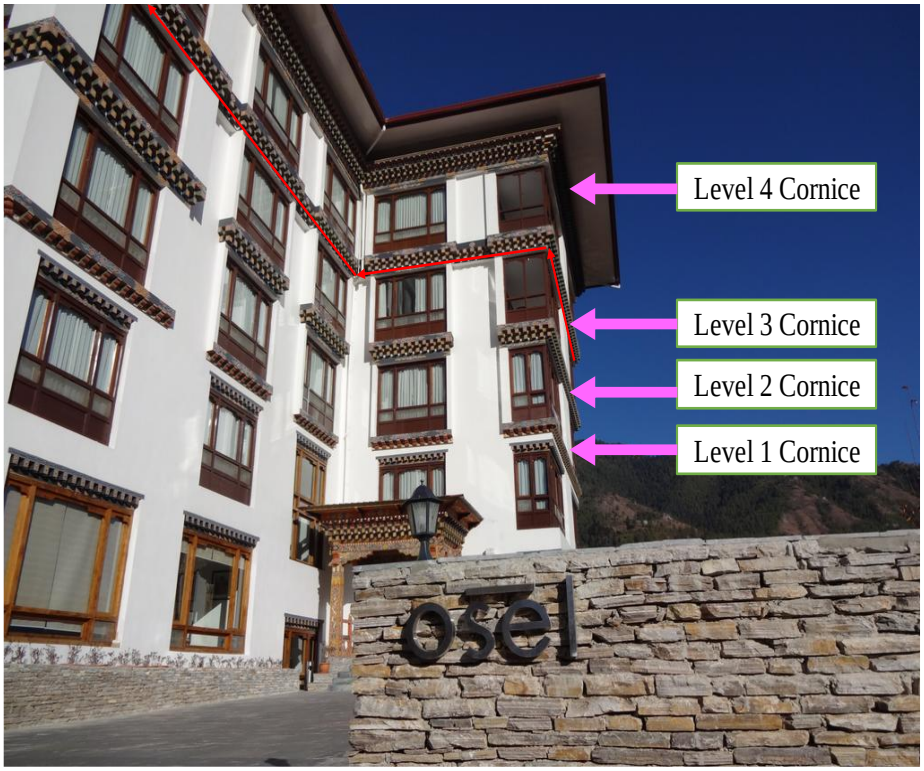

Figure 2-6 Five story modern building with cornice projection (http://www.oselbhutan.com)

There is no adequate detailed study and standard procedure was in place to assess the seismic performance of such type of buildings including the non-structural component called cornice projections. The detail of this major architectural components and its effects when it is exposed to vertical acceleration is the focus of this study.

2.2.3 Cornice projection

In the traditional Bhutanese architecture, cornice are considered to be one of the most significant and beautiful. The cornice ("Rabsel" in Dzongkha means "good clarity") because it provides better light and clarity into a building through its multiple window openings and is the main visible architecture component that adds beauty and sophistication to a Bhutanese house. It mainly consists of three components among

others. First component, Bogh is an end of the extension of the Cham or interior timber joist for ceiling or upper floor levels that are set to project outside the wall as cornice

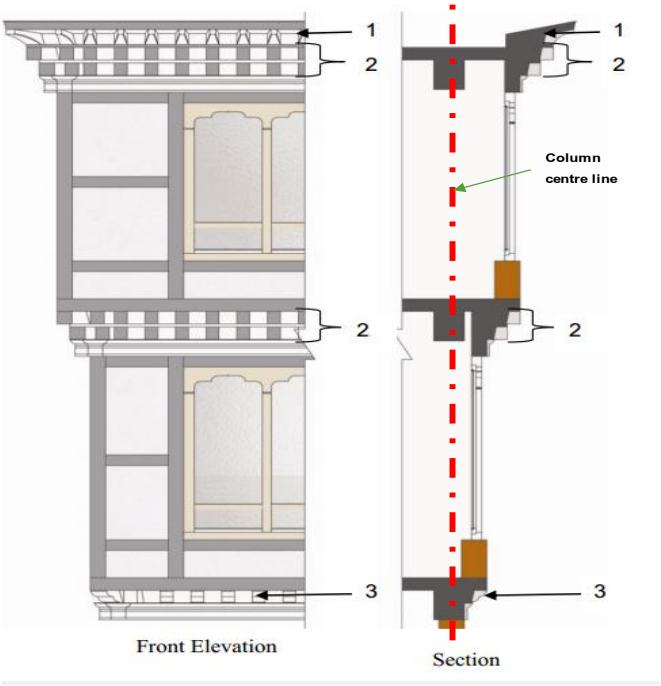

Figure 2-7 Components of cornice projection (MoWHS, 2014)

Second component, phana is a timber/reinforced concrete/ precast cornice shaped like a pig 's nose or neck of a duck is laid over the Bogh (MoWHS, 2014). Third component, tshechu kha is cantilever ring of ground floor joists which support the cornice.

Table 2.1 Width and thickness of cornice range

Components	**Width (mm)**		**Thickness(mm)**	
	Minimum	Maximum	Minimum	Maximum
Phana (1)	125	150	150	175
Bogh (2)	125	150	150	175
Tshechu kha(3)	125	175	150	200

Basically, the bogh and phana are components of cornice projections and it further divided cornice component into other minor architectural details. Cornice design are eight types and form as continuous frame covering the whole of the upper

façade or is divided into smaller units. Cornice usually projects away from main gridline of column out of the main superstructure. It is supported by the cantilever ring ground floor joists known as tshechu kha. Further, cornices are categorized in terms of material used as listed below:

1. Glass fiber Reinforced Concrete (GRC) Cornice
2. Reinforced Concrete (RC) Cornice
3. RC Cornice with timber Phana, Figure 2-8 shows the RC cornice

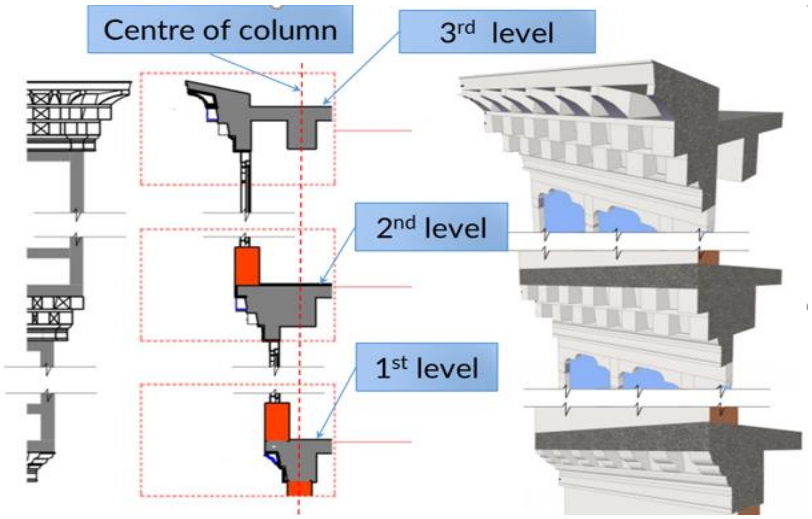

Figure 2-8 Reinforce concrete cornice details (MoWHS, 2014)

A. Cornice recommendations for usage

The requirement of two layers of bogh (charms) with one layer of phana on any cornice is necessary. For single-story building, cornices are not mandatory. For single story ekra building either two layers or one-layer bogh and phana is recommended for double tier cornice, the lowest cornice will rest on tshechu kha and in between the two cornices double layer, bogh shall be provided. Recommended sizes of elements for cornice in cornice are presented in Table 2.1 based on the width of bogh (x).

B. Proportion of cornice

The length of bogh cantilever varies for different cornice projection at different parts of the building. The spacing between the boghs ranges from x + 25mm to 2 times x. In dwellings the length of x ranges from 125mm to 150mm while it is much bigger in important buildings, generally equaling 175mm. Figure 2-9 shows the detail of typical cornice basically used in Bhutan.

Phana is also made from the same timber section as charms. However, when it is placed in position, phana appears much taller than bogh as it is placed on the diagonal face. The guideline ensures the incorporation of traditional architecture in the modern design and is not meant to obstruct any innovative new designs but to add positive aesthetic value to the Bhutanese landscape and the built environment of Bhutan. In order to incorporate cornice features, it is very better to understand the effects on the behavior of structure when exposing to a strong ground motion from the earthquake.

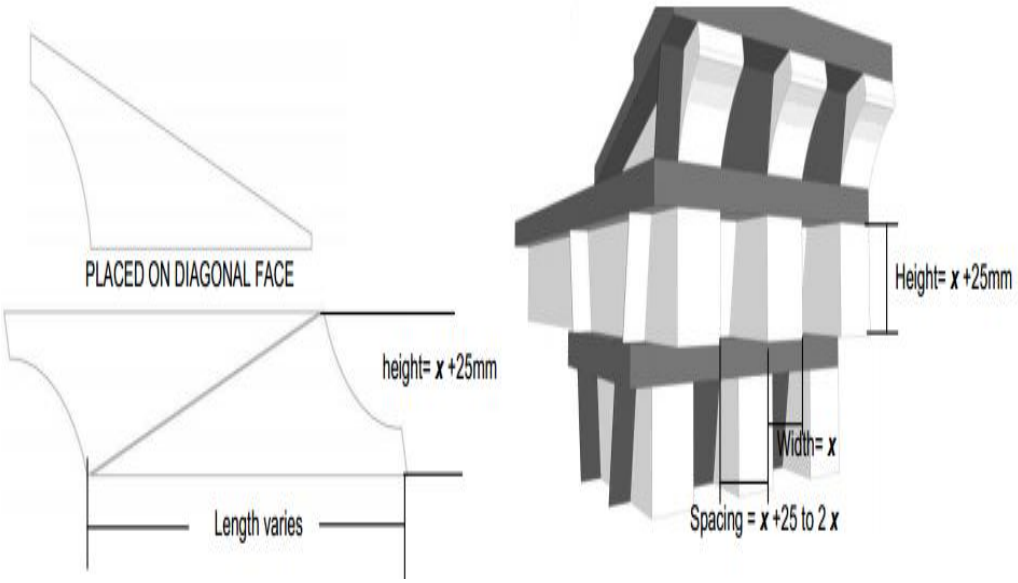

Figure 2-9 Proportion with dimensions (MoWHS, 2014)

At the moment analysis procedure do not capture the cantilever projection of cornice and different material used for the cornice. Also, until now, there is no adequate attempts are made to understand the change in behavior. The traditional cornice need

to be clearly shown in the drawings that need to be submitted to the concerned authority for formal approval.

C. Cornice in various codes

The Indian seismic code (IS1893, 2002) basically used in Bhutan for masonry in-fill RC frame structure. This code does not have adequate provisions for buildings with masonry infill walls (Jain, 2003). Jain emphasis the requirement of detailed provisions in the code for ready references for design engineers.

The cornice projection is included as nonstructural elements in various codes and deemed for analysis check. According to IS Code (IS1893, 2002) all horizontally projected member such as cornice projection and balconies requires to be check for stability. The stability check is carried out considering five times of design vertical coefficient ($10A_h/3$). A_h is the design horizontal coefficient of target spectrum.

The structural-nonstructural interaction under architectural components in FEMA 356 (FEMA356, 2000) has a requirement to include it in a mathematical model to evaluate the forces and deformations. This accounts for the response modification and amplification of floor accelerations and also to predicts the consequent damages. Cornice projection under appendages are considered to be acceleration sensitive especially for out-of-plane direction. Its response is sensitive to inertial loading. The vertical acceleration is considered as a primary concern and it has to conform to the requirements. Use of in-plane drift ratio and acceleration out-of-plane as acceptance criteria to relate the damage state and performance level of such a component. In ASCE41 (ASCE41, 2013), also further highlight the similar requirements and acceptance criteria.

The code currently takes a simplistic approach of requiring dynamic analysis for all irregular buildings. Thus, in this research work, based on necessity other codes such as ASCE41(ASCE41, 2013) ASCE7 (ASCE7, 2010) ACI318 (ACI318, 2014) and FEMA356 (FEMA356, 2000) are also referred.

2.3 Reinforced frame structure with in-filled walls

2.3.1 Behavior of in-filled frame structures

Different terminology (Crisafulli et al., 2000) is normally used depending on the construction techniques. However, “masonry in-filled frame structures " is more appropriated to specifically refer to this type of structure, whereas "in-filled frame" is used in a general sense. Many attempts (Teguh, 2017) has been made by the various researcher to investigate the performance of masonry in-filled frame structures building with in-fill panel under cyclic loading in the direction of in-plane to understand the contribution of in-fill panels for more accurate seismic assessment.

Masonry in-filled frame structure is commonly used around the world and more popular in developing countries in Asia. However, there is still lack of knowledge regarding the seismic behavior of mixed systems. The concept of earthquake resistant design for the medium-high rise building, earthquake load dominates the gravity load. Different countries codes can be broadly grouped into two categories of those that consider and do not consider the role of masonry infill walls while designing masonry in-filled frame structures. Masonry infill walls are highly popular and widely used due to following advantages.

1. Lightweight and better to work with during construction
2. Cost efficiency
3. Locally available material and labor skills
4. Good sound and heat insulations properties

Infill wall can be repositioned to the varying functional requirements of tenants without much effects on global structural performance. The brick walls are generally considered as nonstructural members. The non-linear effects of masonry in-filled frame structures and difficulty in defining material properties accurately for masonry required sophisticated computational techniques in the modeling (Crisafulli et al., 2000). Thus, inadequate knowledge concerning the composite behavior of masonry in-filled frame structures is the main reasons for considering it as non-structural component despite the effects in global responses.

Using masonry infill walls in masonry in-filled frame structures raise two main controversial assumptions as follows:

1. The infill walls are not considered as a structural element and unaccounted for the design assuming it further increase the stiffness of the masonry in-filled frame structures ultimately providing extra deformation control
2. The infill wall may impose damage to the boundary structural elements during the seismic load/lateral in-plane cyclic load. Thus, it is a danger to seismic design philosophy.

Both of the above arguments seem true for structural design when the lateral deformation demands are considered.

A. Effects of in-filled wall

The study (Teguh, 2017) shows that infill walls provide an alternative load path for transferring the load and improve the collapse resistance capacity of the masonry in-filled frame structures however it may reduce the ductility of the masonry in-filled frame structures and may change the failure modes of the frames. Therefore, the effects of infill walls in masonry in-filled frame structure can be summarized as:

1. It enhances maximum resistance (stiffness) but reduces ductility of the frame.
2. Change strains distribution of tie beam and column (confining element)
3. Change the crack development pattern and failure mode of the frame
4. It does not cause shear failure to tie-column.

The masonry (Kaushik et al., 2006) infill can be distributed in masonry in-filled frame structures in different patterns and sometimes the regular building may not remain regular after it is constructed. It is due to uncertain position or asymmetric placement of infill walls and openings in it. Thus, we need to take beneficial of infill walls and mitigate the introduction of irregularities to the building.

B. Failure modes of the in-filled wall

The understanding (Asteris et al., 2011) and crack patterns classification enhance significantly the understanding of behavior of masonry in-filled frame structures to resist earthquake load which leads to more accurate modeling, analysis, and design. The previous study of failure modes with crack patterns of in-filled wall is identified and classified.

Different modes of failure are identified due to tension and shear forces in beams and columns. If the perimeter structural elements of in-filled panel are strong enough to resist exerted loads then another mode of failure come in place that is in-fill wall itself. This leads to a compressive and tensile stresses to the diagonal strut and in the perpendicular direction respectively. The strut modeling do not represent the infill openings; however, we can include stiffness and strength reduction of the in-fill wall by reducing the area of struts.

C. Types of failure with opening

As expected, (Asteris et al., 2011) in presence of opening the diagonal compression(DC) and diagonal cracking(DK) cannot be formed. The experimental specifies that the behavior in presence of openings is considerably different than full in-filled wall without opening. The opening size and location has a substantial effect for global behavior of structures. The mechanism of failure for openings in a weak in-fill wall will be ruled by hinge of column

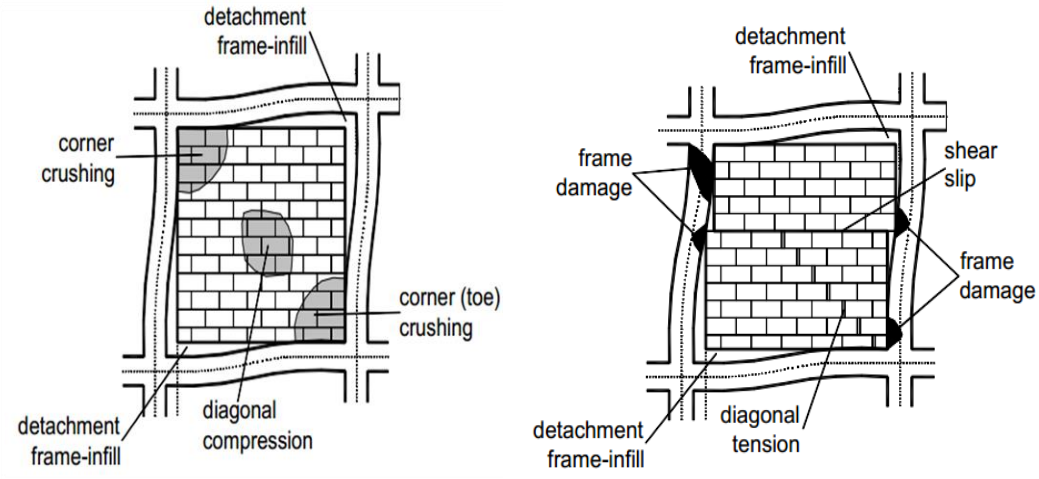

CC mode; DC mode

(b) SS mode; FF mode; DK mode

Figure 2-10 Different failure modes of infill wall (Asteris et al. 2011)

Most codes restrict the use (Kaushik et al., 2006) of demand calculated from dynamic analysis which does not differ significantly from a minimum value calculated from empirical formulae given in the code for period of the structure. This control the building design with unreasonably reduced forces which are considered to be the results

of dynamic analysis and its uncertainties. Further, it had investigated and suggested that it is crucial to identify different means of failure and detrimental effects that need to be prevented are:

1. Shear cracking of the masonry
2. Elongation of the reinforced concrete members
3. Beam-column joint failure
4. Shear failure of the columns

Cracking in the masonry panel due to shear stresses is a very common type of failure observed in masonry in-filled frame structures affected by earthquakes. The longitudinal bars of reinforced concrete members can yield in tension with significant ductility. Consequently, the columns and beams of the surrounding frame should be designed to resist the tensile axial forces resulting from seismic actions without yielding of the reinforcement.

2.3.2 Strength of masonry in-filled frame structures

The Strength of RC framed structure with and without infill panel. The investigation of structural behavior such as stiffness, strength, and ductility had been done by a number of researchers considering different parameters in recent decades. The Structural behavior of high strength reinforced concrete (H.S.R.C) frame with infill walls had been studied (Teguh, 2017). The exterior walls and interior partitions are usually considered as a non-structural element of masonry in-filled frame structure. The interaction effect between masonry in-filled frame structures and infill walls is a much-complexed issue under cyclic in-plane loading while performing the laboratory test.

The study on H.S.R.C (Essa et al., 2014) to see the behavior and ductility under the effect of cyclic loading. The 4 specimen's frames were studied for without infill and with infill walls, varying thickness of infill walls and using a different type of bricks. The study shows that the existence of a vertical gap between columns and infill walls can reduce the strength by 25% approximately. The rough interface between infill and frames can remarkably reduce the frame lateral displacement compared to the smooth interface. They performed the hydraulic jack applied a cyclic loading by a displacement-controlled mechanism.

Another researcher studied that some minimum (Essa et al., 2014) size of a specimen of both beam column frames. The load-displacement relationship for varying sizes of the beam, column and different details of beam-column connections studied. Initially particular size of beam and column with standard connections were taken as control specimen (F1). More specimens were cast for different beam size, column size and following conclusion is drawn. Keeping all same as F1 only if we increase only the depth of beam - there is a slight increase in capacity (7%). The increase the depth of column keeping other same- there is a drastic increase in capacity (118%). When aspect ratio h/L (height to length of the beam) of the frame is changed from 0.81 to 0.625 – there is a decrease in capacity (8%). The previous study (Essa et al., 2014) shows that keeping the same horizontal load corresponding to the presence of diagonal cracks in the infill walls can reduce the strength by 45% approximately.

A. Lateral load sharing for in-fill panel

The lateral earthquake forces are resisted by frame and in-filled panel in different proportions. Brick masonry panels are considered to be highly stiff initially, resist most of the forces exerted by lateral loading however it may lead to sudden failure prematurely due to its brittle behavior. In this case, confining frames must have adequate backup strength in order to avoid the collapse. The load sharing between infill panels and frames (Kaushik et al., 2006) using different countries codes.

Table 2.2 Lateral load sharing between infill and frame

Codes	**Vertical (%)**		**Lateral (%)**	
	Frame	Infill	Frame	Infill
Euro Code 8	100	0	50-65	35-50
Columbian: NSR-98 Egyptian-1988 Ethiopian: ESCP-183	100	0	0	100 (structurally connected)
Algerian code-1988	80	20	0	100
Recommended (IS1893-2002)	100	0	25	75

B. Ductility of masonry in-filled frame structures

The ductility of masonry in-filled frame structures depends on a number of factors such as material properties of in-fill wall, relative strength of confining member and in-fill walls, ductile details of confining member, definition of plastic hinges, rebar in in-fill walls and elevation of the building, in-fill wall distribution (horizontally and vertically) among others.

The material strength of in-fill wall can be increased if the opening size of panel is too large. The minimum (Essa et al., 2014) shows that ductility factor of the frame with infill wall is much less than that without infill wall. And also, ductility factor changes with the thickness and type of material used for the infill walls. When the thickness increases the ductility, factor gets reduced and varies with different material properties of infill walls.

Both the results through pseudo-dynamic tests as well the numerical models confirmed that the presences of non-structural masonry infill walls can significantly modify the global seismic behavior of masonry in-filled frame structures (Negro et al., 1997). This is due to irregular distributions of infills which will lead to unreasonably huge ductility demands. The negative effect may not be compensated by positive effect that is develop due to increase in energy dissipation, stiffness and strengths. Safe seismic resilient design practice should not neglect the effect of the non-structural brick masonry in-fills through simplified mathematic model analysis.

2.3.3 Stiffness of masonry in-filled frame structures

Experimentally shown that masonry infill walls is consider to resist much of initial stiffness but has low deformability (Moghaddam et al., 1987). The same was confirmed by another (Kaushik et al., 2006) researcher infill walls are remarkable in increasing the initial stiffness of reinforced concrete (RC) frames, and being the stiffer component, attract most of the lateral seismic shear forces on buildings, thereby reducing the demand on the masonry in-filled frame structures members. Accordingly, many codes mentioned that masonry in-fill walls supposed to carry any its self-weight only not additional gravity load. The contribution to resist the lateral loads by in-fill wall is substantial. In practice for safety measure RC frame with in-fill panel are design for low earthquake forces. The frame independently should be required to resist at least 25% of the seismic forces in addition to self-weight and gravity loads.

The frame with regular distribution of infill in the plan as well as along height is stiffer than irregular one. The opening will also reduce the stiffness of masonry in-filled frames. Thus the introduction of masonry infill in masonry in-filled frame structures changes the lateral-load transfer mechanism of the structure from predominant frame action to predominant truss action (Murty et al.), which is responsible for the reduction in bending moments and increase in axial forces in the frame member.

Masonry infills in masonry in-filled frame structures cause several undesirable effects under seismic loading besides beneficial effects such as it contributes significantly to lateral stiffness, strength, overall ductility and energy dissipation capacity such as:

1. Short-column effect,
2. Soft-story effect,
3. Torsion,
4. Out-of-plane collapse.

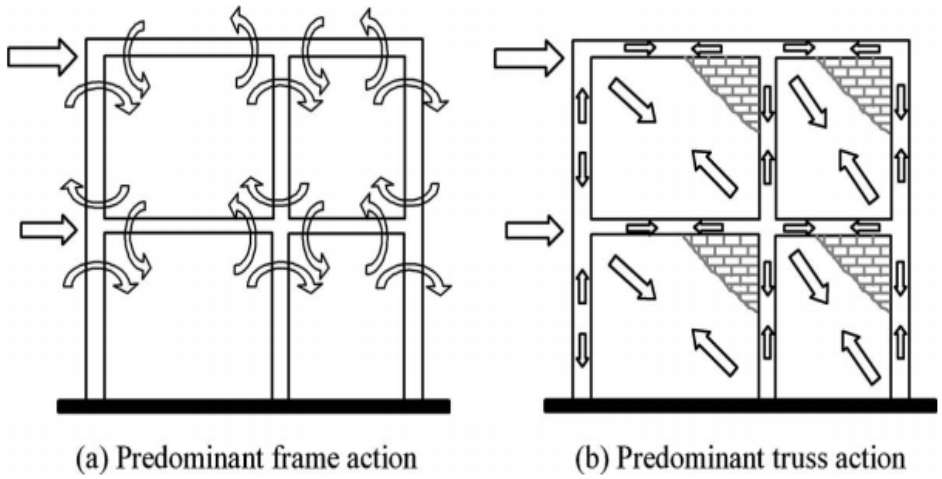

Figure 2-11 Infill truss action-transfer (Murty & Jain, 2000)

By increasing thickness of infill wall increases the stiffness of frame by a substantial value. The initial stiffness of frame with infill wall from holes red bricks is approximately 71% greater than frames with infill wall from cement bricks.

2.3.4 Modeling techniques of masonry in-filled frame structures

Basically, modeling of in-filled frame is done in two different techniques as mentioned below:

1. Micro-Model: It is also called local models. It can simulate the behavior of structure with great detail using constitutive models. The finite element models typically perform this kind of analysis. This technique more intensive computation and it is quite difficult to apply in big building model. It is time-consuming and costly.

2. Macro- Model: It is called simplified form of complex models however it representation the behavior of structure quite accurately but not exact. The computational simplicity and drastically less time consumptions than micro modelling. The compression struts representing in-fill wall is typical example of this kind. The (Smyrou et al., 2011) in-fill modeling with multiple struts can even accounts for local effects of wall panel without much complexity in the analysis.

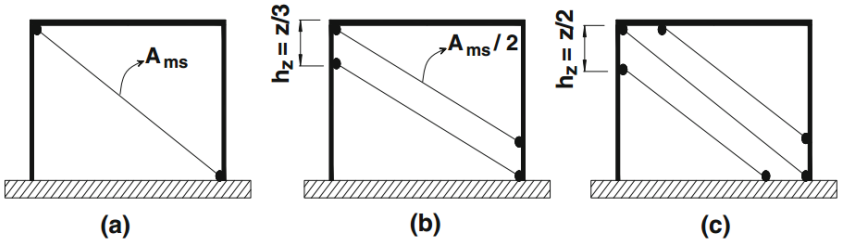

Figure 2-12 Various strut models (a)Single-strut (b)Double-strut (c) Triple-strut (Smyrou, Blandon et al. 2011)

The simplified single-strut model may somewhat a compromise and triple-strut models are more elaborative modalities. The double strut can provide good insight of interaction effects of the in-fill wall. It is assumed that the diagonal struts are active when compressive forces develop in them. This simplified (Asteris et al., 2011) results in significant changes in the internal forces in the surrounding frame especially the axial forces in the columns (tensile forces decreases, whereas compressive forces increases). The compression strut is only considered important considering the bond strength at the panel-frame interfaces and the tensile strength of the masonry are very low. In most refined model tensile behavior is considered but it does not affect significantly the results. So, in this paper, the author would be using double-strut modeling approach.

The (Crisafulli et al., 2007) comparisons between experimental data obtained by the authors and other researchers and analytical results indicate that the cyclic response of in-filled frames can be properly represented by the double strut model.

A. Energy dissipations of masonry in-filled frame structures

The consideration (Essa et al., 2014) and understanding of the energy dissipation are a very crucial component to study the behavior of masonry in-filled frame structures subjected to earthquake loads. In this context ductility behavior is preferable than the rigidity of frame structure as it implies the ability of a structure to withstand large deformation without failure. The area enclosed by the hysteresis loops of the lateral load-displacement relationship gives the total energy dissipation per cycle.

The seismic damage in the building can be controlled by using the dampers in structural components such a device with high damping capacity which drastically reduces the seismic energy entering the building. There are few commonly used seismic dampers which absorb the jerks and reduced the motion of building viscous**,** friction, yielding, and viscoelastic dampers among others**.**

B. In-filled wall and irregularities of structure

The asymmetric placement (Kaushik et al., 2006) of masonry infill walls, the plan irregularities are introduced into buildings and this leads to increase the shear force demand in the frame members, especially columns. In case of server plan irregularities due to the huge uneven positioning of masonry infill walls, 3D-analysis is required in view of stiffness distribution related to the undefined position of masonry in-fill panels. Also, the sensitivity analysis is required for masonry infills wall considering properties and position by disregarding one panel out of 3 or 4 panels on the more flexible side. However, some codes considered accidental eccentricity that may occur due to the probable relocation of infill walls or alteration in the usage of the building during the service life.

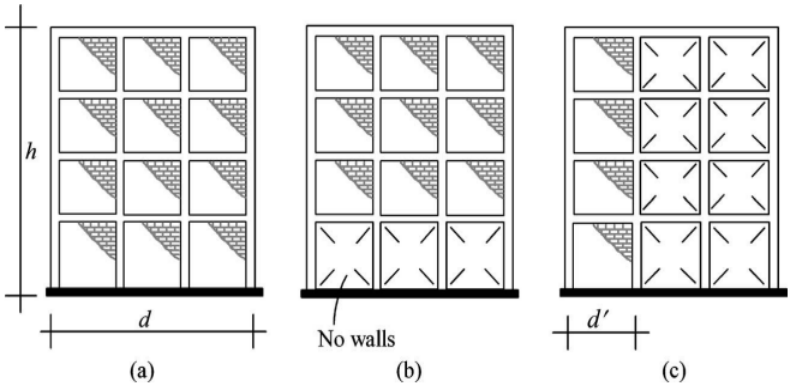

Figure 2-13 Masonry infill walls(a) regular (b) vertical irregular (c) Plan irregular (Kaushik et al., 2006)

The vertical irregularities occur into masonry infill walls masonry in-filled frame structures due to sudden reduction of masonry in-fill panels in particular story compared to stories above and below. The presences of parking space first story (soft story) creates vertical irregularities which introduce irregularities in terms mass, stiffness and strength along the height of structures making horizontal and vertical structural member of those stories susceptible to damage.

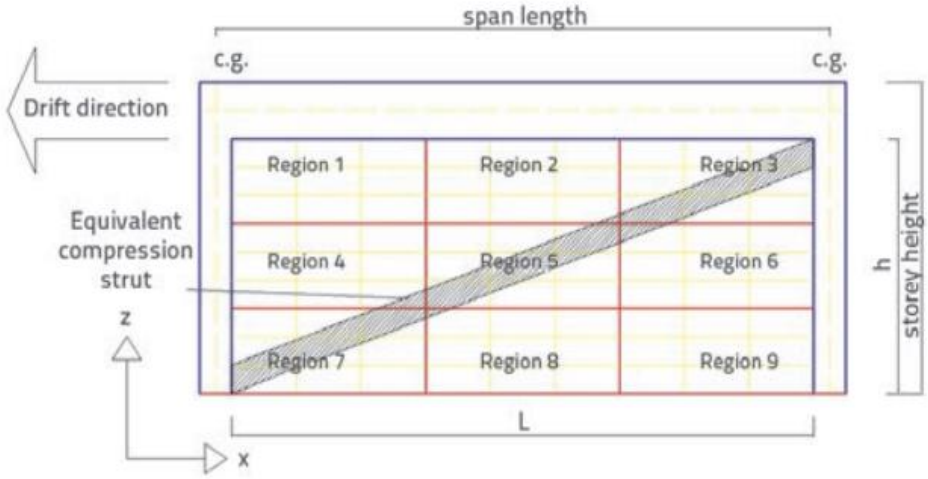

Figure 2-14 Diagonal strut and effects of infill in 9 regions (Asteris et al., 2016)

This study opening in the in-fill wall reduces the strength and stiffness of RC frame. Further, the reduction factor depends on location and dimension of in-fill panel of brick masonry. The opening at joint region of beam and column gets tremendously

affects the resistance. This is visible in Figure 2-15 which represents stress distribution in finite element software.

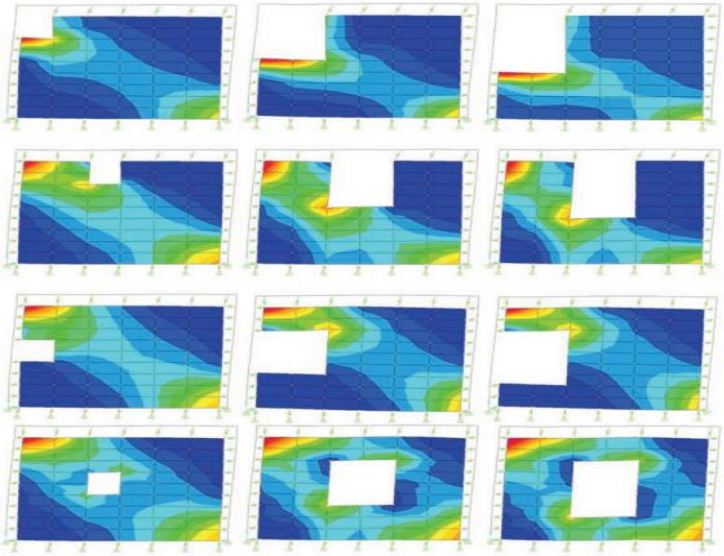

Figure 2-15 Stress distribution for in-fill wall (Asteris et al., 2016)

The opening considerably modifies the structural response of the building (Thinley et al.). Most codes do not mention the effects of opening and its relations to strength and stiffness for RC frame structures with in-filled walls. The prediction of structural response of in-filled frame is quite complex due to followings:

1. The different size of openings
2. The different position of openings

According to the Nepal code (NBC201, 1994) in-fill panel opening more than 10% of gross in-fill panel area is not considered for resisting earthquake lateral loading.

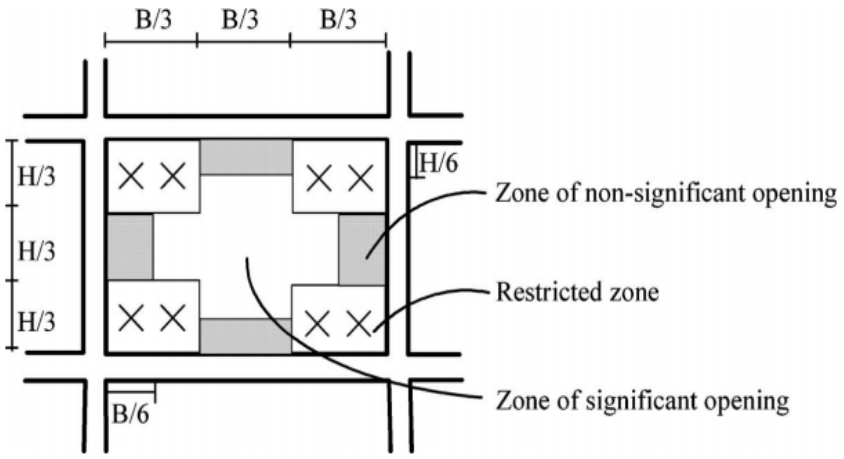

Figure 2-16 Possible location of openings
(NBC201, 1994)

The opening shall be outside restricted zone as shown in Figure 2-16, if the opening is located in the center of the panel then tie bands with longitudinal reinforcement need to be used at the perimeter of the panel opening. When opening size increases shear force decrease in confining elements and flexibility of wall increases reducing the mass. Also, according to the Euro code 8 (EC8, 2004) tie bands or structural elements across at top and bottom of opening similar to NBC201.

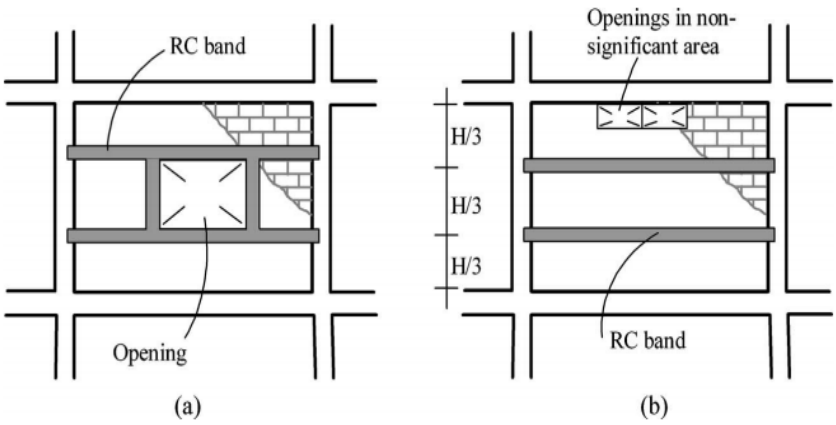

Figure 2-17 Openings , tie bands for in-fill walls (NBC201, 1994)

As an expedite recommendation, (Smyrou et al., 2011) effect in stiffness and strength of in-fill panel due to presence of opening can be accounted pragmatically by reducing the strut area value, the reduction is in proportion to the percentage of opening size of the walls. For the opening of 15 to 30 percentage of the total area of wall good estimation is derived by reducing the strut area value that varies 30 to 50 percentage.

Thus, a number of prominent studies by researchers propose the reduction factor to reduce the stiffness and strength of in-filled wall and are used as described above in terms of strut area to account for the reduction of strength and stiffness, since it was very well validated with the experimental results.

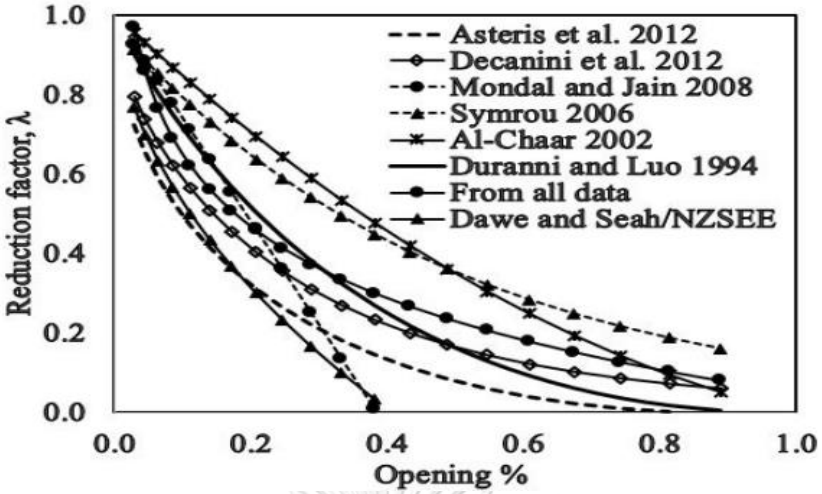

Figure 2-18 Comparison of reduction factors proposed by various studies (Thinley et al., 2015)

A. Fundamental natural period

The fundamental period is one of most critical parameters for the assessment as well as for seismic design of structures. Natural periods of vibration (Kaushik et al., 2006) of buildings mainly depend on two parameters; mass and lateral stiffness. Considering the masonry walls in the buildings increases both the parameters. Thus, the seismic design forces for infill walls frames is drastically more than bare frames. However, various codes recommend empirical formulae to calculate fundamental period of bare frames, however very few specify the formulae for RC frame with masonry in-fill walls.

The researcher (Asteris et al., 2016) more specifically investigated the parameters and he also concluded similar findings that the height of a structure significantly influences its fundamental period. The number of spans does not have a significant effect on the period. For in-filled frames with higher the masonry stiffness with the same opening, the lower the fundamental period. The increase in the opening does not affect the fundamental period of the structure.

In reality, empirical natural period vibration (Kaushik et al., 2006) considered to be more reliable than natural period computed by structural dynamics, which includes many uncertainties from non-structural components and masonry in-fill walls, modulus of elasticity for all materials used, area and inertia of moments of members

taking part. These uncertainties lead to the larger natural periods which results in lower design forces. Therefore, most codes have put an upper limit on period values obtained by Rayleigh method to prevent against very small seismic forces.

2.4 Earthquake ground motions

2.4.1 Horizontal components

The concurrent seismic effects are considered in the analysis by establishing orthogonality of X and Y axes. For the linear and non-linear static 100% and 30% combinations to each direction are used. However, in pushover analysis, an additional technique is permitted that may be simpler to implement, in this technique amounts to pushing to 100% of the target displacement applied separately along each frame axis. For non-orthogonal frames, additional pushover cases would be applied with the load vector aligned along the direction of each frame. For non-linear dynamic procedure more than 5km from an active fault 100% and 30% combination are used in each direction however near fault site less than 5km, if the fault-normal to fault-parallel ratio is close to unity, then it may be simpler to calculate everything conservatively using the larger fault-normal spectrum (ASCE41-13).

When random earthquake accelerations are applied to structure it can vibrate the structure in three mutual direction simultaneously. The largest direction of vibration is usually horizontal. Vertical accelerations induced vertical inertia forces that are to be considered in design unless calculated values are not substantial. Ground motion at any point or location consist of six components, 3 translations which are orthogonal to each other and rotations about these 3 axes.

Normally, we consider only translational components as only these components are recorded during earthquakes. The factors that affect characteristics of ground motion at a location are:

1. Source (magnitude, fault mechanism)
2. Path (distance from the epicenter, geology, direction)
3. The site (soil condition at the location considered)

2.4.2 Vertical components

The maximum considered earthquake of vertical response spectrum is bascially considered as 2/3 of horizontal component amplitude (ASCE7-16). The use of the 2/3 spectral ratio may leads to an under or overestimation of expected vertical components. Designing of most building in practice does not include the vertical accelerations however it is indirectly included in terms of modification of dead/permanent load factors. The vertical component consists of greater proportion of high frequency (short-period) spectral content than horizontal component of same set of ground motions. This difference will change with the soil condition of the site, for high stiffness of soil the differences increases.

The previous studies and codes (Bane, 2006) and IS 1893:2002 mentioned the usage same 2/3 ratio for vertical accelerations. However, Bane suggest that 2/3 ratio is conservative and this usage has been justified in terms of greater variations than the median and uncertainties of ground motion in the vertical direction.

Recently, it is the focus of attention looking at the damage patterns that is mainly caused by severe vertical vibrations. Majority of structures and their foundations has a deficiency of resisting vertical earthquake-induced vibrations. The study recommended for vertical seismic analysis and design at varying damping ratios to safeguard future infrastructure establishment from severe damage. The vertical spectra are representative of the available worldwide earthquake data bank today and are therefore suitable for use in modern design practice.

The vertical component of earthquake acceleration should be considered for large span structures and stability is a criterion in design analysis. Gravity load reduction due to excitation of vertical acceleration of earthquakes develops detrimental effect in case of cantilevered members. Thus, it effects structure such as pre-stressed horizontal members or cantilevered beams, girders and slabs.

In the IS1893 (IS1893, 2002) has three performance level of the structure as mentioned below:

1. Basis Earthquake (DBE) frequently occurring but without damage.

2. DBE without substantial structural damage though non-structural member may suffer damage to some extent.

3. Maximum considered earthquake (MCE) rarely occur and get damages but structure should not be collapse.

During the earthquake actual forces may be much more than design one however structural element can withstand all that large forces in the form of ductility that develops from inelastic behavior of material, extra rebar provided by designer in detailing pattern and from reserved over-strength which compensate the differences.

CHAPTER 3
THEORETICAL BACKGROUND

3.1. Analysis methods

Selection of appropriate procedure is important structural analysis. Higher modes effects are not important for static analysis. The nonlinear dynamic analysis capture explicitly nonlinearity (inelastic) of material in the form of hinges and also geometric nonlinearity is included as P-Delta in the modeling.

3.1.1 Static analysis

A. Linear static analysis

The free vibration analysis of the whole model is carried out by means of established methods using correct masses and its stiffness and get natural period as well as modes shapes for its mode of vibrations. The building can be analyzed for the design forces considered as static forces.

3.1.2 Dynamic analysis

The earthquakes cause immeasurable damage structures and it is important to understand the response of inelastic systems. The applications of the theory of structural dynamics can be used to analyze the responses caused by an earthquake. The dynamic analysis performed by Response History or Response Spectrum Method. In both the methods design base shear (V_B) and base shear (V_{Bcal}) calculated using a period (T_a) as per Indian seismic code (IS1893, 2002).

Approximate period (T_a) of the structure can be calculated as:

$$T_a = 0.075h^{0.75} \quad (3\text{-}1)$$

where h is height of structure in the meter. If $V_B < V_{Bcal}$, all the response demands should be multiplied by the ratio of V_{Bcal}/V_B which is called scaling factor.

A. Nonlinear dynamic analysis (NDA)

The Non-linear Response History Analysis (NLRHA) is the popular NDA which provide a more accurate demands quantities on each component of structures

when the structure is loaded meaningfully beyond their elastic-range of behavior than do linear procedures (FEMA274-1997). The usage of the solution requires a set of ground motions records that account for the uncertainties and differences in severity, frequency characteristics, and duration due to rupture characteristics and distances of the various faults that may cause motions at the site. It is a refined approach to investigating the inelastic demands of the structure by a specific set of ground acceleration histories.

NLRHA is performed based on an appropriate ground motion and following accepted principles of dynamics. This method involves integration for a time-step by step of dynamic equilibrium equation and it is term as time stepping method. An analytical solution is usually not possible when excitation varies arbitrarily with time and when the system is nonlinear. Such problems can be solved by numerical time-stepping methods for integration of differential equations fulfilling the requirements of convergence, stability, and accuracy.

The direct-integration time-history analysis Hilber-Hughes-Taylor alpha (*HHT*) method is used by ETABS 2015 where single alpha parameters are used with the value range 0 to -1/3. For alpha = 0, the method is equivalent to the Newmark method with gamma = 0.5 and beta = 0.25 and called the trapezoidal rule and offers the highest accuracy of the available methods. The Newmark equations are as given in Equations 3-2 and 3-3.

$$u_{i+1} = u_i + \left[\ 1-\gamma\ \right]\ddot{u}_i + \ \gamma\Delta t\ \ddot{u}_{i+1} \tag{3-2}$$

$$u_{i+1} = u_i + (\Delta t)\dot{u}_i + \left[\ 0.5-\beta\ \ \Delta t^{\ 2}\right]\ddot{u}_i + \left[\beta\ \Delta t^{\ 2}\right]\ddot{u}_{i+1} \tag{3-3}$$

The values of β as well as γ are define as the acceleration variation over a time step to determine accuracy and stability characteristics of the method. Where the values of γ is 0.5 and β range from 1/6 to 1/4. HHT accounts for energy dissipation and 2nd order accuracy which is not accounted in Newmark Method.

The relationship between lateral forces, $f_s(u,\dot{u})$ and lateral displacement, u depends on the history of displacements, thus equation 3-3 is slightly get modified. The acceleration $\ddot{u}_g(t)$, the deformation $u(t)$ of a single degree of freedom system be highly depends on natural (vibration) period of the system and damping ratio. For constant

given damping ratio, the only change in natural period is responsible for difference in deformations. Similarly, keeping the natural periods constant and change in damping will also make a big difference in the deformations. The governing equations of an inelastic system to the given ground motion is as follows:

$$m\ddot{u} + c\dot{u} + f_s(u,\dot{u}) = p_{eff}(t) \tag{3-4}$$

$$p_{eff}(t) = -m\iota\ddot{u}_g(t) \tag{3-5}$$

where ι is influence vector, each element equals to one, m, c, k is same as stated in equation Once the deformation response history $u(t)$ has been evaluated by dynamic analysis of the structure, the internal forces can be determined by static analysis of the structure at each time instant. The preferred approach in earthquake engineering is based on the concept of the equivalent static force (f_s).

$$f_s(t) = ku(t) \tag{3-6}$$

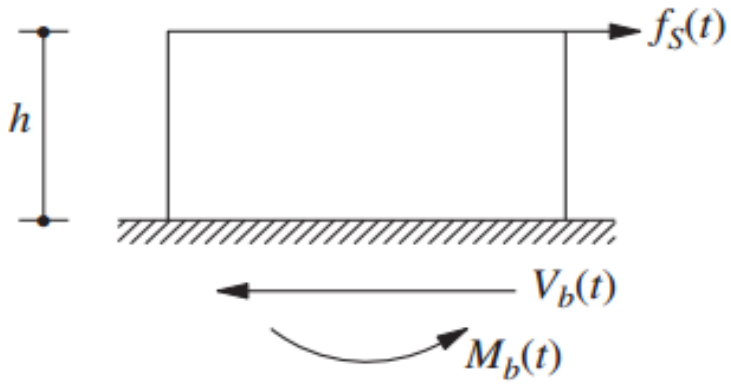

Figure 3-1 Equivalent static force (Chopra, 2012)

$$f_s(t) = m\omega_n^2 u(t) = mA(t) \tag{3-7}$$

where,

$$A(t) = \omega_n^2 u(t) \tag{3-8}$$

The equivalent force (static) is product of m and *A(t)*, the pseudo-acceleration and is directly calculated from deformation response *u(t)*. The static analysis is performed at each instant whenever response is desired. Damping matrix cannot be computed from the dimensions of structural elements of the model thus it should be

constructed from modal damping ratios. To construct the diagonal classical damping matrix [C] from Rayleigh damping matrix as follows:

$$C = a\ M + b\ K \tag{3-9}$$

where C, M, and K are already defined above, in general, 5% damping ratio is used for reinforced concrete structures (Chopra, 2012) and damping ratio for in-filled framed structure is not clear.

where,

$$a = \xi_i \frac{2\omega_i\omega_j}{\omega_i + \omega_j} \qquad b = \xi_j \frac{2}{\omega_i + \omega_j} \tag{3-10}$$

The coefficient a and b mass proportional damping coefficient and stiffens proportional coefficient which depends on the modal damping ratios selected for two modes. If we want the damping ratios of mode i and j to be ζ_i and ζ_j, and the modal frequencies are ω_i and ω_j.

3.1.3 Design acceleration spectrum

Response acceleration spectrum is main concept to seismic engineering in order to determine maximum response of structure directly from response spectrum. The site-specific response spectrum is used as target design spectrum. It provides sufficiently good estimate of peak response applicable to design of structures.

Design horizontal seismic coefficient is given by Equation (3-11):

$$A_h = \frac{ZIS}{2Rg} \tag{3-11}$$

where, Z-zone factor for maximum considered earthquake (MCE), I-importance factor, depending on the functional use of structure-response reduction factor depending on the perceived seismic damage performance of the structure characterized by ductile or brittle deformations. Sa/g is average response acceleration coefficient of rock or soil sites base on natural periods and damping of the structure.

$$m\ddot{u}(t) + c\dot{u}(t) + ku(t) = -m\ddot{u}_g(t) \tag{3-12}$$

$$\ddot{u}(t) + 2\xi\omega_n\dot{u}(t) + \omega_n^2 u(t) = -\ddot{u}_g(t) \tag{3-13}$$

we get from (3-12) by dividing both sides by m and replacing c/m and k/m by $2\xi\omega_n$ and ω_n^2 respectively. Where m, c, k, ω_n, ξ and T_n are mass, damping, lateral

stiffness, natural frequency, natural period respectively for the single degree of freedom system (SDoF). The response spectrum can be obtained repeatedly by solving the Equation (3-13) with varying natural period (t) and obtained the following responses of SDoF by plotting their peak values versus natural period:

Deformation response

The peak value of deformation, $D = \max_t |u(t)|$ (3-14)

Pseudo- velocity response

The peak value of Pseudo-velocity, $V = \omega_n D = \frac{2\pi}{T_n}$ (3-15)

Pseudo-acceleration response

The peak value of Pseudo- acceleration, $A = \omega_n^2 D = \left(\frac{2\pi}{T_n}\right)^2 D$ (3-16)

The earthquake excitation is represented in the form of smooth design spectrum and in reality, it is obtained by combining many different ground motions of the different earthquake in that specific region as one is shown in Figure 3-2 from IS1893-2002 based on 5% damping. The medium soil type more frequently used in design based on the site condition, thus medium soil type is used in this research.

For any structure, the fundamental period is less than 0.1sec the value of A_h will not be taken less than Z/2 whatsoever the value of I/R. For the different percentage of damping ratio, we use the multiplying factors for obtaining values for the response spectra curves which represent free-field ground motion:

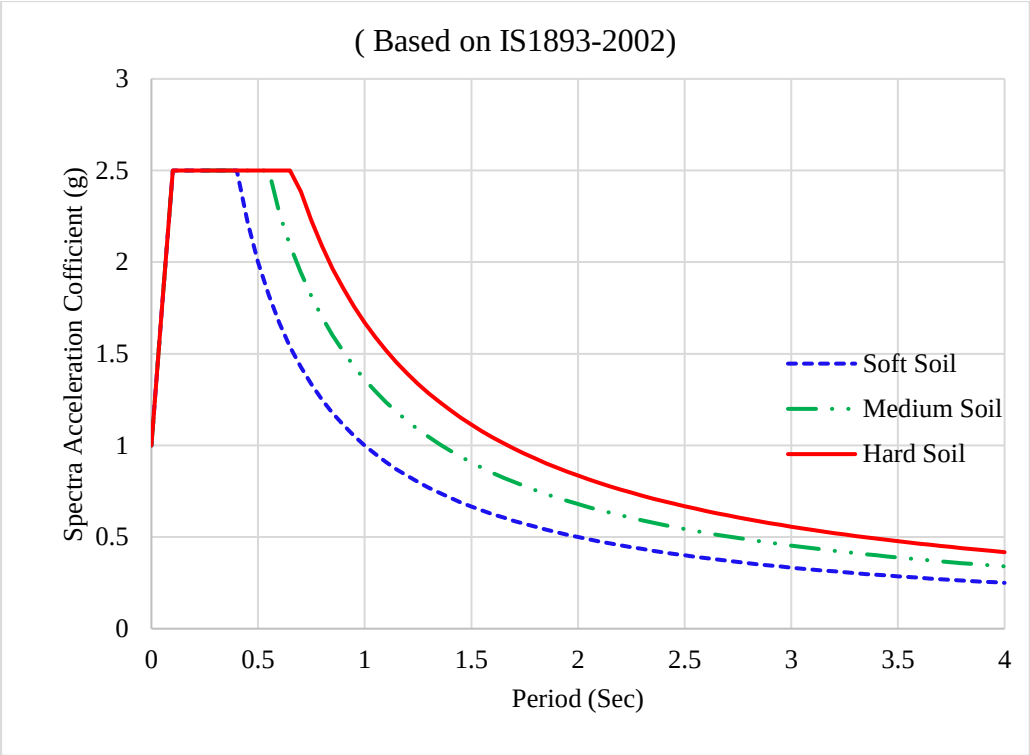

Figure 3-2 Response for different type of soil at 5% damping (IS1893, 2002)

3.2 Modal analysis

3.2.1 Equation of motions

The procedures to formulate the equations of motions for multi-degree of freedom (MDF) system subjected to dynamic forces have coupled equations of motions and simultaneous solutions are not feasible, thus modal analysis procedure developed.

The equations (Chopra, 2012) are changed to modal coordinates which uncoupled the set, each equation is then solved and determine the modal contribution of response. The general equation of motion for MDF system is given by

$$m\ddot{u} + c\dot{u} + ku = p(t) \tag{3-17}$$

Transforming the equation of motions by expanding the displacement vector u of MDF system.

$$u(t) = \sum_{r=1}^{N} \phi_r q_r(t) = \Phi q(t) \tag{3-18}$$

$$\phi_n^T m \phi_n \ddot{q}_n(t) + \phi_n^T c \phi_n \dot{q}_n(t) + \phi_n^T k \phi_n q_n(t) = \phi_n^T p(t) \tag{3-19}$$

From Equation 3-19 reducing the generalized terms of mass, damping, lateral stiffness and force by normalizing and using the orthogonal properties of modes we get,

$$M\ddot{q} + C\dot{q} + Kq = P(t) \tag{3-20}$$

To uncoupled the modal equation of the MDF system with classical damping is given by:

$$p_{eff}(t) = -m\iota\ddot{u}_g(t) \tag{3-21}$$

Expand the spatial distribution of the effective earthquake force $m\iota$ as a summation of modal inertia force distribution s_n.

$$m\iota = \sum_{n=1}^{N} s_n = \sum_{n=1}^{N} \Gamma_n m\phi_n \tag{3-22}$$

where,

$$\Gamma_n = \frac{L_n}{M_n} \; L_n = \phi_n^T m\iota \; M_n = \phi_n^T m\phi_n \tag{3-23}$$

The contribution to nth mode to excitation vector $m\iota$ is

$$s_n = \Gamma_n m\phi_n \tag{3-24}$$

The governing equation of the modal coordinate q_n:

$$\ddot{q}_n + 2\zeta_n\omega_n\dot{q}_n + \omega_n^2 q_n = -\Gamma_n\ddot{u}_g(t) \tag{3-25}$$

The displacement due to the nth mode is computed as

$$u(t) = \phi_n q_n(t) = \Gamma_n\phi_n D_n(t) \quad q_n(t) = \Gamma_n D_n(t) \tag{3-26}$$

3.2.2 Modal combination

The peak response quantities of a structure such as member forces, displacements, story forces, story shears and base reactions are commonly combined as Complete Quadratic Combination (CQC) method and the square root of the sum of square (SRSS) method as formulated below equations:

CQC Method (for closely spaced modes):

$$\lambda = \sqrt{\sum_{i=1}^{r}\sum_{j=1}^{r} \lambda_i \rho_{ij} \lambda_j} \tag{3-27}$$

$$\rho_{ij} = \frac{8\zeta(1+\beta)\beta^{1.5}}{(1+\beta^2)^2 + 4\zeta^2\beta(1+\beta)^2} \tag{3-28}$$

$$\beta = \frac{\omega_j}{\omega_i} \tag{3-29}$$

where, r, $\rho_{ij}, \lambda_i, \lambda_j$ are a mode number considered, coefficient of cross-modal, responses mode i and j respectively. $\zeta, \beta, \omega_j, \omega_i$ are modal damping ratio, frequency ratio, circular frequency in ith mode, and circular frequency in jth mode respectively.

SRSS Method (not closely spaced modes):

$$\lambda = \sqrt{\sum_{k=1}^{r} \lambda_k^2} \tag{3-30}$$

where r is the absolute value of the quantity in mode k and number of modes being considered respectively.

3.2.3 P- Δ effects

P-Δ effects are included in linear and nonlinear analysis procedures. In the static P-Δ effects is basically caused by gravity loads on deformed configuration of structural member consequently which leads to increase in lateral displacements.

The dynamic P-Δ effects are due to the negative post-yield stiffness that increases story drift and the target displacement. To capture the P-Δ effects NLRHA is suitable. The parameter that affects the P-Δ effects are mainly by ratio of post yield stiffness to elastic stiffness, natural period, ratio of strengths, story load-deformation (hysteretic) and earthquake duration and types of frequencies.

CHAPTER 4
METHODOLOGY AND NUMERICAL MODELS

4.1 Approach

The seismic performance in terms of global response such as natural period, lateral displacement and inter-story drift and local response such as internal forces and vertical deflections of projected elements of structures with RC cornice projections are

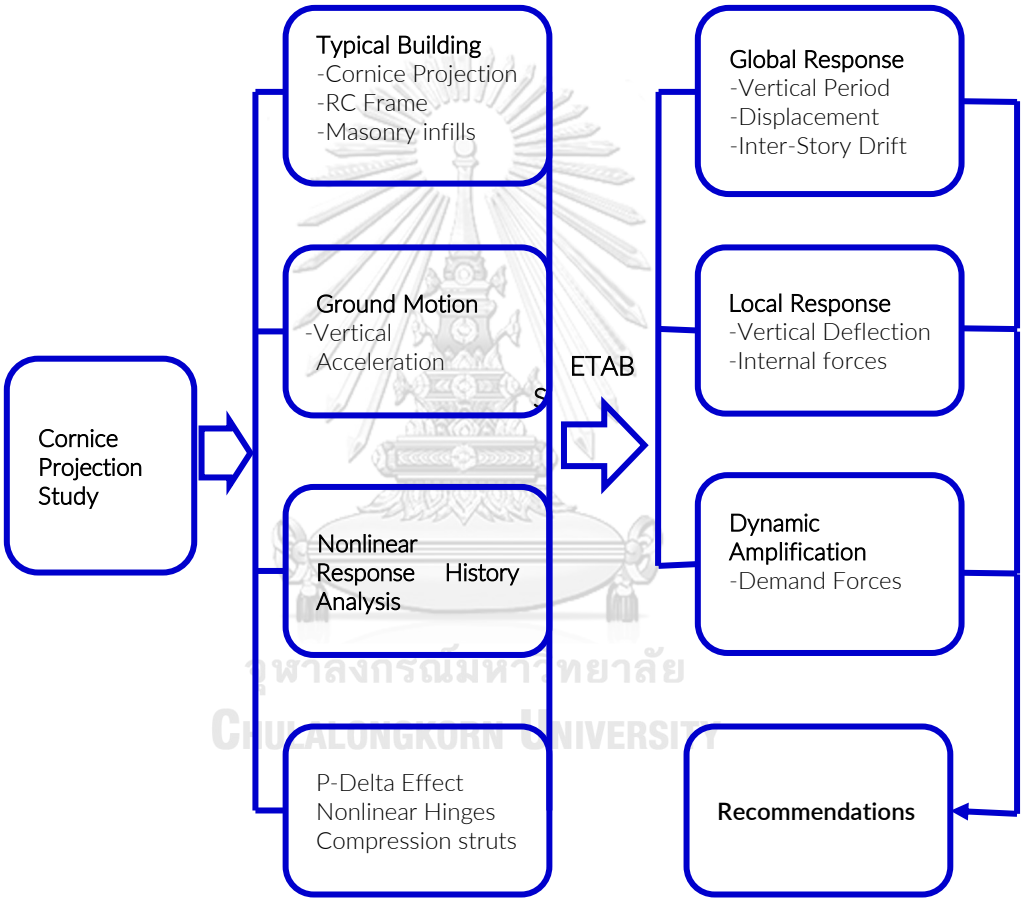

Figure 4-1 Flow chart for structured approach of methodology

investigated. Figure 4.1 clearly shows the approach including each step to study the building model and capture the response that can achieve the objective of research as expected. To study the effects of cornice projection, preparation of models with typical building layout, relevant input ground accelerations including P-Delta, nonlinear hinges and diagonal compression struts is done. After that NLRHA is performed for all eight different models. The responses in terms of global and local as well as dynamic

amplification factor are calculated from the NLRHA and compared with acceptance criteria of the ASCE41, ACI318 and section capacity.

4.2 Analysis procedures

4.2.1 Analysis considerations

The analysis by equivalent lateral force method (ELF) based on the IS1893 code is carried out. Simple way to capture inelastic dynamic responses is using equivalent lateral force (ELF) method. It is helpful for preliminary checking of model.

ELF is normally use of real design of many structures. However, application of the ELF is limited to the structures without substantial discontinuities in terms of mass and stiffness throughout the height. In this ELF method, base shear and vertical force distribution of structure are determined by Equation 4-1 and 4-2 respectively.

$$V_B = A_h W \tag{4-1}$$

$$Q_i = V_B \frac{W_i h_i}{\sum_{j=1}^{n} W_j h_j} \tag{4-2}$$

where, A_h is horizontal acceleration spectrum (design) using the fundamental natural period (T), W is seismic weight and h_i is story height.

4.2.2 Nonlinear response history analysis (NLRHA)

Figure 4-2 represent relationships of lateral force and deformation for a typical moment frame (ASCE7-16). Initial yield is represented by a first plastic hinge formed on nonlinear curve. Firstly, over-strength is a direct result of material strengths in excess to nominal material strengths specified in the design, such and concrete and steel stronger than the strength determined after applying reduction factor reducing the probability of failure to the design loading. Normally ϕ is not included while evaluating response of structure by NLRHA. Thirdly, additional strength comes from providing reinforcements and choice of sections that exceed computations requirements.

The interaction of applied gravity load to over-strength of elements and lateral force produce successive plastic hinges. The maximum strength point form along the curve substantially higher than that at first significant yield and the margin is referred

to as the system over-strength capacity. The ratio of these strengths is denoted as Ω. The difference between actual elastic demand and one considering the limit to the period (C_uT_a) with 100% participation of mass in first mode. Inter-story drift is affected by this variation.

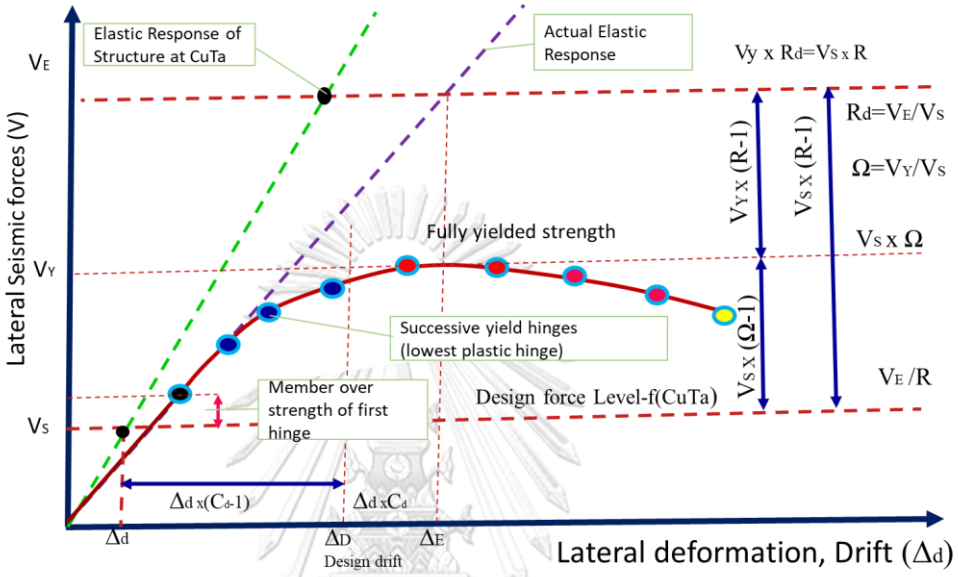

Figure 4-2 Inelastic force-deformation curve (ASCE7-16)

Response modification; the deflection amplification and the over strength factors are also shown in Figure 4-2. The yielded strength (V_y) and elastic seismic force demand (V_E), Seismic force demand (Vs) and lateral deformations (Δ) are also presented in the diagram.

4.3 Numerical Modeling

Models consist of mainly three interacting sub-system such as structural framing (beams, columns, diaphragms and masonry walls), the foundations (footings) and supporting soils. The foundation is provided with fixed supports and supporting soil characteristics is not considered due to lack of data for the actual site. The complex interaction of earthquake acceleration and model produces the responses. From this response we understand the behavior of excited structure. The ground accelerations depend on site characteristics and the effects are considered independent of main building model as soil-structure interaction (SSI) considering the soil site is medium or hard soil. Normally, in the conventional design methods SSI effects are neglected in

case of light structures (low rise buildings) in the stiffer soil, however, SSI becomes prominent for heavy structures resting on soft soils (high rise buildings). The SSI usually results in a reduction of base shear because of flexibility of the foundation to soil. This is the reason that most structural designer neglect SSI. The pin support may be used which restrained horizontally and vertically but when column extends to through basement, it may be restrained to rotations so it is more preferable and consistent to provide fixed support.

4.3.1 Effective seismic weight

The effective seismic weight (W) consists of dead load (DL) plus suitable amounts of the imposed loads which contribute to inertial forces such storage loads, permanent equipment and others that are tied to the structural element. The structure accelerates laterally due to earthquake force and these accelerations of the structural mass produce inertia forces. These inertial forces, accumulated over the height of the structure, produce the total force of applied lateral acceleration term as seismic base shear (V_b). Thus, base shear is an important parameter to see the responses due to lateral loading. In this study models, the effective seismic weight consists of seismic weight (W) consist of summation of dead load (DL) and masonry load (ML). The seismic mass (M) consist of the seismic weight divided by acceleration due to gravity (M=W/g), where g is acceleration due to gravity.

4.3.2 Structural parameters and modeling

The suitable mathematical model is developed for typical school building of a structure is carried out to capture the story drifts and forces in the structural members especially projected components. The most (ASCE41, 2013) realistic analytical model of 3D includes stiffness from different sources in the structure, effects of P-delta and nonlinear inelastic response is allowed for critical elements for investigation.

This study investigates the performance of frame structures with RC cornice projections and infill walls. Structural details of these models such as loads, structural elements, reinforcement and material properties are obtained from structural drawings of School Planning and Building Division (SPBD, 2009). The traditional building

normally has projections on the front side or three sides. In this study, the only variation in front projection is assessed. Figure 4-3 is the plan view which includes dimensions of roof floor without projection. The same plan view of masonry in-filled frame model with incremental projection of 650mm (IFP_650) is shown in Figure 4-4. The floor slabs and projection slab are also clearly shown with arrows in Figure 4-4. Figures 4-5-4-7 presents the elevation view in X direction, Y direction and 3D view.

The proportionally increased length of complex cornice projections is simplified as cantilever beam and slabs. The base supports are fully restrained. The bracing represents the compression struts to represent the infill panel. The sections and reinforcement details used in the model development are given in Table 4-1. Eight different models are considered for the analysis of the performance assessment. First one is a bare frame, the second one includes masonry wall considering the openings effects and its strength reduction, other 6 models have infill, as well as a different range of projection length with an incremental of 150mm, are used as given in Table 4-2. The simplified mathematical model of cornice components and cornice elevation detail are shown in Figure 4-8 to 4-9 respectively.

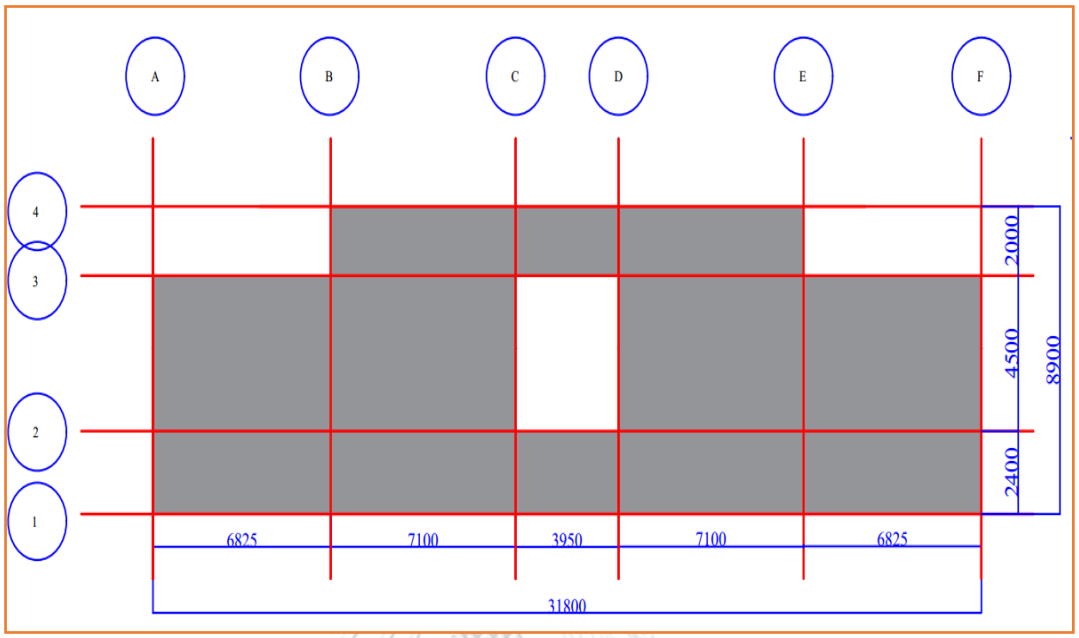

Figure 4-3 Plan dimensions without projection

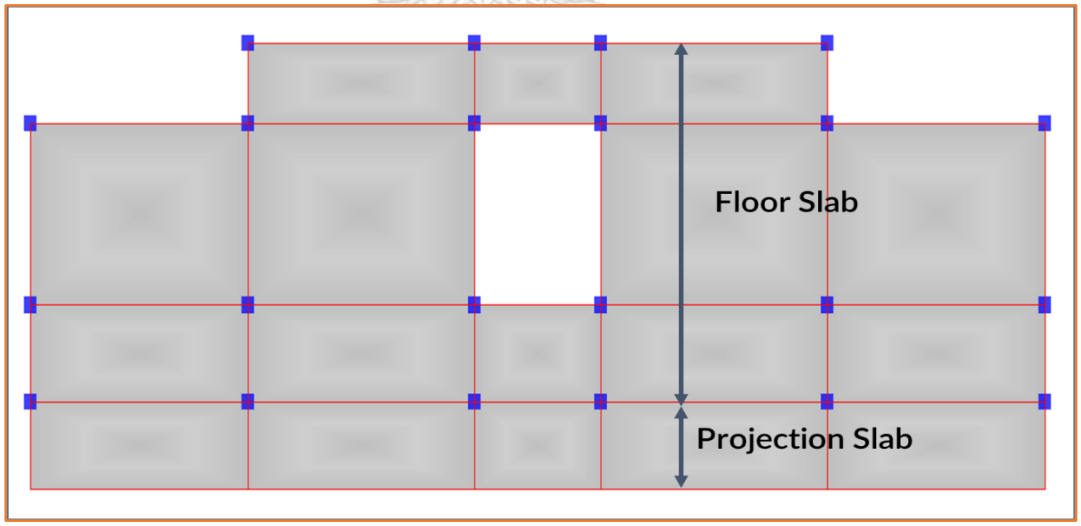

Figure 4-4 Plan of model showing the front projection

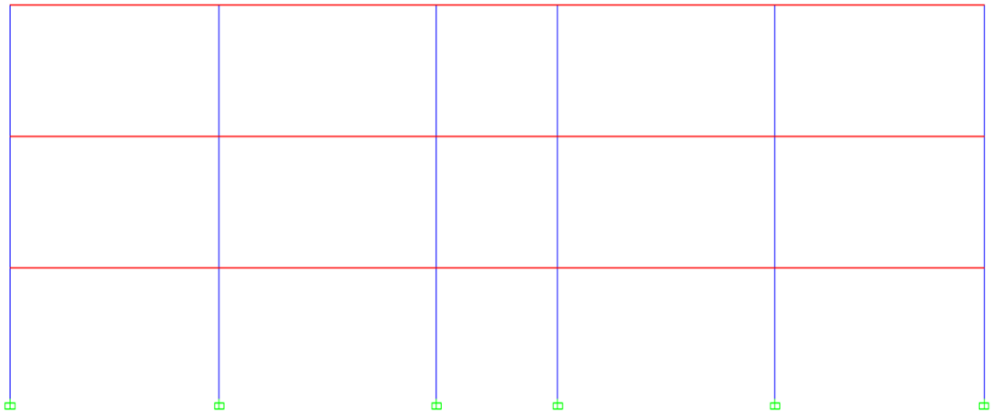

Figure 4-5 Elevation view in X direction (Grid 3-3)

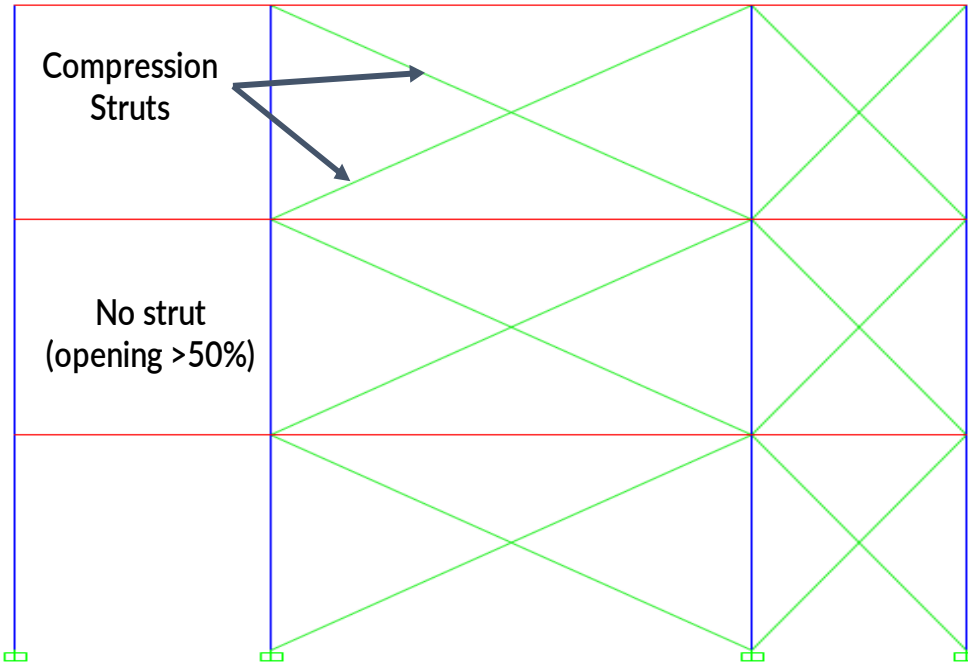

Figure 4-6 Elevation view with projection in Y direction (Grid C-C)

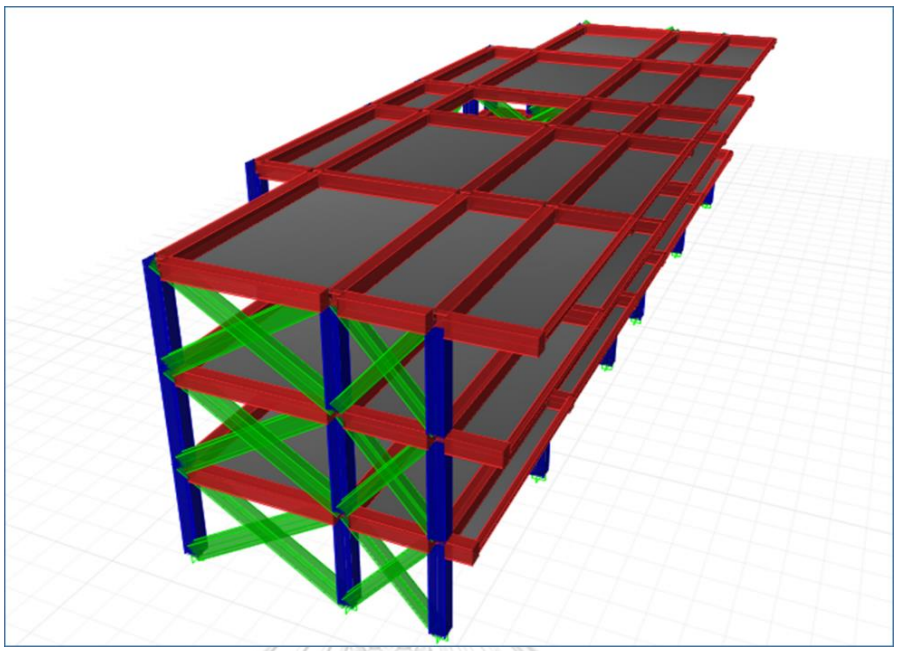

Figure 4-7 3D View of IFP_650 model

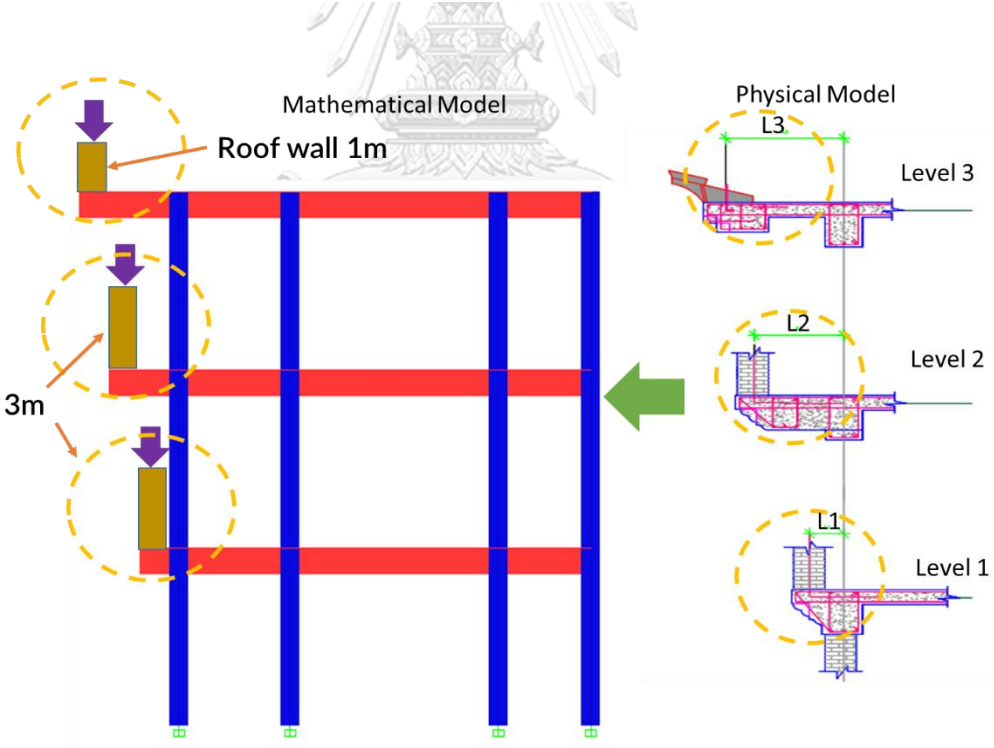

Figure 4-8 Simplified mathematical model of projection

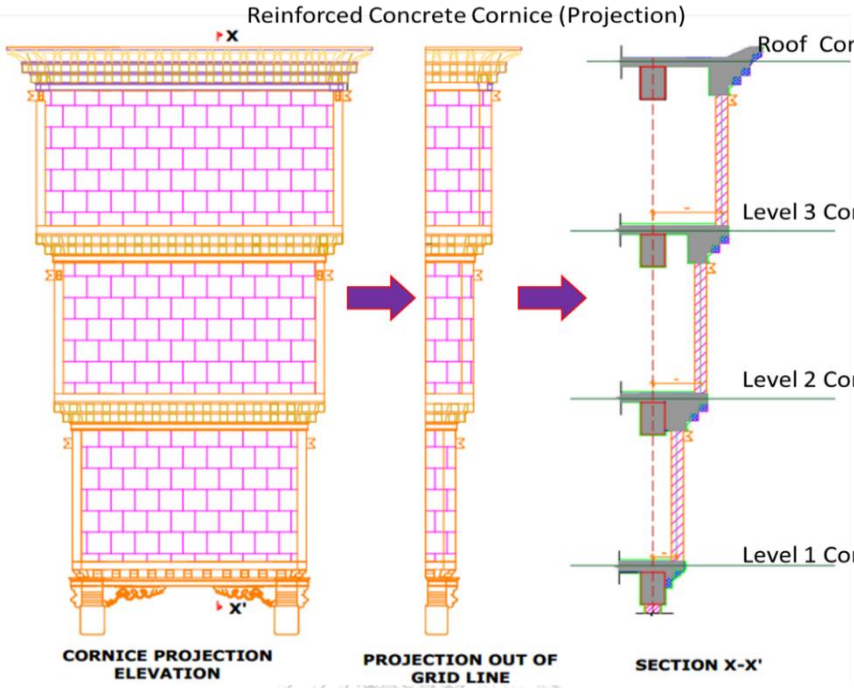

Figure 4-9 Typical cornice projections

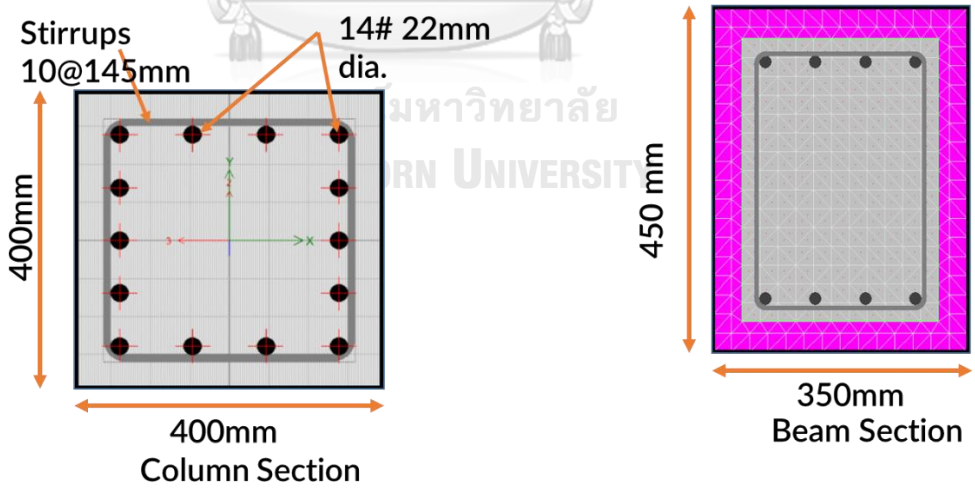

Figure 4-10 Typical column and beam sections

Table 4.1 Details of structural elements (SPBD,2009)

Beams	Width (mm)	Depth (mm)	Top Rebar (mm^2)	Bottom Rebar (mm^2)
B126	350	450	1964	943
B4	350	450	829	628
B35	350	450	1183	1183
Bho-beam	150	150	314.2	314.2
Column	Width (mm)	Depth (mm)	Rebar	Stirrups(mm)
C1	400	400	5#22mm dia	10dia@145 c/c
C2	400	400	4#22mm dia	10dia@145c/c

Table 4.2 Eight models with different projections

Model Name	1^{st}Floor (mm)	2^{nd}Floor (mm)	3^{rd}Floor (mm)	Proportional increments(mm)
BF	0	0	0	0
IFP_0	0	0	0	0
IFP_150	350	500	650	150
IFP_250	450	700	950	250
IFP_350	550	900	1250	350
IFP_450	650	1100	1550	450
IFP_550	750	300	1850	550
IFP_650	850	1500	2150	650

BF-Bare Frame, IF-In-filled frame
IFP_0 to the 650-masonry in-filled frame models with incremental projection
IFP_150: Centre to surface of column 200mm + incremental 150=350mm

4.3.3 Material properties

Structural details of these models such as loads, RC member dimensions, and reinforcement and material properties are obtained from structural drawings of SPBD, 2009. It is a typical structure with the proportionate cornice projections which represent

a trend for the current construction practice. It is worth to note very similar properties used for other commercial and government building across the country.

The very similar structural material properties used for other commercial and government building across the country. In absence of the structural details of the brick masonry critical parameter, the compressive strength of brick masonry wall was obtained from Kaushik [10]. Both numerical and experimental investigation on Indian brick masonry. Based on the numerous tests, the mean compressive strength of brick masonry with intermediate (1:4) mortars are estimated to be 6.6 MPa (f_b). In this study, 6.6MPa is used. Further, they found the modulus of elasticity of brick masonry to vary from $250f_b$ to $1100f_b$. The mean value of $550f_b$ was recommended to be used for the design, thus $550f_b$ has been adopted in this study. The details of material properties are presented in Table 4.3.

4.3.4 Brick masonry in-fill wall properties

NRHA finite element method is used to determine masonry in-fill in-plane stiffness and strength which accounts for openings, post-yield cracking, and cyclic degradation of wall.

Table 4.3 Material properties

Strength structural materials properties (MPa)	
Compressive Strength of concrete (f_c)	20
Rebar yield strength (f_y)	415
Compressive strength of bricks wall (f_b)	6.6 (for 1:4 cement-mortar)
Unit Weight (KN/m^3)	
Cement Concrete (γ_c)	25
Brick Masonry(γ_b)	20
Steel (γ_s)	78.5
Modulus of elasticity (MPa)	
Modulus of elasticity, E_c	$2.102x10^4$
Modulus of elasticity, E_s	$2x10^5$
Brick Masonry, E_b	$3.63x10^3$

In this model, the infill wall at the cornice projection is not confined to the horizontal and vertical members. Depending upon the geometry of wall, component drifts ratio important parameter that is effective displacement (Δ_{eff}) effective height

(h_{eff}) between each end of the element of the component (ASCE06, 2006) as shown in Figure 4-11. Masonry in-filled panels is main elements of lateral force resisting system. One major hazard in past earthquakes is the separation of heavy masonry walls from floors or roofs (FEMA, 2009). The wall components can create anchorage force (tension) at connections in out-plane or in-plane.

The unreinforced masonry walls or un-filled walls due to projections evaluated (ASCE06, 2006) for out-of-plane inertial forces by two-way actions: components to span vertically between diaphragm levels when effective wall-to-diaphragm connections are present, or to span horizontally between intersecting columns. The acceptance criteria based on flexural cracking caused by out-of-plane inertial loading. The wall cracked segments during excitation of acceleration time histories using numerical time-step integration models at top and bottom of panel should remain in stable condition. Further, at collapse prevention level, height-to-thickness (h/t) ratio of masonry panel spanning should not be less than that given in ASCE41 (ASCE06, 2006). This ratio mainly depends on input peak ground acceleration (PGA). The ratio decreases for higher PGA indicating that thicker walls are more stable to dynamic excitations.

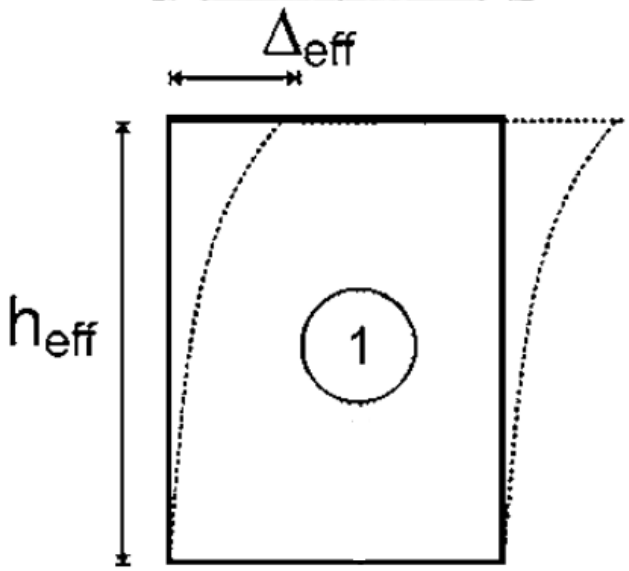

Figure 4-11 Effective height and displacements of the wall (ASCE06, 2006)

B. Diagonal strut properties

Stiffness masonry in-fill in-plane actions under seismic forces, column and beam elements tend to separate forming gap from in-fill panel at small lateral deformations. This separation leads to the reduction of the lateral stiffness, which onsets the nonlinear behavior of the structure. The strength at this point is noted up to 60% of the peak lateral force (Asce, 2006).

As infill panel act as a diagonal compression strut, however, it is difficult to clearly define the locations and orientations of the strut. Different researcher as mentioned in the literature review proposed at different locations. The results significantly depend on the location of struts.

The stiffness of masonry infill with openings to the in-plane actions is important to comprehend. The stress field is considerably affected by presences of openings. The clear mechanism is still unknown. The strength of in-fill wall to the in-plane actions is a deformation-controlled and determined in-plane shear strength for solid infill panels by-product of the area of the mortared section of infill panel (A_{in}) and shear strength of masonry infill bed joints (F_{vi})

$$V_{in} = A_{in}F_{vi} \qquad (4\text{-}3)$$

The diagonal compressive force in the in-fill should not be more than the compressive strength of the in-filled panel. The bearing (compressive) strength of the infill is obtained by following equations:

$$F_{mc} = f_m'(\frac{h}{3})t_w \qquad (4\text{-}4)$$

where; the f'm=compressive strength of the masonry; h=height of in-fill wall; and, t_w=thickness of in-fill wall. The shear modulus of masonry shall be measured or calculated by ASCE41-13:

$$G_m = 0.4E_m \qquad (4\text{-}5)$$

where; E_m = Young's modulus of masonry. The bearing strength of the in-fill can be considered as a cap of the force the infill can carry and shall be compared with the diagonal force carried by each strut. If the force is lower than the strength, the infill can

transfer the estimated force. If the force is higher, the lateral resistance should be accordingly adjusted downward.

B. Determination of the equivalent strut width

The stiffness properties of infill are developed based on previous studies and FEMA356. The diagonal compression strut property is then used in the 3 story model in 2D to verify the zero tension diagonal struts. The single strut is highly used due to its simplicity and suitable for large structural system. The study by Abdelkareem gives review on different expressions used to calculate width of equivalent diagonal struts (Abdelkareem, Sayed, Ahmed, & Al-Mekhlafy, 2013).

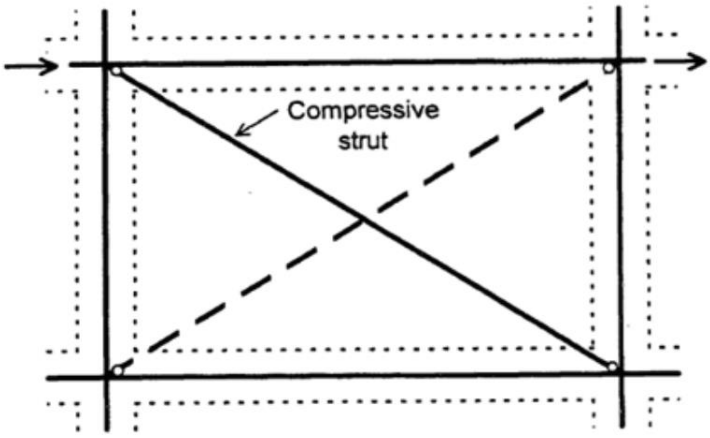

Figure 4-12 Diagonal equivalent single strut

The comparative study of different strut width calculations by various expression proposed are reviewed and further the force-deformation relations diagonal struts using different expression from previous studies are plotted in Figure 4-13.

$$W_m = 0.25 d_{\text{in}} \qquad (4\text{-}6)$$

where W_m is diagonal strut width d_{in} is the diagonal length of the in-fill panel

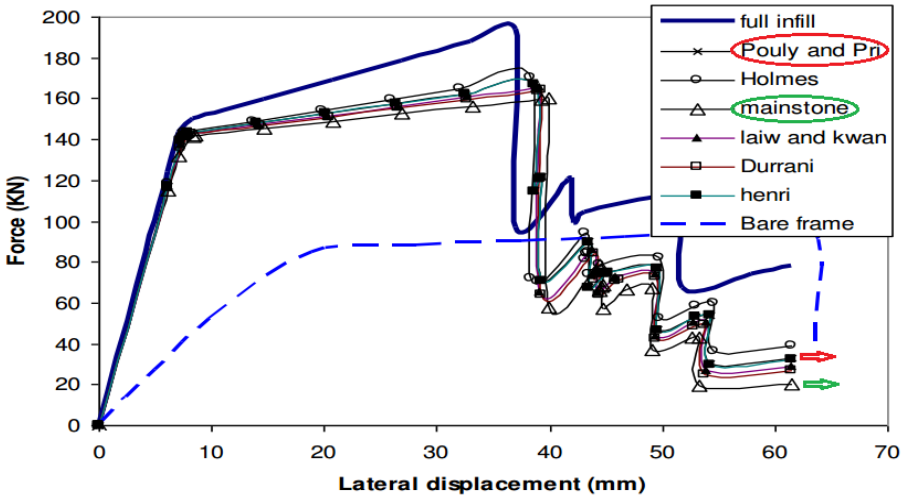

Figure 4-13 Strut width comparison for different models

(Abdelkareem et al., 2013)

The high value of W_m leads to stiffer model and attracts higher seismic response and suggested a conservative width value is better for design purpose. The modeling of single diagonal (Das & Murty, 2004) strut joints in this study are done as pin joint as shown below in the diagram. The allowable shear is calculated on the bed joint area as per IS 1905 or other codes and compared with the value obtained from the analysis. If wall failed in shear we have to increase the thickness of walls. However, in this study, we take all wall thickness as 250mm initially and carry out the analysis.

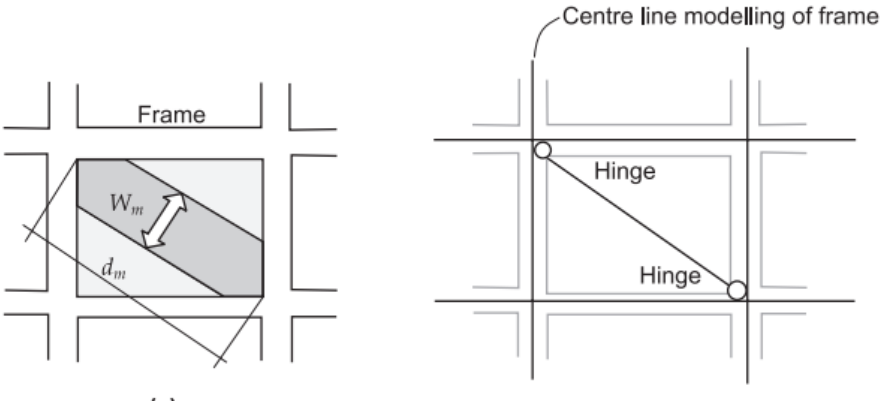

Figure 4-14 Modeling of the strut with hinge connection with concentric joints

$$W_m = 0.175(\lambda_1 h_{col})^{-0.4} r_{inf} \quad (4\text{-}7)$$

where,

$$\lambda_1 = \left[\frac{E_m t_{\inf} \sin 2\theta}{4 E_{fe} I_{col} h_{\inf}}\right]^{\frac{1}{4}} \qquad (4\text{-}8)$$

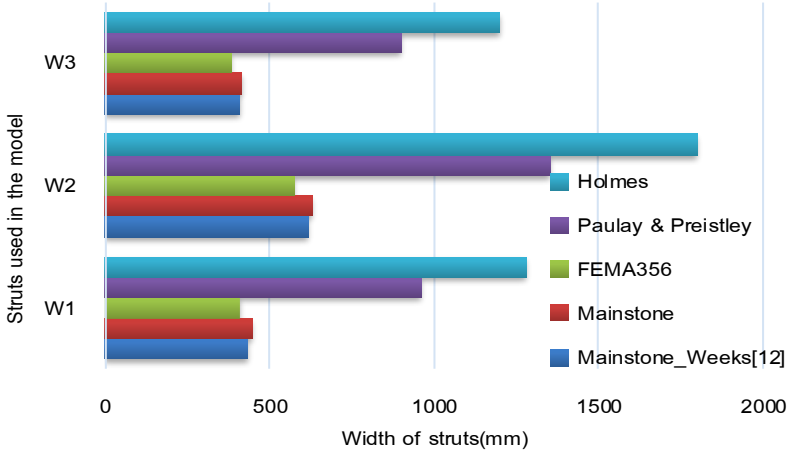

Figure 4-15 Comparison of model strut width calculations

Infill walls, brick masonry panels built partially or fully within the concrete frames and confined horizontally by beams and vertically by columns. However, if the opening is more than 50% diagonal compression struts are not used as the stiffness (Asteris et al., Smyrou et al., 2011) drastically reduced, specifically stiffness reduction factor tends to zero. The strut modeling at the cornice projection length is not required as the masonry walls are not confined within the RC frame. The walls are also offset from the main superstructure, thus only the mass of masonry wall is considered. The width of compression strut is compared by using a number of empirical formulae proposed by various studies such as Abdelkareem (Abdelkareem et al., 2013) in Figure 4-15. The widths calculated using FEMA356 is smallest in size and same empirical formulae are used to calculate the force-deformation relationships using the infill brick properties. The cracking, yielding and ultimate strengths of each strut as well as corresponding limiting drift are determined based on FEMA356 and previous studies for brick walls.

The three-different size infill panel is evaluated using various empirical formula with the width of W1, W2, and W3 respectively as shown in Figure 4-15. The FEMA 356 used the equation 4-5 to determine the width of the strut. h_{col} is column height between centerlines of beams, h_{inf} is height of in-fill panel, in. E_{fe} is expected Young's

modulus of frame material, E_m is expected Young's modulus in-fill material, I_{col} is moment of inertia of column, r_{in} is diagonal length of in-fill panel and t_{if} is thickness of in-fill panel and equivalent strut. After reviewing and comparing as mentioned in Figure 4-15, the width calculation from FEMA 356 is used. The struts are modeled zero-tension bracing partially or fully only in Y-direction and X-direction strut modeling is not required as the opening is more than 50% or not confined in RC frames.

The force-deformation relation for three struts is calculated and plotted as shown in Figure 4-116 for three different sizes of infill panels that are taken from the model. The maximum (F_{max}) and cracking forces (F_{cr}) are calculated using the Equation 4-9 and 4-10 other parameters remain same as above for diagonal struts (Kadysiewski et al., 2009).

$$F_{\max} = 0.818 \frac{L_{\text{in}}\, \text{t}_w\, f_{tp}}{C_1} \left(1 + \sqrt{C_1^2 + 1}\right) \quad (4\text{-}9)$$

where, $C_1 = 1.925 \frac{L_{in}}{H_{in}}$

$$F_{cr} = 0.6 F_{\max} \quad (4\text{-}10)$$

FEMA 356 (FEMA 2000) provides empirical formula to calculate In-Plane lateral deformation of the in-fill wall at the collapse prevention limit state referring Table 7.9. The detail of calculations of ultimate force, yielding force and cracking force of wall are also presented in Appendix A.

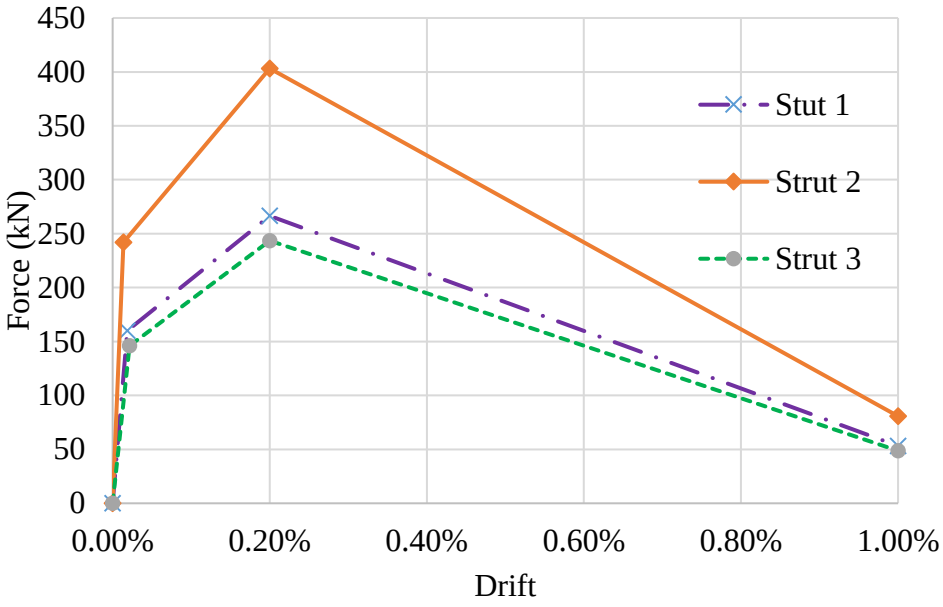

Figure 4-16 Force-deformation relationships for struts

C. Plastic hinges

When a column is subjected to lateral loading due to an earthquake, substantial inelastic rotation may experience at the end of column. In the design of RC structures or during seismic analysis plastic hinge length needs to be calculated. There is no direct way of calculating the plastic hinge length (L_p). Flexural hinges (plastic) shall form near the ends of the component. If it is located away from ends it needs to be accounted during modeling and analysis. Yu-Chen Ou reviewed and proposed simplified formulas for the plastic hinge length of circular reinforced concrete columns,

$$L_p = 0.8k_1k_3(L/d)c \quad (4\text{-}11)$$

$$L_p = d/2 + 0.2L/\sqrt{d} \quad (4\text{-}12)$$

$$L_p = d/2 + 0.05L \quad (4\text{-}13)$$

$$L_p = 0.08L + 0.022d_b f_y \, (f_y \, in \, MPa) \quad (4\text{-}14)$$

$$L_p / h = \left[0.3 \; P/P_0 \; + 3(A_s/A_g) - 0.1\right](L/h) + 0.25 \geq 0.25 \quad (4\text{-}15)$$

Several previous studies have proposed numerous formulas to approximate the plastic hinge length. Equations 4-11 to 4-15 are suggested empirical formulas, respectively,

by Baker and Amarakone (1964), Corley (1966), Mattock (1967), Paulay and Priestley (1992), and Bae and Bayrak (2008) (Ou et al., 2012).where L_p is plastic hinge length; $k_1$is coefficient related to type of steel (mild or cold work steel); k_3 is coefficient related to concrete strength; d is effective beam depth; L is distance between critical section and point of contra-flexure; c is neutral axis depth at ultimate condition; d_b is diameter of longitudinal rebar; f_y is yield strength of longitudinal rebar; P is applied axial force; P_0 is nominal axial load capacity ,A is area of longitudinal reinforcement; A_g is gross cross section area; and h is total column depth. The I_p estimated can be used in calculating flexural displacements to approximate the descending part of the lateral load response of concrete columns. The previous studies show that axial load, L/h and the amount of longitudinal reinforcement are main parameters for estimating the length of a plastic hinge based on that equation (4-15) is more appropriate proposed by Sungjin Bae and Oguzhan Bayrak (Sungjin et al., 2008). The five parameters are identified that are significant to the plastic hinge length, namely:

1. Axial force,
2. Shear span-to-depth ratio,
3. Longitudinal reinforcing ratio,
4. Concrete compressive strength, and
5. Yield strength (material type) of longitudinal reinforcement, However, all the above parameters are not used in one equation.

Observations by Mehmet Inel (Inel et al., 2006) length of plastic hinge and transverse stirrups reinforcement with different spacing has no effect on the base shear capacity but it does strongly affects the capacity of frames for displacement. Therefore, increases in transverse reinforcement can improve the displacement capacity. Modeling with default hinges requires special attention. The user defined hinges in the modeling has advantages over default hinge definition in order to reflect the nonlinear behavior. However, default-hinge definition is more user friendly than user defined, which has ready definition built in some programs based on different codes such as FEMA-356, ASCE 41 and ATC-40 guidelines.

4.4 Gravity and earthquake loads

4.4.1 Gravity loading

Gravity loading for Structural analysis used for numerical simulation of all models are as mentioned below:

Table 4.4 Gravity loads used to combine with seismic load cases

SN	Description of loads	Load (kN/m^2)
A	Live loads (LL)	
	Classrooms, staircases, corridors & Stores	3
	cessible Roof	2
B	Superimposed Load-Masonry wall (ML)	Load (kN/m)
	Story Walls	15
	Roof walls	5

The seismic mass consists of dead load and superimposed dead load only, however, the P-Delta or non-linear dead load to combine with seismic loads includes all dead loads and 25% of the live load.

4.4.2 Earthquake loading

In absence of real recorded ground motions due to lack of recording instrumentation and seismic stations in Bhutan, the selection is done based on similarity in magnitudes, fault distance, and source mechanisms from the available online database (https://ngawest2.berkeley.edu). The chosen data magnitude ranging from 6.9 to 7.9 aims to represent earthquakes that probably would occur in Bhutan. To investigate the performance of buildings in the event of a real earthquake such as Gorkha Earthquake of Nepal on 25th April 2015 is used along with similar other ground

motions as mentioned in Table 6. Nepal and North East India earthquakes could provide a more realistic response behavior since seismicity and geographical locations are similar.

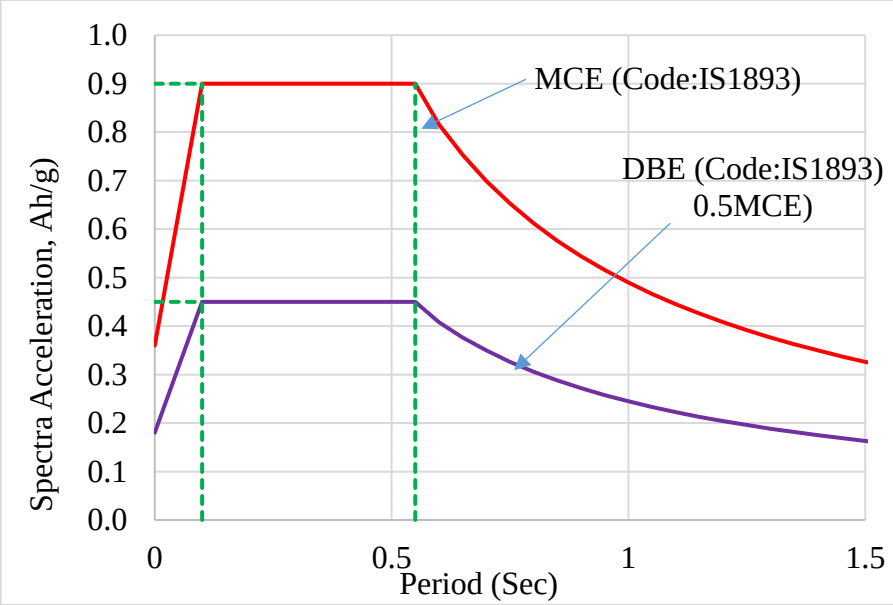

Figure 4-17 MCE and DBE based on IS 1893 Code

Design Base Earthquake (DBE) is 0.5 of MCE

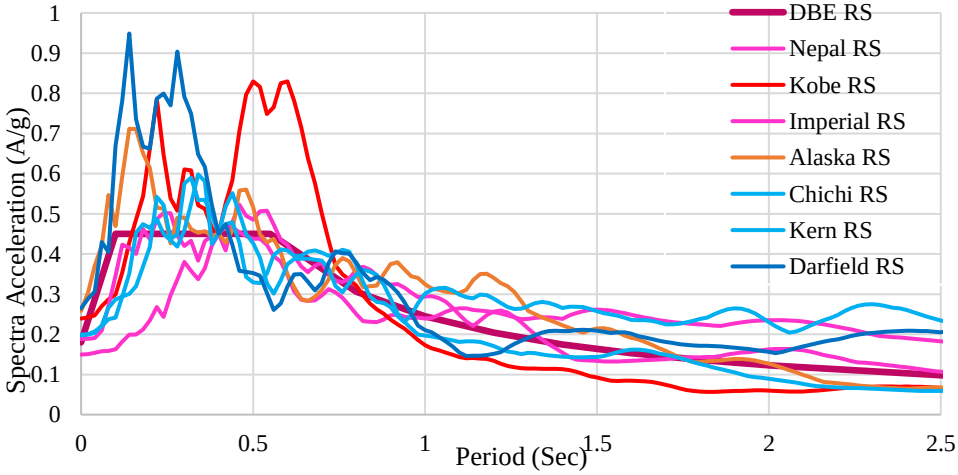

Figure 4-18 Amplitude scaling to target spectrum with conditioning period

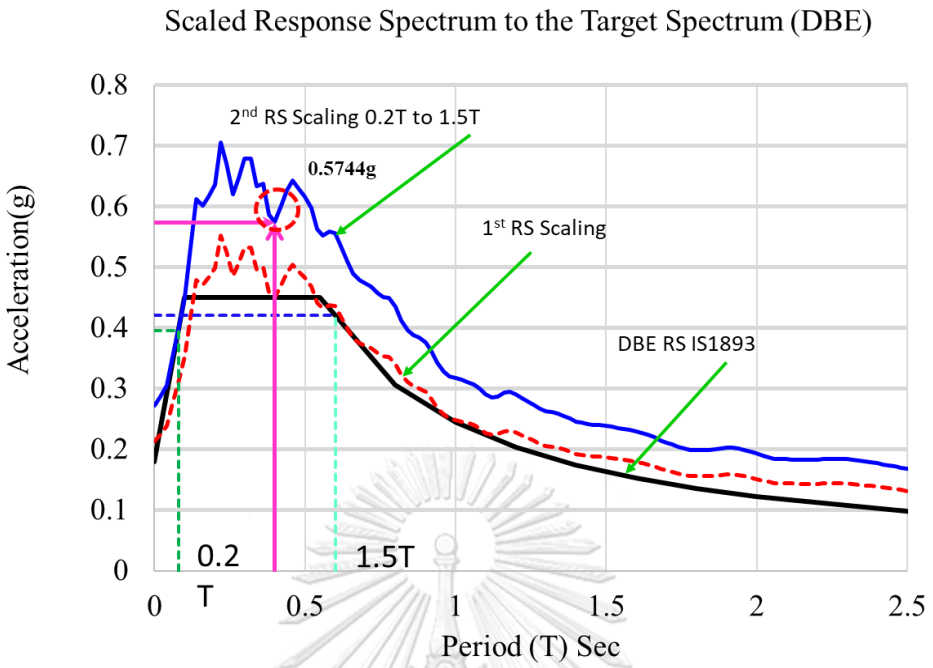

Figure 4-19 Earthquake acceleration scaled response spectrum

The 3D NLRHA using the sets of earthquake accelerations consist of both horizontal and vertical components as selected after amplitude scaling done for individual sets based on ASCE 7. For horizontal components, a square root of the sum of the squares (SRSS) are calculated and constructed response spectra for 5 percent-damp where an identical scale factor for both horizontal and vertical components is applied.

Table 4.5 Ground motions with horizontal & vertical components

Earthquake	Magnitude	Year	Rrup (km)	Fault
Gorkha, Nepal	7.80	2015	15	Strike Slip
Kobe, Japan	6.90	1995	69	Strike Slip
Imperial, USA	6.95	1940	6	Strike Slip
Alaska, USA	7.90	2002	50	Strike Slip
Chichi, Taiwan	7.62	1999	40	Reverse convergence
Kern, USA	7.36	1952	39	oblique
Darfield	7.00	2010	15	Strike Slip

Second scaling is carried out to scaled up response spectra such that its value shall be greater in the period range from 0.2T to 1.5T, where T is fundamental period of the building from empirical formula. Thus, average response spectra fall above the

target spectrum. The target spectrum considered is based on Design-Based Earthquake (DBE) according to Indian seismic code, IS1893-2002 which is half of Maximum Considered Earthquake (MCE) as shown in Figure 4.17. All response spectrum of each ground motions is then scaled up to Target Spectrum (DBE) using the building period as presented in Figure 4-18.

The seismic mass (M) considered is the modeling consist of total self-weight of the structure that is self-weight of frame elements and slabs as well as lumped mass of masonry in-filled walls. The mass of wall is lumped in the form of line mass or joint mass as appropriate, presence of wall is represented by zero tension diagonal struts. The P-Delta included and it is defined using total self-weight of frame and slab along with superimposed dead load of masonry in-filled wall and 25% of live load as the non-linear load case.

The seismic code used in Bhutan is mostly Indian seismic code unless necessary, Similarly, in this study IS1893 as well as ACI318-14, FEMA356 are used wherever necessary. These codes are updated with latest techniques to compute nonlinear dynamic analysis and has well-established acceptance criteria and are widely used in many countries. The modeling is done by using simultaneously both horizontal accelerations, vertical acceleration resembling the occurrence of a real earthquake.

4.5 Lateral force distribution and vertical period

4.5.1 Lateral force distribution of ELF

The lateral force distributions model with masonry in-filled frame structures with projections by ELF is presented in Figure 4-20. The vertical distributions lateral forces for both the direction X and Y are equal. In this case the calculations are based on fundamental period (T_a) calculated by using an empirical formula based on IS1893.

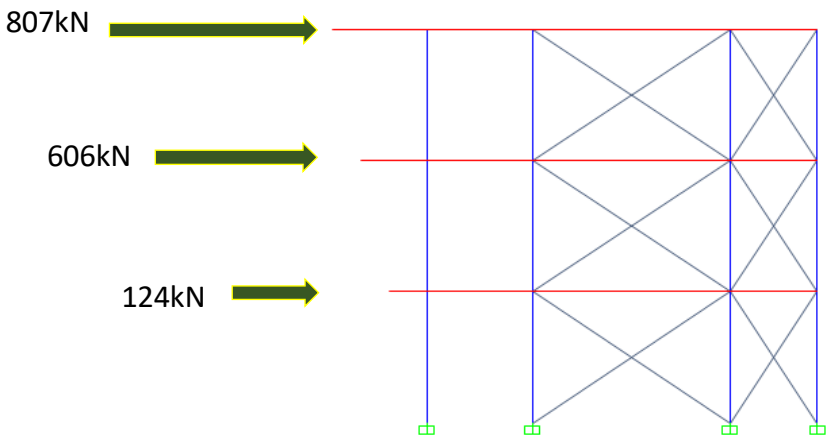

Figure 4-20 Equivalent lateral force distribution along the height

(Appendix B)

The base shear is the summation of distributed lateral force along the height of building (1537kN). The model is checked for total seismic weight by comparing the hand calculations and ETABS value. This is useful to verify unintended seismic mass presence and correctness of the model. Table 4.6 is the check of the model developed with all elements such as RC frame, slabs, diagonal strut with fixed base support.

Table 4.6 Total gravity load check for the model (IFP650)

Total self-weight of structure including masonry wall		
Etabs Model (kN)	Hand calculation (kN)	% Differences
5916	5909	0.118%

4.5.2 Natural period (*T*)

The fundamental period of vibration is important parameters for the seismic design and assessment of structures. Natural periods of vibration (Kaushik et al., 2007) of buildings mainly depend on two parameters; mass and lateral stiffness. The inclusion

of the masonry walls in the mathematic model increases both the parameters. However, most codes do not explicitly mention the empirical formulae for period calculations specifically for masonry in-filled frame structures. Besides height of the building, percentage of in-fill panel and the number of bays in each direction had almost the equal effect on the natural period (Kose, 2009).

The fundamental period of vibration (T) is estimated by empirical Equation 4-16 for RC frame only and by Equation 4-17 for RC frame with brick in-fill panel based on IS1893-2002. Where, h is the building height, b is the base dimension at plinth level in the direction of the lateral force. According to ASCE7-10 period is estimated by Equation 4-18. The detail calculations are included in Appendix C. The approximate fundamental period (Ta) calculated from IS1893 are calculated.

From IS code

$$T_a = 0.075h^{0.75} \quad (4\text{-}16)$$

$$T_a = \frac{0.09}{\sqrt{d}} \quad (4\text{-}17)$$

ASCE7-10

$$T_a = C_t H_n^{\ x} \quad (4\text{-}18)$$

where,

$C_t = 0.0466^a$, $a = 0.9$ (in metric units)

The upper limit coefficient (C_u) calculates the period and it is use in design which depends on design spectral response acceleration as specified in Table 12.8-1 of ASCE7-10. However, elastic drifts can be determined using seismic force based on the computed period of building without upper limit restriction.

The correctness of the model is verified by basically comparing the consistency of the natural period and base shear for different models. The model IFP_0 has included macro modeling of the diagonal strut in Y-direction representing bricks panels. However, the struts are not included in the X-direction where there opening more than 50% of the total panel area. Thus, a period in X-direction remain consistent, however natural period drastically reduced in Y-directions, this itself indicates the effects of infill wall which increase the stiffness and strength accordingly. The uniform placement of

infill walls with the appropriate size of opening plays an important role. The consistent small increments in periods are noted with an increase in the length of the projection merely because of increase in mass only but no contribution from stiffness.

4.5.3 Vertical periods (T_v) of cantilever components

The natural periods of the projected components for different lengths are plotted in Figure 4-21 subjected to different masonry wall as a superimposed load for three stories. Periods are determined from multi-degree of freedom (MDoF) system of the model. Determining vertical period is important as it gives the probable potential for dynamic amplification to the cantilever components. This amplification primarily affects the vertical loads and it may ultimately lead to the amplification of vertical deflections and internal forces (shear and moment). The stiffness used in single degree of freedom (SDoF) is referred to the ratio of external force to deflection of the real system considered at the degree-of-freedom. Equation 4-19 and 4-20 provides the stiffness and deflection respectively.

$$K = \frac{F}{\Delta_{max}} \qquad K = \frac{3EI}{L^3} \tag{4-19}$$

where Δ_{max} is calculated as

$$\Delta_{max} = \frac{FL^3}{3EI} \tag{4-20}$$

The mass applied in the SDoF is the lumped mass (M) and the mass contributes to the inertia effect of the motion in a real structure. It is therefore required to define the shape of vibration before we can compute the mass, M, of SDoF. The system vibration also is characterized by the natural frequency f (Hz), which is computed from the circular eigenfrequency.

Story 1	
Projection	Period
mm	sec
350	0.038
450	0.046
550	0.056
650	0.067
750	0.077
850	0.09
Story 2	
500	0.043
700	0.071
900	0.098
1100	0.125
1300	0.154
1500	0.185
Story 3	
650	0.047
950	0.07
1250	0.102
1550	0.127
1850	0.158
2150	0.192

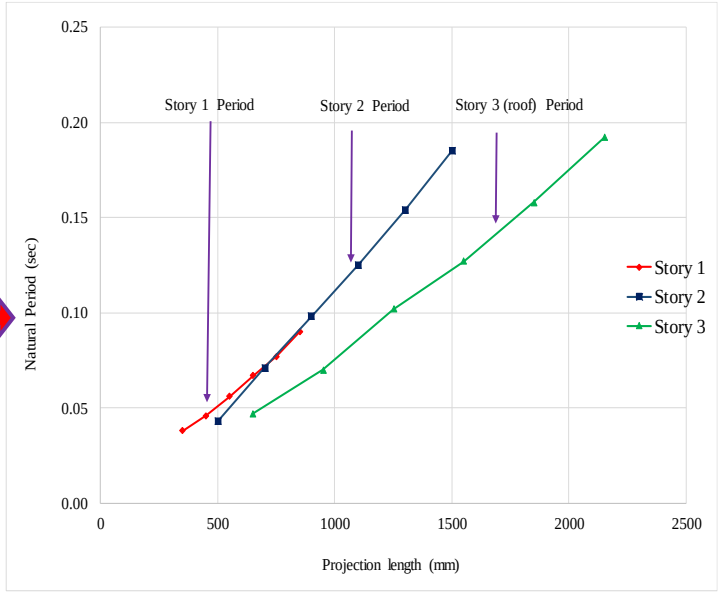

Figure 4-21 Projection length and vertical period from MDoF system

The natural period can be calculated from the eigenfrequency as well as directly using the stiffness and lumped mass of the structure as given in Equation 5-6.

$$T = \frac{1}{f} = \frac{2\pi}{\omega} = 2\pi\sqrt{\frac{k}{m}} \qquad (4\text{-}21)$$

The period from the model computation in MDoF system and SDoF system by hand

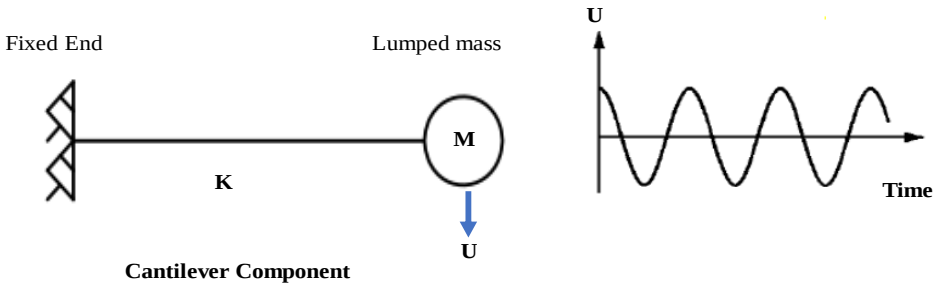

Figure 4-22 SDoF with lumped mass of projection

calculations are compared and presented in Table 4.7 and same is reproduced in Figure 4-23.

Table 4.7 Vertical period comparison for projected components

Projection Length (m)	T_v, SDoF Calculation	T_v, MDoF model
2.15	0.189	0.192
1.50	0.176	0.185
1.30	0.141	0.154
1.10	0.109	0.125
0.90	0.080	0.098
0.70	0.055	0.071
0.50	0.033	0.043

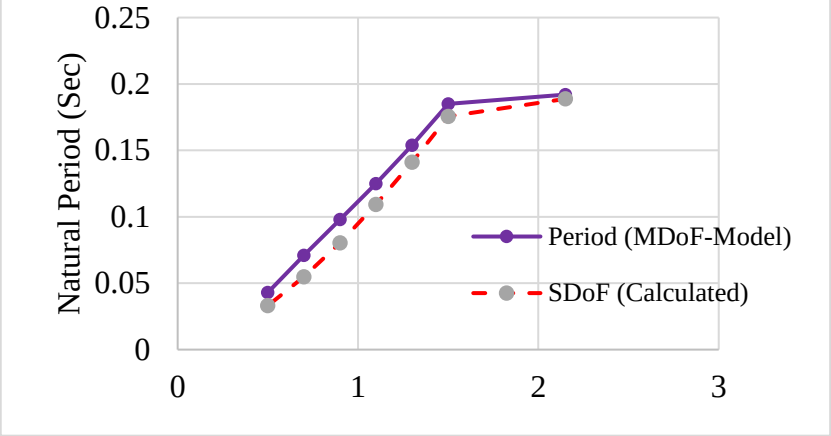

Figure 4-23 Vertical period comparison for projected components

Both the curve blue line and dotted line are close to each other, however, the vertical period calculated from MDoF model is slightly larger. This may be due to end support condition, that is more flexible than the fully restrained joint for the projected components.

Modes for 90% mass participation is higher for the model with increased projection component where there is in-filled wall however in-X direction where there is no in-filled wall, mass participation requirement of 90% is fulfilled in initial few modes. For model with in-filled wall as well as presence of projection many modes need to be included to attend the 90% mass participation.

CHAPTER 5
NONLINEAR RESPONSE HISTORY ANALYSIS

5.1 Nonlinear response history analysis (NLRHA)

Response from NLRHA mainly depends on input accelerations and structural properties of the models. In this study response calculations are as mentioned below:

1. NLRHA was performed with scaled ground motions with typical structural properties.
2. Absolute maximum responses from each set of earthquake and gravity loading are calculated.
3. Further an average of 7 maximum responses from each earthquake and gravity loading are calculated as the NLRHA responses
    a. Lateral displacements in X and Y direction.
    b. Inter-story drift in each direction (X and Y).
    c. Internal forces -moment and shear force demands.
    d. Deformations – vertical deflection of projection.
    e. Dynamic amplification factor for the response especially internal forces and deflections.
4. Responses are compared with code acceptance criteria/limits and capacity of section as appropriate.
5. Based on results, conclusions and recommendations were provided.

5.2 Results and discussions

5.2.1 Story lateral displacements

The mean lateral displacements of eight 3D models in X and Y for each set of seismic load case calculated and presented in Figure 5.1 and Figure 5.2 respectively. The story lateral displacement with the in-filled frame with first projection (IFP150) has minimum displacement followed by bare frame and consistent slight increase in displacement within increases in projections from IFP150 to IFP650. In Y-direction,

there is a large difference between BF and in IFP (IFP150-650). The huge reduction of displacement in Y direction only is noted due to the presence of infill walls as there is a drastic increase in stiffness. However, the differences of relative displacement for each model with increased projections is not much as obtained in Figure 5.6.

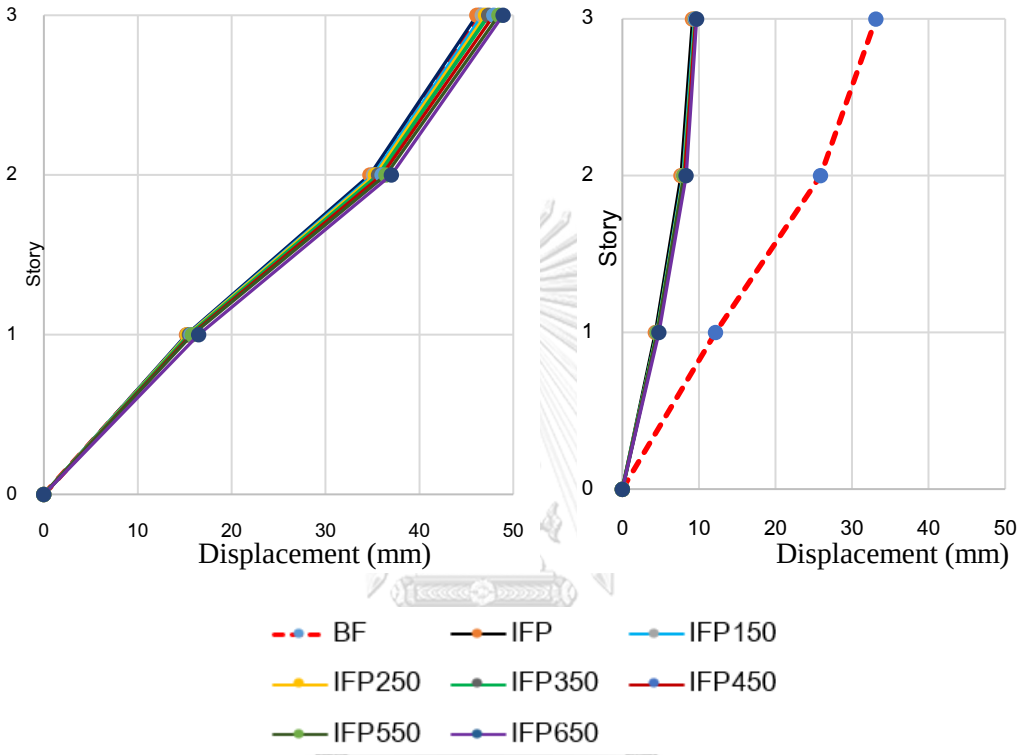

Figure 5-1 Lateral displacement in X in direction

Figure 5-2 Lateral displacement in Y in direction

5.2.2 Inter-story drifts

Determination of lateral drift is important as it provides seismic behavior and stability of structure to lateral loading. The inter-story drifts and its relationship with the performance levels are defined as indicative of the range of drift for different types of structures (ASCE41-06) as shown in Table 5-1. In this study Table 5.3 limits from codes as well as and Table 5.4 from the previous study are used as appropriate.

Table 5.1 Structural performance levels and damage (ASCE41-06)

Elements	Type	Collapse Prevention	Life Safety	Immediate Occupancy
URM (In-filled Walls	Drift	0.6%	0.5%	0.1%
URM (Non-infill) Walls	Drift	1.0%	0.6%	0.3%
RM Walls	Drift	1.5%	0.6%	0.2%
Concrete Frames only	Drift	4.0%	2.0%	1.0%
URM-Unreinforced Masonry; RM- Reinforced masonry				

Table 5.2 Drift relationship (Ghobarah)

Performance Levels	Damage state	Inter-story drift limit (%)
Immediate Operational (IO)	Slight	0.1
Life Safety (LS)	Irreparable	0.4
Collapse Prevention (CP)	Severe	0.7

The studies on the correlation of inter-story drift to the performance levels and damage state of masonry in-filled frame buildings done. Ghobarah and Kalman-Sipos (Ghobarah, Šipoš et al.) found very similar relationships of performance level with damage state and inter-story drift. Relationship proposed by Ghobarah are used in this paper for limiting the inter-story drift. The average inter-story drift of 8 models are calculated from peak responses are presented in Figure 5-3 and Figure 5-4 for X and Y direction respectively.

For the selected material properties, section properties and combined seismic and gravity loading, response behavior in terms of inter-story drift is plotted for X and Y independently against the allowable drift limits proposed by previous studies. The regular drift demand profile is observed; this may be due to fixed support base without consideration of soil-structure interaction (SSI). The maximum demand drift in the X-direction is in the second story exceeds the limiting IO and LS and almost reach the CP level. However, the drift percentage of the in-filled frame is comparatively lower than other models. it is apparent that none of the models would be satisfying for near IO

requirement under the given ground motions in X-directions for chosen structural properties.

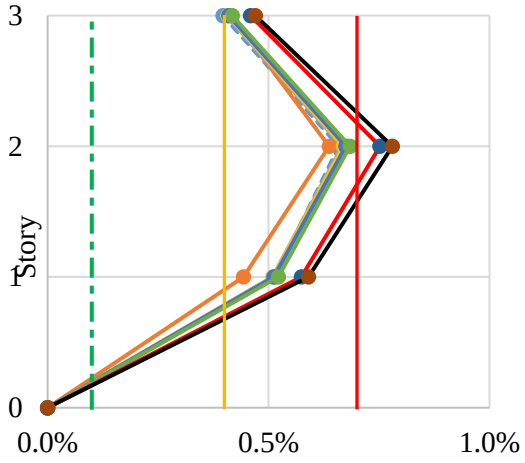

Figure 5-3 Inter-story drift in X direction

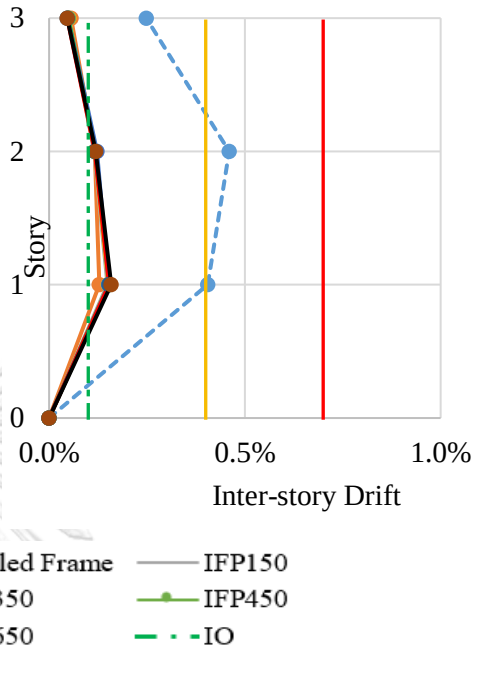

Figure 5-4 Inter-story drift in Y direction

In Y-direction the drift percentage in mostly falls on IO level except for the bare frame which reaches to LS level. It is evident that in each incremental projection, the story drift also increased accordingly. Although, the increase is not much due to the small incremental size of projection length. Judging by the inter-story drift values, the performance of 3 stories building, the bare frame seems more vulnerable to lateral deformation to earthquakes.

5.2.3 Vertical deflections of the projected components

The vertical deflection is sensitive to vertical acceleration of ground motions. In this study vertical components are used along with two horizontal components after proper scaling. The out-of-level condition of floor slabs needs to be controlled, it is important for the stability of masonry wall resting above it as well as aesthetics and sense of comfort for occupants. The limiting values for deflections (L/240) are referred to ACI318-14 (Table 24.2.2) for the floor supporting non-structural elements for

immediate deflection with sustained or any additional live load. The deflection limit for cantilever member is not defined clearly in the code for earthquake load combined with gravity load, thus two times of L/360 i.e. L/180 is more reasonable and used as second limiting values in this study, where L is projection length. The maximum deflection for each floor for models (IFP150 -IFP650) are assessed for seismic loads and the average of absolute maximum response is plotted against the projection length. The new proposed limits (L/180) for earthquake loads is also presented in Figure 5-5.

Figure 5-5 shows that comparison of vertical deflection of cantilever beam due to seismic and gravity loading. There is an increase in deflection with the increase of cantilever lengths. The deflection due to seismic loading is comparatively larger than the gravity loading. The deflection of the cantilever beam exceeds both the limiting values in story 2 and 3 due to seismic load.

Table 5.3 Proposed Projection Limits

Story	Loading	Deflection (mm)	Projection Length Limit (mm)
2	EQ	-7.60	1375
3	EQ	-12.05	2100
2	Gravity	-5.59	1400
3	Gravity	-8.90	2150

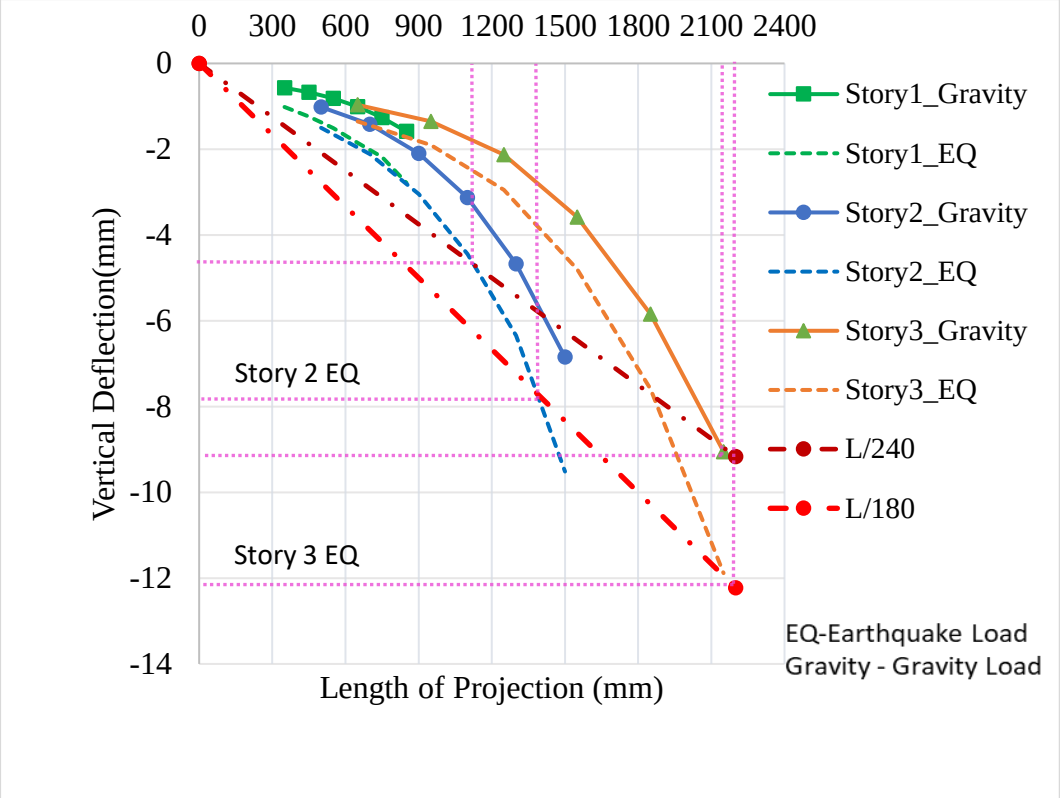

Figure 5-5 Deflections of cantilever projection and with limits

The projection limit points for all three story are determined in Table 5-5 and proposed for a suitable range of projection for story 2 and story 3. The projection of for story one within both the limits.

5.2.4 Internal forces

Figure 5-6 shows the internal force, a moment in the cantilever beam that is extended from the main super-structure to provide extra flooring space and carry the masonry wall loads at the end of the beam which then transfers to the column. The length vs moment demand along with the capacity of the cantilever beam section in dotted line is plotted in Figure 5-6.

Table 5.4 Shear demand and amplification factor for varying length of projection

Models	Projections	Gravity (kN)	Seismic (kN)	Amplification factor
Story 1 Shear force demand				
IFP150	350	7.20	12.64	1.75
IFP250	450	14.08	23.8	1.69
IFP350	550	22.22	36.13	1.63
IFP450	650	29.89	46.19	1.55
IFP550	750	37.02	54.76	1.48
IFP650	850	43.66	63.75	1.46
Story 2 Shear force demand				
IFP150	500	18.05	30.59	1.69
IFP250	700	33.41	51.42	1.54
IFP350	900	46.68	67.81	1.45
IFP450	1100	54.90	74.21	1.35
IFP550	1300	63.11	80.6	1.28
IFP650	1500	77.42	96.36	1.24
Story 3 Shear force demand				
IFP150	650	10.01	15.03	1.50
IFP250	950	17.29	23.83	1.38
IFP350	1250	22.15	28.36	1.28
IFP450	1550	31.43	38.77	1.23
IFP550	1850	39.91	48.00	1.20
IFP650	2150	43.79	53.44	1.22

There is an increase in demand with an increase in the length of projections, the demand does not exceed the capacity of the beam in this case. Figure 5-7 shows the amplification due to shear and moment demand due to seismic and gravity loading with respect to length. The amplification due to vertical acceleration is higher for the shorter projection length and it decreases till 1.4m and slope becomes almost gentle and remain constant as the length of projection increases.

Table 5.5 Average dynamic amplification factor of shear forces

Story	Projection Range (m)	Average amplification factor
Story 1 Projection	0.35-0.85	1.59
Story 2 Projection	0.50-1.50	1.43
Story 3 Projection	0.65-2.15	1.30

Table 5.6 Moment demand and amplification factor for varying projection

Models	Projections	Gravity (kN-M)	Seismic (kN-m)	Amplification factor
Story 1 Moment Demand				
IFP150	350	-4.45	-8.36	1.88
IFP250	450	-8.17	-14.26	1.75
IFP350	550	-12.78	-21.38	1.67
IFP450	650	-18.28	-29.04	1.59
IFP550	750	-24.62	-37.49	1.52
IFP650	850	-31.77	-47.88	1.51
Story 2 Moment Demand				
IFP150	500	-10.29	-17.98	1.75
IFP250	700	-21.27	-33.73	1.59
IFP350	900	-35.52	-53.32	1.50
IFP450	1100	-52.74	-74.67	1.42
IFP550	1300	-73.00	-96.91	1.33
IFP650	1500	-95.58	-123.37	1.29
Story 3 Moment Demand				
IFP150	650	-6.42	-9.7	1.51
IFP250	950	-14.61	-20.39	1.40
IFP350	1250	-25.15	-33.96	1.35
IFP450	1550	-38.46	-50.15	1.30
IFP550	1850	-53.8	-68.12	1.27
IFP650	2150	-70.56	-89.27	1.27

Tables 5.6 to 5.9 present response demand and dynamic amplification due to gravity load as well as earthquake load including average amplification factors. The calculations of dynamic amplification factor for shear forces and moments carried out and the Table 5-6 and 5-7 represents for a different story with various length of projections.

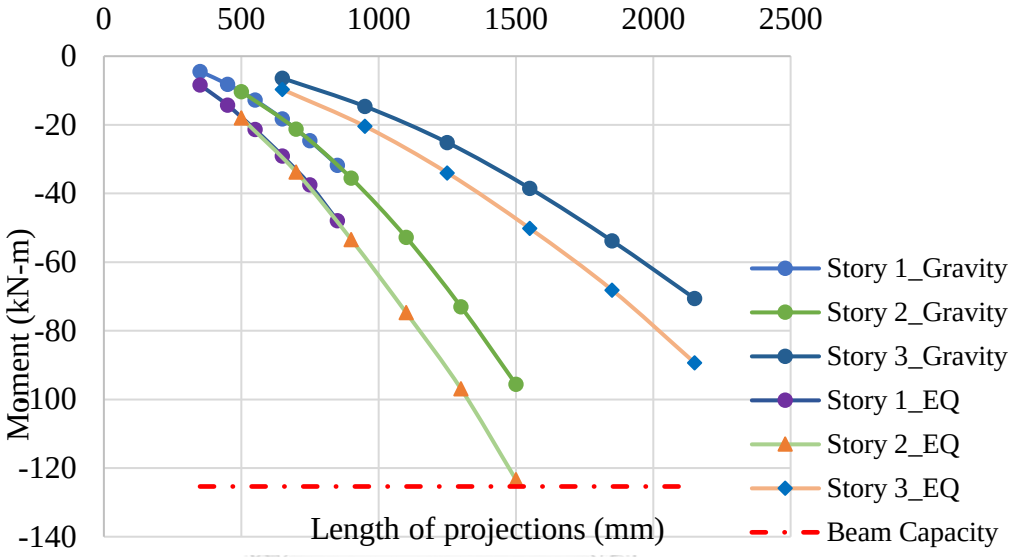

Figure 5-6 Moment demand and projection length for different stories

5.2.5 Dynamic amplification factors

The moment and shear dynamic amplification factor have similar trend that that is the amplification is higher for the shorter projection length. However, it reduces as the length increases till 1500mm and it gets stabilizes becoming almost constant for both the moments and shear as shown in Figure 5-11

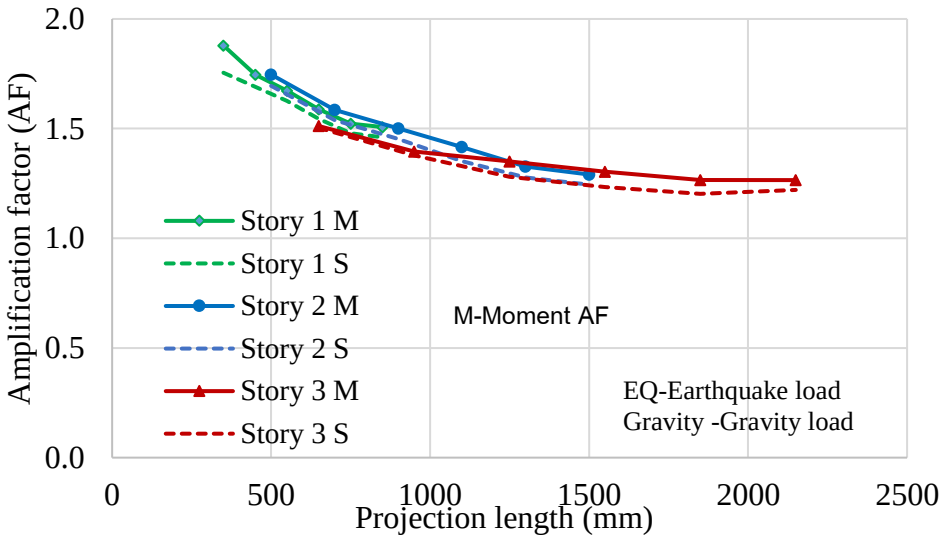

Figure 5-7 Moment and shear dynamic amplification factor

Based on the results of NLRHA, safe limits of cornice projection length and dynamic amplification factors (DAF) for vertical deflections, shear forces, and bending moments are presented in Table 5.7 and Table 5.8 respectively. Note that cornice projections at the 1st and 2nd story support 3 m-high masonry wall, whereas the 3rd story (top roof level) supports 1 m-high masonry wall on the building perimeter.

Table 5.7 Safe limits of cornice projection length to resist earthquake loading.

story	projection range (m)	projection length(m)
1	0.35 - 0.85	safe
2	0.50 - 1.50	1.40
3	0.65 - 2.15	2.15

Table 5.8 Dynamic amplification factors (DAF) for seismic demand.

story	projection range (m)	vertical deflection	shear force	bending moment
1	0.35 - 0.85	1.80	1.59	1.65
2	0.50 - 1.50	1.43	1.43	1.48
3	0.65 - 2.15	1.36	1.30	1.35

CHAPTER 6
CONCLUSIONS AND RECOMMENDATIONS

6.1 Conclusions

By using three-story typical building representing stocks of frame structures in Bhutan with incremental cornice projection lengths in the numerical analysis, the main results of this studies are summarized as below:

1. Dynamic amplification factor (DAF) need to be considered for projected component for exposed to similar vertical accelerations and typical section properties is proposed. The minimum DAF to the gravity loading demands should not be less than 1.8 for the performance base design.
2. The projection length limit proposed based on typical design and acceptance criteria of ACI318-10 is 1.4m.
3. Due to the presence of projection for full length of the front façade of the building, masonry walls which are not confined in the RC frames affect the responses. This is indicated in response demands of lateral displacement and inter-story drift. The walls that do not fall on the grid line of perimeter column should be considered as un-filled masonry wall. This highly effects the lateral stiffness due to seismic load of the structure.
4. The vertical period of the projection component keeps increasing and it depends on the size of wall, length of projection and section properties of cantilever component. For the same wall section period increases with increasing of projection length indicating reduction stiffness and stability of the structure.

6.2 Recommendations

Cornice projection to the typical RC frame structure of low rise building gets affected by the vertical acceleration of strong ground motions when the cantilever length is long. The projection length should vary within the limit depending upon the section properties, and type of wall resting at the edge of cornice slab. The dynamic amplification may lead to the damages of non-structural/architectural components making it unstable or pull out from the main structure. It may further initiate the damage

to structural component connecting to it and creating a bigger risk of damage to the whole structure. Thus, unique cornice projection of Bhutanese types covering the whole façade deemed to be included in the structural analysis. This provision is also mentioned in ASCE41 and IS1893 under non-structural components.

The following recommendations are proposed:

1. Cornice projection longer than 1.4m gets affected by vertical acceleration resulting high amplification that may lead to the damages of architectural components making it unstable or pull out from the main structure. It may further initiate the damage to structural component connecting to it and creating greater risk of damage to structural element of the structure.
2. Projection length cornice should vary within safe limit depending upon the section properties, and type of wall resting at the edge cantilever component.
3. Provisions in ASCE41, FEMA356 and IS1893 should be adopted to check the unique cornice projection in performance-based design.

6.3 Future study

Projections are many types and, in this paper, covered only front full-length cornice projections. The plan and structural details modeled is only for 3 stories typical plan of school building without considering actual soil-structure interaction (SSI) to Response History Analysis. In-depth study of further increased in projection lengths including increased number of stories, site-specific SSI, including cornice projection of other sides of the building can be useful to reconfirm the findings. However, the further in-depth study of numerical simulation along with a laboratory test is deemed to reconfirm the projection length limit by investigating relevant responses. This can be useful to provide recommendations in design and reviewing of existing codes. These limitations are part of the author's future course of study.

REFERENCES

Abdelkareem KH, Sayed FKA, Ahmed MH and Al-Mekhlafy N (2013), "Equivalent Strut Width for Modeling R.C. Infilled Frames," *Journal of Engineering Sciences, Assiut University, Faculty of Engineering*, **41**(3): 851-866.

ACI318 (2014), *American Concrete Institute ,Building Code Requirements for Structural Concrete* ACI, Farmington Hills, MI.

ASCE06 (2006), *American Society of Civil Engineers,Seismic Rehabilitation of Existing Buildings (ASCE/SEI-06)*, American Society of Civil Engineers, Reston, Virginia 20191,USA.

ASCE7 (2010), *American Society of Civil Engineers,Minimum Design Loads for Buildings and Other Structures*, American Society of Civil Engineers, Reston, Virginia,United States of America.

ASCE41 (2013), *American Society of Civil Engineers ,Seismic Evaluation and Retrofit of Existing Buildings* American Society of Civil Engineers Reston, Virginia,USA.

Asteris PG, Giannopoulos IP, Chrysostomou CZ and Smyrou E (2011), "Masonry Infilled Reinforced Concrete Frames with openings," Proceedings of the III ECCOMAS Thematic Conference on Computational Methods in Structural Dynamics and Earthquake Engineering, Corfu, Greece.

Asteris PG, Kakaletsis DJ, Chrysostomou CZ and Smyrou EE (2011), "Failure Modes of In-filled Frames " *Electronic Journal of Structural Engineering* **11(1)**.

Asteris PG, Repapis CC, Repapi EV and Cavaleri L (2016), "Fundamental period of infilled reinforced concrete frame structures," *Structure and Infrastructure Engineering,Maintenance, Management, Life-Cycle Design and Performance*, **13**(August): 1-13.

Chopra AK (2012), *Dynamics of Structures:Theory and Applications to Earthquake Engineering*,, Prentice Hall, Upper Saddle River, NJ.

Crisafulli FJ, Carr AJ and Park R (2000), "Analytical modelling of infilled frame structures-a general review," *Bulletin-New Zealand Society for Earthquake Engineering*, **33**(1): 30-47.

Crisafulli FJ and Carr AJ (2007), "Proposed macro-model for the analysis of infilled frame structures," *Bulletin of the New Zealand Society for Earthquake Engineering*, **40**(2): 69-77.

Dorji J and Thambiratnam DP (2009), "Modelling and analysis of infilled frame structures under seismic loads," *The Open Construction & Building Technology Journal*, **3**: 119-126.

Drukpa D, Velasco AA and Doser DI (2006), "Seismicity in the Kingdom of Bhutan (1937-2003): Evidence for crustal transcurrent deformation," *Journal of Geophysical Research: Solid Earth*, **111**(6): 1-14.

DuDH (2002), *Development & Housing Royal Government ; Bhutan Building Rules ,epartment of Urban of Bhutan*, Thimphu,Bhutan.

EC8 (2004), *Eurocode 8 Design of structures for earthquake resistance,Part 1: General rules, seismic actions and rules for buildings*, BRITISH STANDARD, United Kingdom.

Essa ASAT, Badr MRK and El-Zanaty AH (2014), "Effect of infill wall on the ductility and behavior of high strength reinforced concrete frames," *HBRC Journal*, **10**(3): 258-264.

FEMA356 (2000), *Federal Emergency Management Agency, Presetandard and commentary for the seismic rehabilitation of buildings*, Federal Emergency Management Agency Washington, D.C., Reston, Virginia, United States of America.

Ghobarah A (2004), "On drift limits associated with different damage levels," Proceedings of the Performance-Based Seismic Design concepts and Implementations, 28, Bled, Slovenia, 321-332.

Inel M and Ozmen HB (2006), "Effects of plastic hinge properties in nonlinear analysis of reinforced concrete buildings," *Engineering structures*, **28**(11): 1494-1502.

IS1893 IS (2002), *IS1893-Part 1:2002 Criteria for earthquake resistant design of structures* Bureau of Indian Standard, New Delhi, India.

Jain SK (2003), "Review of Indian seismic code, IS 1893 (Part 1): 2002," *Indian Concrete Journal*, **77**(11): 1414-1422.

Kadysiewski S and Mosalam KM (2009), *Modeling of unreinforced masonry infill walls considering in-plane and out-of-plane interaction*, Pacific Earthquake Engineering Research Center Berkeley, CA.

Kaushik HB, Rai DC and Jain SK (2006), "Code approaches to seismic design of masonry-infilled reinforced concrete frames: A state-of-the-art review," *Earthquake Spectra*, **22**(4): 961-983.

Kaushik HB, Rai DC and Jain SK (2007), "Uniaxial compressive stress–strain model for clay brick masonry," *Current Science*, **92**: 497-501.

Kose MM (2009), "Parameters affecting the fundamental period of RC buildings with infill walls," *Engineering Structures*, **31**(1): 93-102.

Moghaddam HA and Dowling PJ (1987), "ESEE Research Report No. 87-2, The State of the Art in Infilled Frames, Imperial College of Science and Technology," *Civil Eng. Department, London, UK*.

MoHCA (2009), *Ministry of Home and Cultural Affairs,Joint Rapid Assessment for Recovery, Reconstruction and Risk Reduction, 21 September 2009 Earthquake*, Thimphu, Bhutan.

MoHCA (2011), *Ministry of Home and Cultural Affairs,Joint Rapid Assessment for Recovery and Reconstruction and Risk Reduction Joint; 18 September 2011 Earthquake*, RGoB, Thimphu, Bhutan.

MoWHS (2014), *Minstry of Work and Human Settlements;Bhutanese Architecture Guidelines,Royal Government of Bhutan*, Thimphu, Bhutan.

Murty CVR and Jain SK (2000), "Beneficial influence of masonry infill walls on seismic performance of RC frame buildings," Proceedings of the 12th World Conference on Earthquake Engineering (12WCEE2000) ,30 January - 4 February 2000, 12, Auckland, New Zealand, 1-6.

NBC201 (1994), *Nepal National Building Code (NBC)*, Ministry of Physical Planning and Works, Babar Mahal, Kathmandu, NEPAL

Negro P and Colombo A (1997), "Irregularities induced by nonstructural masonry panels in framed buildings," *Engineering Structures*, **19**(7): 576-585.

Ou Y-C, Kurniawan RA, Kurniawan DP and Nguyen ND (2012), "Plastic hinge length of circular reinforced concrete columns," *Computers & Concrete*, **10**(6): 663-681.

Šipoš TK and Sigmund V (2014), "Damage assessment of masonry infilled frames," Proceedings of the 2nd European Conference on Earthquake Engineering and Seismology, Istanbul, Turkey.

Smyrou EE, Blandon C, Antoniou S, Pinho R and Crisafulli F (2011), "Implementation and verification of a masonry panel model for nonlinear dynamic analysis of infilled RC frames," *Bulletin of Earthquake Engineering*, **9**(5): 1519-1519.

Sungjin B and Bayrak O (2008), "Plastic hinge length of reinforced concrete columns," *ACI Structural Journal* **105**: 290-300.

Takai N, Shigefuji M, Rajaure S, Bijukchhen S, Ichiyanagi M, Dhital MR and Sasatani T (2016), "Strong ground motion in the Kathmandu Valley during the 2015 Gorkha, Nepal, earthquake," *Earth, Planets and Space*, **68**(1): 10-10.

Teguh M (2017), "Experimental Evaluation of Masonry Infill Walls of RC Frame Buildings Subjected to Cyclic Loads," *Procedia Engineering*, **171**: 191-200.

Thinley K and Hao H (2015), "Seismic assessment of masonry infilled reinforced concrete frame buildings in Bhutan," Proceedings of the Tenth Pacific Conference on Earthquake Engineering Building an Earthquake-Resilient Pacific 6-8 November 2015, Sydney, Australia.

Walling MY and Mohanty WK (2009), "An overview on the seismic zonation and microzonation studies in India," *Earth-Science Reviews*, **96**(1): 67-91.

APPENDIX

APPENDIX A: DIAGONAL STRUTS

Masonry expected compressive strength (from Kaushik,2007)

$f_{me} := 6.6MPa$

(expected and lower bound in FEMA Tables 7-1 and 7-2)

Thickness of infill masonry (SPBD,2009)

$t_{inf} := 0.25m$

Height of the infill panel (SPBD,2009)

$h_{inf} := 2.55m$

Length of the infill panel (SPBD,2009)

$L_{inf} := 2m$

Height of the Column (center to center of beam)

$h_{col} := 3m$

Length of the infill panel

$L_{col} := 2.4m$

FEMA356 Formula for masonry elastic modulus (expected and lower bound) (Tables 7-1 and 7-2)

$E_m := 550 \cdot f_{me}$

$E_m = 3.63 \times 10^{3} \cdot MPa$

Compressive strength of concrete (SPBD,2009)

$f_c := 20MPa$

$E_c := 4700\sqrt{(f_c \cdot MPa)} = 2.102 \times 10^{4} \cdot MPa$ (ACI318-14)

Gross moment of inertia of the concrete column

$I_g := 213333.3cm^4$

Effective cracked moment of inertia of concrete column (ACI318-14, Table 6.6.3.1.1(a)

$I_{col} := 0.7 \cdot I_g = 1.493 \times 10^{-3} m^4$

$\phi_{inf} := atan\left(\frac{h_{inf}}{L_{inf}}\right) \quad \phi_{inf} = 0.906$

$r_{inf} := \sqrt{\left(h_{inf}^2 + L_{inf}^2\right)} = 3.241m$

$L_{diag} := \sqrt{\left(h_{col}^2 + L_{col}^2\right)} = 3.842m \quad L_{diag} = 3.842m$

Calculation of the width of the compression strut which represents the infill, based on given in FEMA 356, Section 7.5.2

$$\phi_{diag} = 0.896$$

$$\lambda_1 := \left(\frac{E_m \cdot t_{inf} \cdot \sin(2 \cdot \phi_{inf})}{4 \cdot E_c \cdot I_{col} \cdot h_{inf}} \right)^{\frac{1}{4}}$$

$$\lambda_1 = 1.288 \cdot m^{-1}$$

$$a := 0.175 \cdot (\lambda_1 \cdot h_{col})^{-0.4} \cdot r_{inf}$$

$$a_1 := 0.355m$$ width of the compression strut 1

Similarly strut width of other sizes are calculated

$$a_2 := 0.513m$$ Width of the compression strut 2

$$a_3 := 0.382m$$ Width of the compression strut 3

Calculate the axial stiffness of the infill strut

$$k_{inf1} := \frac{a_1 \cdot t_{inf} \cdot E_m}{r_{inf}} = 9.941 \times 10^4 \frac{kN}{m}$$

For other struts also similarly calculated.

Strut 2 (4.5x3)

$L_{in2} := \mathbf{4.1}m \qquad H_{in2} := \mathbf{2.55}m$

$A_{in2} := L_{in2} \cdot H_{in2} = \mathbf{10.455}m^2 \qquad C_{12} := \mathbf{1.925} \cdot \frac{L_{in2}}{H_{in2}} = \mathbf{3.095}$

$f_{tp2} := \mathbf{350}\frac{kN}{m^2} \qquad t_{w2} := \mathbf{0.25}m$

$$F_{max2} := \mathbf{0.818} \cdot \frac{L_{in2} \cdot t_{w2} \cdot f_{tp2}}{C_{12}} \cdot \left(\mathbf{1} + \sqrt{C_{12}^{\,2} + \mathbf{1}}\right) = \mathbf{4.032} \times \mathbf{10}^{\mathbf{5}} N$$

$$F_{max2} = \mathbf{403.208}kN \qquad (\mathbf{2.1})$$

$$F_{cr2} := \mathbf{0.6} \cdot F_{max2} = \mathbf{241.925}kN \qquad (\mathbf{2.2})$$

Shear modulus (*ASCE41* − **13**)

$G_{w2} := \mathbf{0.4} \cdot E_b = \mathbf{1.452} \times \mathbf{10}^{\mathbf{3}} \cdot MPa$

Initial Stiffness of diagonal strut

$$K_{i2} := \frac{G_{w2} \cdot L_{in2} \cdot t_{w2}}{H_{in2}} = \mathbf{5.836} \times \mathbf{10}^{\mathbf{5}} \cdot \frac{kN}{m}$$

Table 1 Parameters of strut calculations

Strut	Shear Modulus Gm (MPa)	Initial stiffness K_i(kN/m)	F_{max} (kN)	F_{cr} (kN)- 60% F_{max}
1	1452000	284706	267	160
2	1452000	583647	403	242
3	1452000	227765	244	146

Strut 3 (2mx3m)

$L_{in3} := \mathbf{1.6}m \qquad H_{in3} := \mathbf{2.55}m$

$A_{in3} := L_{in3} \cdot H_{in3} = \mathbf{4.08}m^2 \qquad C_{13} := \mathbf{1.925} \cdot \frac{L_{in3}}{H_{in3}} = \mathbf{1.208}$

$t_{w3} := \mathbf{0.25}m \qquad f_{tp3} := \mathbf{350}\frac{kN}{m^2}$

$$F_{max3} := \mathbf{0.818} \cdot \frac{L_{in3} \cdot t_{w3} \cdot f_{tp3}}{C_{13}} \cdot \left(\mathbf{1} + \sqrt{C_{13}^{\,2} + \mathbf{1}}\right) = \mathbf{2.435} \times \mathbf{10}^{\mathbf{5}} N$$

$F_{max2} = \mathbf{403.208}kN$

$F_{cr3} := \mathbf{0.6} \cdot F_{max3} = \mathbf{146.094}kN$

Shear modulus (*ASCE41* − **13**)

$G_{w3} := \mathbf{0.4} \cdot E_b = \mathbf{1.452} \times \mathbf{10}^{\mathbf{3}} \cdot MPa$

Initial Stiffness of diagonal strut

$$K_{i3} := \frac{G_{w3} \cdot L_{in3} \cdot t_{w3}}{H_{in3}} = \mathbf{2.278} \times \mathbf{10}^{\mathbf{5}} \cdot \frac{kN}{m}$$

APPENDIX B: LATERAL LOAD DISTRIBUTION

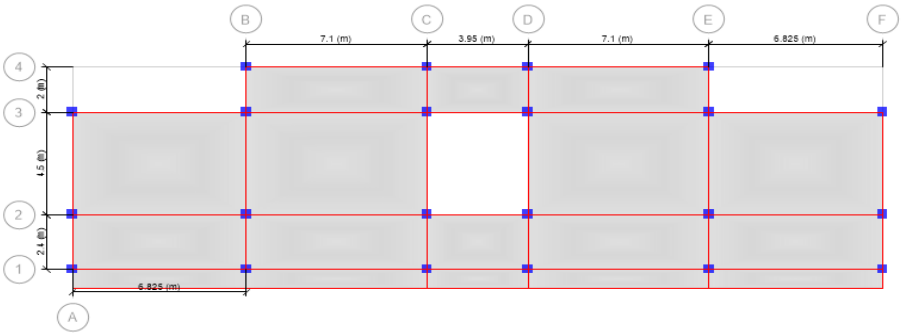

First Floor Plan

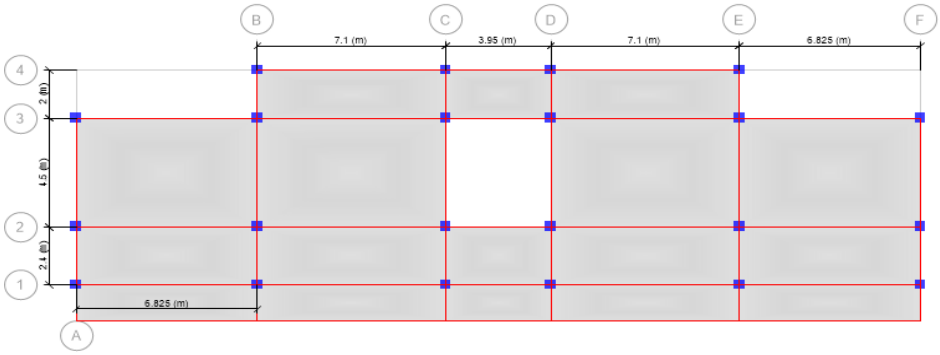

Second Floor Plan

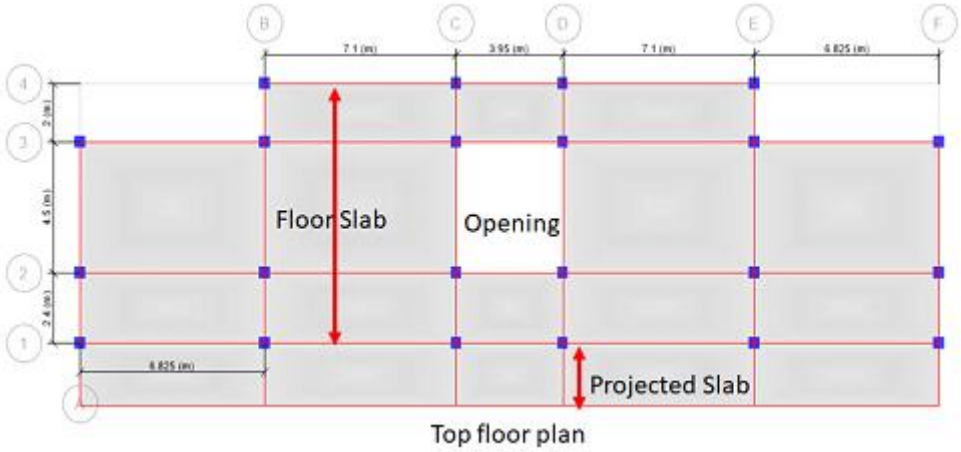

Plan of Model IFP650

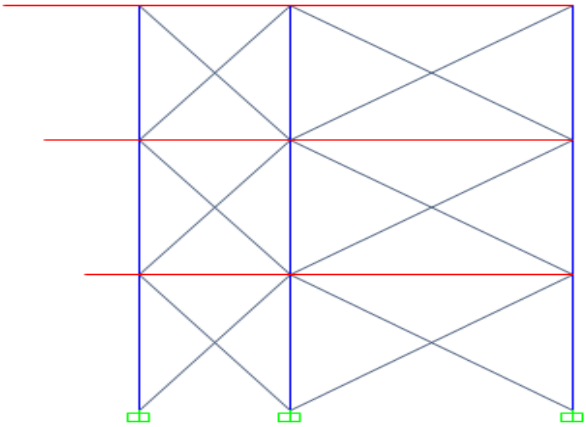

Elevation view A-A

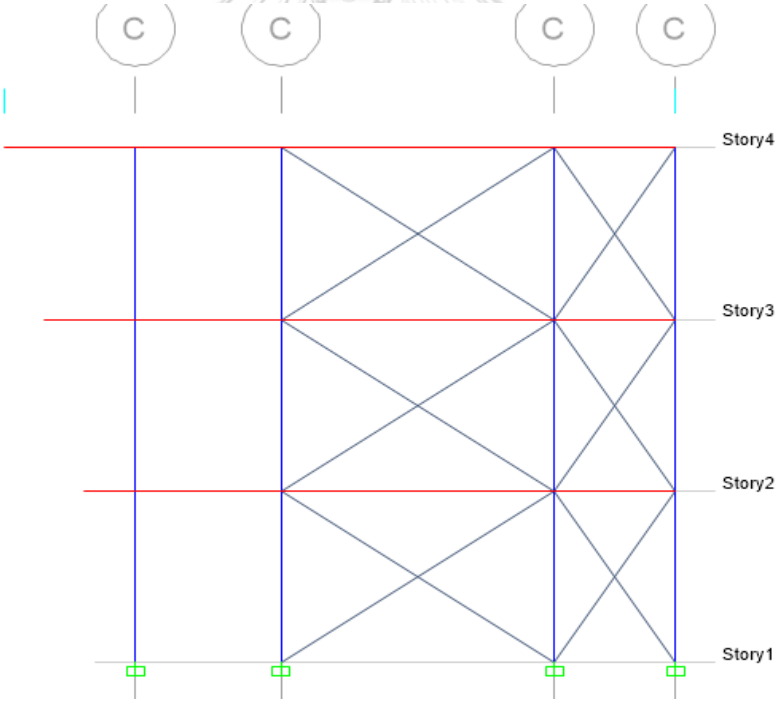

Elevation View C-C

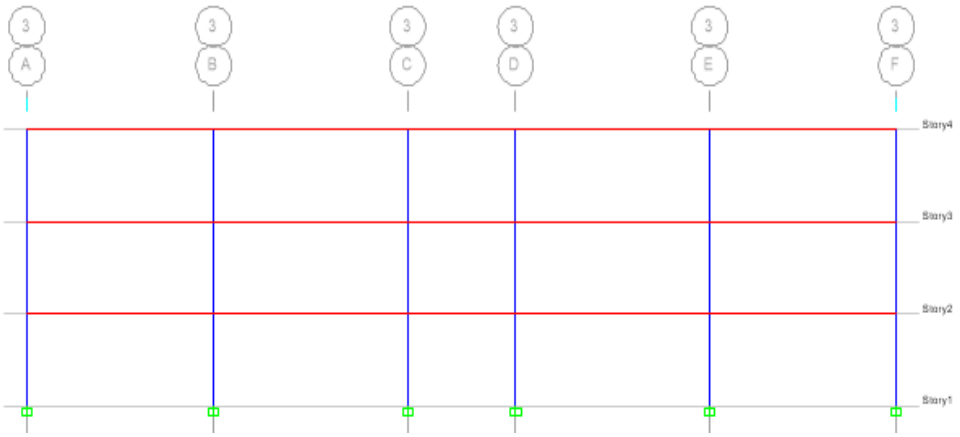

Elevation View C-C

Calculation of Design Seismic Force by Static Analysis

School Building Importance factor

$R_f := 5$ Building with Special RC Moment Resisting Frame detailed as per IS1893 Table 7 Hence Response Reduction factor is 5

Floor Area level 1

$F_{3a} := 2\cdot\left(14.2m^2 + 30.71m^2 + 31.95m^2 + 16.38m^2 + 17.04m^2\right) + 9.48m^2 + 7.90m^2 = 237.94m^2$

$F_{1a} := F_{3a}$ $F_{1p} := 2\left(5.8m^2 + 6.04m^2\right) + 3.36m^2 = 27.04m^2$

Same floor area

$F_{2a} := F_{3a}$

Projected Floor

$F_{3p} := 2\left(14.67m^2 + 15.27m^2\right) + 8.49m^2 = 68.37m^2$

$F_{2p} := 2\left(10.24m^2 + 10.65m^2\right) + 5.93m^2 = 47.71m^2$

Dead load and superimposed load calculations:

$W_{sa} := W_D + W_M = 1.025 \times 10^4 \cdot kN$

$W_{ds} := 2570.82 kN$ Slab self-weight

$W_{db} := 1437.82 kN$ Beam self-weight

$W_{dc} := 1900.80 kN$ Column self-weight

$W_D := W_{ds} + W_{db} + W_{dc} = 5.909 \times 10^3 \cdot kN$ Total dead loads from self-weight of structural members

Total Seismic Weight of the Model considered

$W_{si} := 0.5 W_L + W_D + W_M = 1.138 \times 10^4 \cdot kN$

(ASCE7-10, Section 12.7.2 Effective Seismic Weight W, includes dead loads and other live load is included however in areas used for storage, a minimum of 25 percent of the floor live load)

Natural period and base shear calculations

The lateral earthquake load resistance is provided by framed masonry with Reinforced concrete and 2nd class brick masonry panels modelled as diagonal compression struts.

IS: 1893 Part 1 Section 7.6.2

$d_x := 31.8$

$d_y := 11.0$

$$T_{ax} := \frac{0.09 h_b}{\sqrt{d_x}} = 0.144$$

$$T_{ay} := \frac{0.09 h_b}{\sqrt{d_y}} = 0.244$$

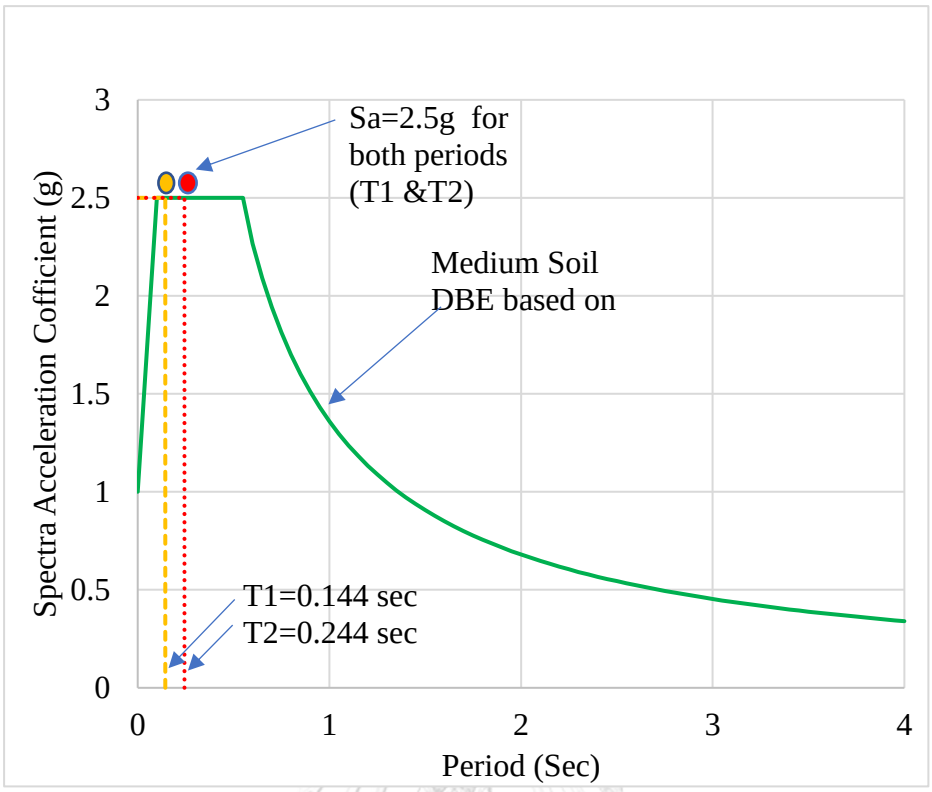

Response Spectra acceleration to the empirical periods of model

$Z = 0.36$ Seismic zone factor Z

$S_{ax} := 2.5g$

$I = 1.5$ Importance factor (I)

$S_{ay} := 2.5g$

$R_r := 5$ Response reduction factor (R)

$A_{hx} := \frac{Z \cdot I}{2 \cdot R_r} \cdot 2.5 = 0.135$ Section 6.4.2 of IS: 1893 Part 1 Ah is calculated

$A_{hy} := \frac{Z \cdot I}{2 \cdot R_r} \cdot 2.5 = 0.135$

Story	Weight (Wi)	Height (Hi)	Lateral Force each level (kN)	
			X	Y
3	2779.01	9	807.00	807.00
2	4691.83	6	605.54	605.54
1	3826.10	3	123.45	123.45
Total lateral force (Base Shear)			1536.00	1536.00

The lateral forces in terms of base shear is presented in the above table for both x and y direction. The base shear is same in both direction as it is controlled by the design response spectrum accelerations which depends on the building natural period in each direction.

APPENDIX C: VERTICAL PERIOD FOR PROJECTION

Stiffness and mass calculations:

$$K_b := \frac{P}{\Delta_{max}} \qquad \Delta_{max} := \frac{P \cdot L_b^{3}}{3 \cdot E \cdot I_b} \qquad K_b := \frac{3 \cdot E \cdot I_b}{L_b^{3}}$$

$$K_{b1} := \frac{3 \cdot E \cdot I_b}{L_{b1}^{3}} = 1.015 \times 10^{4} \frac{1}{m} \cdot kN \qquad K_{b2} := \frac{3 \cdot E \cdot I_b}{L_{b2}^{3}} = 2.99 \times 10^{4} \frac{1}{m} \cdot kN$$

$$K_{b3} := \frac{3 \cdot E \cdot I_b}{L_{b3}^{3}} = 4.592 \times 10^{4} \frac{1}{m} \cdot kN \qquad K_{b4} := \frac{3 \cdot E \cdot I_b}{L_{b4}^{3}} = 7.58 \times 10^{4} \frac{1}{m} \cdot kN$$

$$K_{b5} := \frac{3 \cdot E \cdot I_b}{L_{b5}^{3}} = 1.384 \times 10^{5} \frac{1}{m} \cdot kN \qquad K_{b6} := \frac{3 \cdot E \cdot I_b}{L_{b6}^{3}} = 2.942 \times 10^{5} \frac{1}{m} \cdot kN$$

$$K_{b7} := \frac{3 \cdot E \cdot I_b}{L_{b7}^{3}} = 8.072 \times 10^{5} \frac{1}{m} \cdot kN$$

Seismic mass calculations

$g = 9.807\frac{m}{s^2}$

$M_1 := \frac{90.351kN}{g} = 9.213\times 10^3 kg$

$M_2 := \frac{229.51kN}{g} = 2.34\times 10^4 kg$

$M_3 := \frac{227.311kN}{g} = 2.318\times 10^4 kg$

$M_4 := \frac{225.101kN}{g} = 2.295\times 10^4 kg$

$M_5 := \frac{222.901kN}{g} = 2.273\times 10^4 kg$

$M_6 := \frac{220.701kN}{g} = 2.251\times 10^4 kg$

$M_7 := \frac{219.631kN}{g} = 2.24\times 10^4 kg$

Natural Period of cantilever components

$T_{b1} := 2\cdot 3.142\sqrt{\frac{M_1}{K_{b1}}} = 0.189s$

$T_{b2} := 2\cdot 3.142\sqrt{\frac{M_2}{K_{b2}}} = 0.176s$

$T_{b3} := 2\cdot 3.142\sqrt{\frac{M_3}{K_{b3}}} = 0.141s$

$T_{b4} := 2\cdot 3.142\sqrt{\frac{M_4}{K_{b4}}} = 0.109s$

$T_{b5} := 2\cdot 3.142\sqrt{\frac{M_5}{K_{b5}}} = 0.081s$

$T_{b6} := 2\cdot 3.142\sqrt{\frac{M_6}{K_{b6}}} = 0.055s$

$T_{b7} := 2\cdot 3.142\sqrt{\frac{M_7}{K_{b7}}} = 0.033s$

VITA

My name is Tek Nath Kararia, born on 10 February 1983. I completed secondary education from Damphu Higher Secondary School in Bhutan based on the Indian School Certificate Examination and gained a distinction in 2004. After that, I pursue higher studies in an institute, Maulana Azad National Institute of Technology, Bhopal under the Government of prestigious scholarship and successfully completed in 2009.

After the higher studies, I got the opportunity to work as a civil servant under the Ministry of Work and Human Settlement passing the entrance exam of Royal Civil Service Examination in 2010. I worked as a Project Engineer for implementing the 10 five-year plans for Trongsa District, Central part of Bhutan. Besides, implementing engineering projects, I also served in various capacities for preparing plans and assisting administrative works with the Chief Engineer for the 11 five-year plans.

In 2012, I got a transfer to Thimphu City Corporations and implement some of the visible projects working under the Environment Division creation of public parks, structural mitigation of flood and fire risk, and initiation of the development of first Thimphu City Disaster Management Plan forming technical task group especially focusing on the earthquake hazards.

The requirement of adequate technical knowledge to deal with bigger challenges inspire me to take the opportunity to pursue my graduate study. Consequently, in 2016 through open competition, I availed the full scholarship under Bhutan-Thailand full support program to study Master of Civil Engineering at Chulalongkorn University, Bangkok, Thailand for two years. Accordingly, I completed my studies with this research work successfully in 2018.